Geological Field Trips and Maps

SOCIETÀ GEOLOGICA ITALIANA ETS
FONDATA NEL 1881 - ENTE MORALE R. D. 17 OTTOBRE 1885

ISPRA
Istituto Superiore per la Protezione e la Ricerca Ambientale

Sistema Nazionale per la Protezione dell'Ambiente

2024
Vol. 16 (2.4)

INDEXED IN EMERGING SOURCES CITATION INDEX THOMSON REUTERS

ISSN: 2038-4947

Calabria coast to coast: a nearly complete cross-section of continental crust, with a 13 km-thick late Variscan batholith

Post-conference Field Trip of the "10th Hutton Symposium on Granites and Related Rocks"
Baveno, 10-15 September 2023

https://doi.org/10.3301/GFT.2024.09

GFT&M - *Geological Field Trips and Maps*

Periodico semestrale del Servizio Geologico d'Italia - ISPRA e della Società Geologica Italiana
Geol. F. Trips Maps, Vol.**16** No.2.4 (2024), 84 pp., 66 figs. (https://doi.org/10.3301/GFT.2024.09)

Calabria coast to coast: a nearly complete cross-section of continental crust, with a 13 km-thick late Variscan batholith

Post-conference Field Trip of the "10th Hutton Symposium on Granites and Related Rocks" Baveno, 10-15 September 2023.

Patrizia Fiannacca[1], Rosolino Cirrincione[1], Eugenio Fazio[1], Damiano Russo[1]

[1] Dipartimento di Scienze Biologiche, Geologiche e Ambientali – Università degli Studi di Catania, Corso Italia 57 - 95129 Catania (Italy).

Corresponding author e-mail: patrizia.fiannacca@unict.it

Cover page Figure: Panoramic view of tonalitic cliffs and reefs at "Grotticelle Bay" (Ricadi, Vibo Valentia).

ISSN: 2038-4947 [online]

http://gftm.socgeol.it/

https://doi.org/10.3301/GFT.2024.09

INDEX

INFORMATION

EXCURSION NOTES

ITINERARY

https://doi.org/10.3301/GFT.2024.09

ABSTRACT

Southern Calabria is one of the rare places in the world where a nearly complete section of late Paleozoic continental crust is exposed with regularity, from basal metagabbros equilibrated at a depth of ~ 35 km, through mafic and felsic granulites and overlying metapelitic migmatites, to upper crustal paragneisses and phyllites. The crustal section also includes the late Variscan Serre Batholith (~ 297-292 Ma), a ~ 13 km-thick composite and zoned batholith, consisting of a stack of tabular granitoid units, from strongly deformed to apparently undeformed, and ranging in composition from quartz diorite-tonalite to granodiorite-granite, which were emplaced sequentially, at decreasing depths from about 23 to 6 km.

In this field trip, we will be exploring the entire crustal section from bottom to top, with a central focus on the role of granitoid magmatism in the growth and evolution of the continental crust in collisional zones, together with several more specific topics related to the large variety of rock structures and compositions.

Keywords: crustal section, magma petrogenesis, tectono-metamorphic evolution, Serre Batholith, southern Italy.

PROGRAM SUMMARY

Day 1 – The deep Variscan crust exposed in the northwestern Serre Massif: mafic and felsic granulites and overlying metapelitic migmatites
Stop 1.1 Metagabbro from the bottom of the crustal section - Curinga
Stop 1.2 Felsic granulites – Francavilla Angitola
Stop 1.3 Garnet-rich metapelitic migmatites – Vibo Marina
Stop 1.4 Metapelitic migmatites from the top of the lower crust – Stefanaconi
Overnight in Ricadi, Tyrrhenian coast

Day 2 – From the top of the lower crust to the deepest granitoids of the Serre Batholith: migmatite border zone, deep syn-tectonic tonalites/quartz diorites and overlying two-mica porphyritic granodiorites and granites from Capo Vaticano Promontory
Stop 2.1 Migmatitic Border zone – Santa Maria Beach, Ricadi
Stop 2.2 I-type tonalites with MME swarms and felsic dykes – Scogli della Galea, Ricadi
Stop 2.3 Two-mica porphyritic granodiorites and granites and underlying tonalites – Michelino Beach, Parghelia
Overnight in Ricadi, Tyrrhenian coast

Day 3 – Mid- to upper crustal granitoids, but also «geology and human life»
Stop 3.1 Swabian-Norman castle of Vibo Valentia
Stop 3.2 Serra San Bruno: the granite town

https://doi.org/10.3301/GFT.2024.09

Stop 3.3 Quarry of two-mica equigranular granodiorites and granites – Mongiana
Stop 3.4 The Nardodipace "megaliths"
Stop 3.5 The batholith roof: Bt ± Am granodiorites and MME at Fiumara Allaro
Stop 3.6 The end of late Variscan magmatism: subvolcanic dacites-rhyodacites – Santo Todaro
Overnight in Riace Marina, Ionian coast

Day 4 – The upper crust exposed in the southern Serre Massif: contact aureole in the Stilo phyllites, Variscan mylonites and late- to post-tectonic dykes in the Mammola paragneisses.
Back to the lower crust: migmatitic paragneisses and Alpine mylonites from the Palmi area.
Stop 4.1 Spotted schists – Torrente Pardalà, Bivongi
Stop 4.2 Boulder granite quarry – Fiumara Stilaro, Stilo
Stop 4.3 Mylonitic paragneisses intruded by felsic dykes – Mammola
Stop 4.4 Alpine mylonites at the batholith-lower crust interface – Ulivarella Beach, Palmi
Stop 4.5 Metapelitic migmatites just outside the Palmi shear zone – Scoglio dell'Isola, Palmi
Arrival in Reggio Calabria and end of the field trip.

SAFETY

Most outcrops are on the beach, along roadsides and riverbeds; only short walks in rough terrains are planned, but solid field boots are anyway recommended. The equipment should also include sun protection and a sun hat. The weather in mid-late September is usually warm and dry in Calabria, but some warm clothes and a waterproof jacket are also recommended.
Safety in the field is anyway related to self-awareness. All attendees participate to the excursions at their own risk.

USEFUL PHONE NUMBERS

General Emergency – Tel: 112

https://doi.org/10.3301/GFT.2024.09

HOSPITALS

Presidio Ospedaliero “Giovanni Paolo II”, Via Sen. Arturo Perugini, 88046 Lamezia Terme. Tel. +39 0968 2081.

Hospital G. Jazzolino, Piazza Fleming, 89900 Vibo Valentia. Tel. +39 0963 962111.

Hospital Tropea, Via Provinciale, 89861 Tropea. Tel. +39 0963 962800.

Hospital Serra San Bruno, Via A. Scrivo, 89822 Serra San Bruno. Tel. +39 0963 777111.

First aid Palmi, Via Bruno Buozzi 167, 89015 Palmi.

Grande Ospedale Metropolitano Bianchi Melacrino Morelli, Via S. Cristoforo 24, 89128 Reggio Calabria. Tel. +39 0965 1870549.

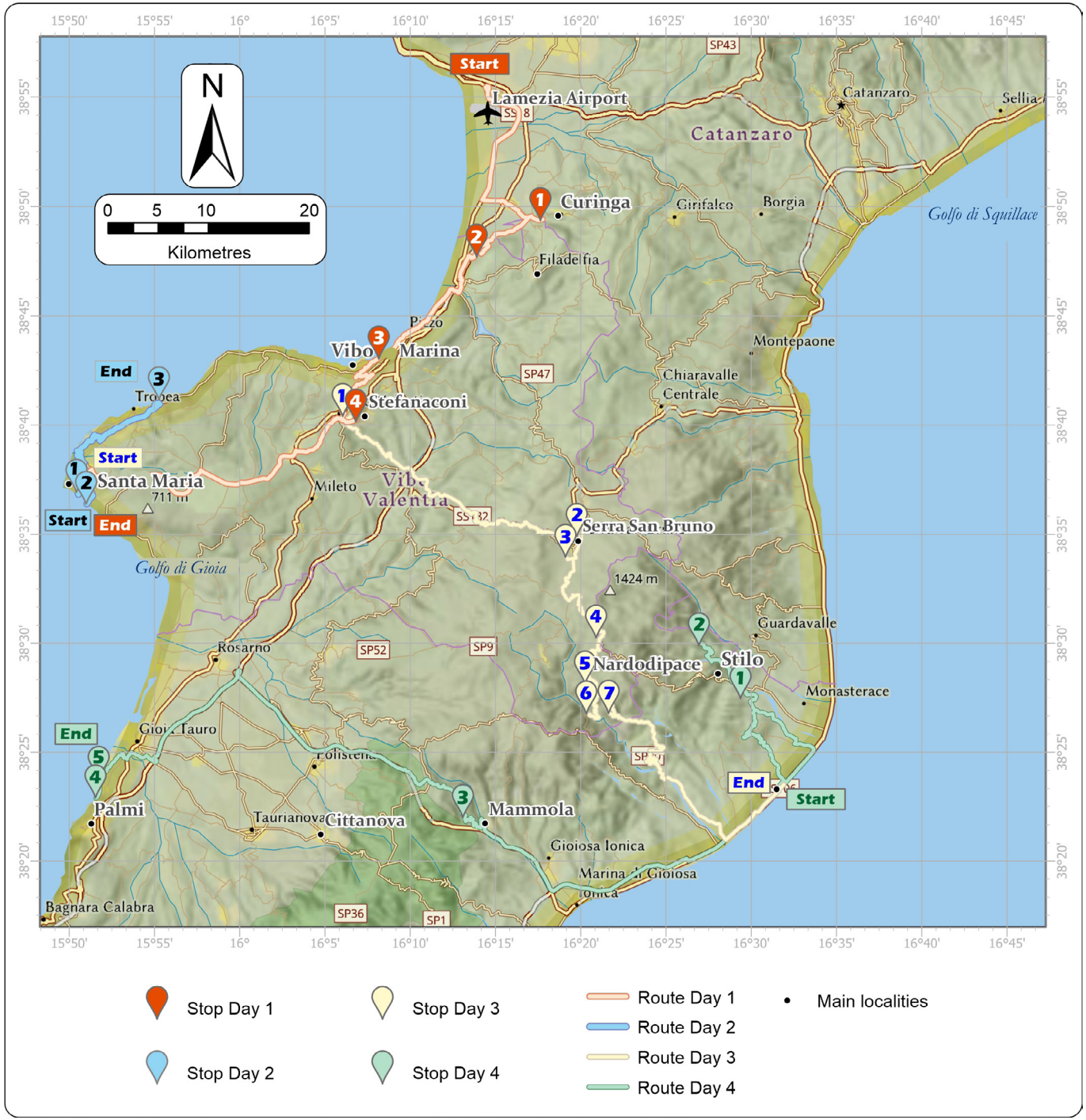

https://doi.org/10.3301/GFT.2024.09

INTRODUCTION

Complete cross sections of continental crust are uncommon occurrences in the global geological record, especially when dealing with ancient collisional orogens, which are usually deeply eroded or dismembered by subsequent geodynamic events.

Despite Italy is well known for hosting one of the best exposed and more complete of such crustal sections – the famous Ivrea-Verbano Zone and adjacent Serie dei Laghi in the Western Alps (northern Italy) – the presence of another outstanding cross-section of late Variscan continental crust in southern Calabria (southern Italy) is much less known.

Portions of the southern Calabria crustal section crop out in the Serre Massif, Capo Vaticano Promontory and Palmi-Bagnara area, with the most complete and continuous cross-section exposed in the Serre Massif; here, field observations combined with petrological investigations have revealed that the massif represents a coherent tilted crustal section, with a thickness of ~ 25 km (Schenk, 1990; Caggianelli et al., 2007; Angì et al., 2010).

In the Serre Massif, the crustal rocks are exposed with regularity from NW to SE, from metagabbros equilibrated at a depth of ~ 35 km, through mafic and felsic granulites and overlying metapelitic migmatites, to upper crustal paragneisses and phyllites.

The crustal section also includes the late Variscan Serre Batholith (~ 300 Ma; Rottura et al. 1990, 1991; Fornelli et al., 1994; Langone et al., 2014; Fiannacca et al., 2015, 2017), a ~ 13 km-thick composite and zoned batholith, consisting of a stack of tabular granitoid units, from strongly deformed to apparently undeformed, and ranging in composition from quartz diorite-tonalite to granodiorite-granite, which were emplaced sequentially, at decreasing depths, from about 23 to 6 km (Caggianelli et al., 1997, 2000; Fiannacca et al., 2017, 2021; Russo et al., 2023).

The Serre Batholith offers a great opportunity to investigate, in a comparatively restricted spatial area of ~ 1200 km^2, many aspects of great petrological and geological relevance including, but not limited to, the processes involved in the generation of the compositional spectrum of granitoids and related rocks, the timescales and mechanisms of batholith construction, and the relationships between tectonics and granitoid magmatism.

In fact, despite the relatively modest area extension of the Serre Batholith, its compositional variety is wide, being dominated by weakly peraluminous tonalites and strongly peraluminous granodiorites, but also including all the compositional range from rare quartz gabbros, much more common quartz diorites and monzogranites, quartz monzodiorites (only as mafic microgranular enclaves) and minor syenogranites and leucogranites, the latter exclusively as pegmatite and aplite dykes intruding all the granitoid rocks and their host rocks. This allows the investigation of the genetic relationships between the different granitoid types and of the processes responsible for their compositional diversity, as well as of their possible I- versus S-type affinity and, in turn of the petrogenetic processes leading to the generation of the granitoid magmas. As an important added value, the exposure of a ~ 7 km-thick section of lower crust underlying the batholith, makes it possible to directly study the crustal rocks potentially involved in the petrogenesis of the granitoids, also investigating the relative role of crust and mantle

https://doi.org/10.3301/GFT.2024.09

and its implications in terms of intracrustal recycling of older crust, or formation of new continental crust.
In addition, the different granitoid bodies that make up the batholith were emplaced sequentially at progressively shallower crustal levels (Fiannacca et al., 2017; and references therein), forming a continuous stack of tabular intrusions; the contacts between the batholith and its underlying and overlying metamorphic host rocks are also locally exposed, all of which provides an opportunity to investigate the architecture, mechanisms and timing of batholith construction.
Finally, as for the relationships between tectonics and magma emplacement, a tight connection with the activity of a crustal-scale shear zone has long been proposed for the foliated quartz diorites and tonalites that make up the oldest and deepest magmatic unit of the batholith (e.g., Caggianelli et al., 2000, 2007; Angì et al., 2010; Fiannacca et al., 2017; Ortolano et al., 2022). A shear zone-linked emplacement has been suggested also for the progressively younger, shallower and apparently undeformed granitoids (e.g., Angì et al., 2010; Fiannacca et al., 2017, 2021); nevertheless, several important aspects including the shear zone geometry, kinematics and tectonic regime are still to be understood in detail, as well as the cause-effect relationship between magma emplacement and shear zone activation: was the emplacement of the earliest granitoid magmas shear-zone controlled or was the nucleation of the shear zone assisted by magma emplacement? New information and interpretations about the shear-zone kinematics and tectonic regime have been recently proposed by Ortolano et al. (2022) (see Stop 4.3), and further studies are in progress.
In this field trip, we will be exploring the entire crustal section exposed in southern Calabria from bottom to top, with a central focus on the role of granitoid magmatism in the growth and the compositional and structural evolution of the continental crust in collisional zones, together with several more specific topics related to the wide variety of rock structures and compositions.

https://doi.org/10.3301/GFT.2024.09

GEOLOGICAL BACKGROUND

GENERAL OUTLINE

The Serre Massif (SM), the adjacent Capo Vaticano Promontory (CVP) and the Palmi-Bagnara area, which will be visited in this field trip, make up the central part of the Calabria–Peloritani Orogen (CPO), an arcuate mountain belt connecting the southern Apennines and the Sicilian Maghrebides (Fig. 1).

The CPO consists of a poly-orogenic basement complex made up of remnants of Variscan and older mountain chains incorporated into the Alpine–Apennine orogenic system (Cirrincione et al., 2015; and references therein). In particular, although the present-day geological setting is due to Alpine tectonics and the subsequent opening of the Tyrrhenian basin (e.g., Langone et al., 2006; Festa et al. 2020), and a pre-Variscan origin has been documented or suggested for some of the CPO basement rocks (Cirrincione et al., 2005; Micheletti et al. 2007; Fazio et al., 2015), most of the basement formed during the Variscan Orogeny (~ 300 Ma; e.g., Graessner et al., 2000; Micheletti et al., 2008; Fiannacca et al., 2008, 2017; Appel et al., 2011; Langone et al., 2014; Fornelli et al., 2020).

The CPO is indeed considered one of the crustal blocks making up the former Galatian superterrane (e.g., von Raumer

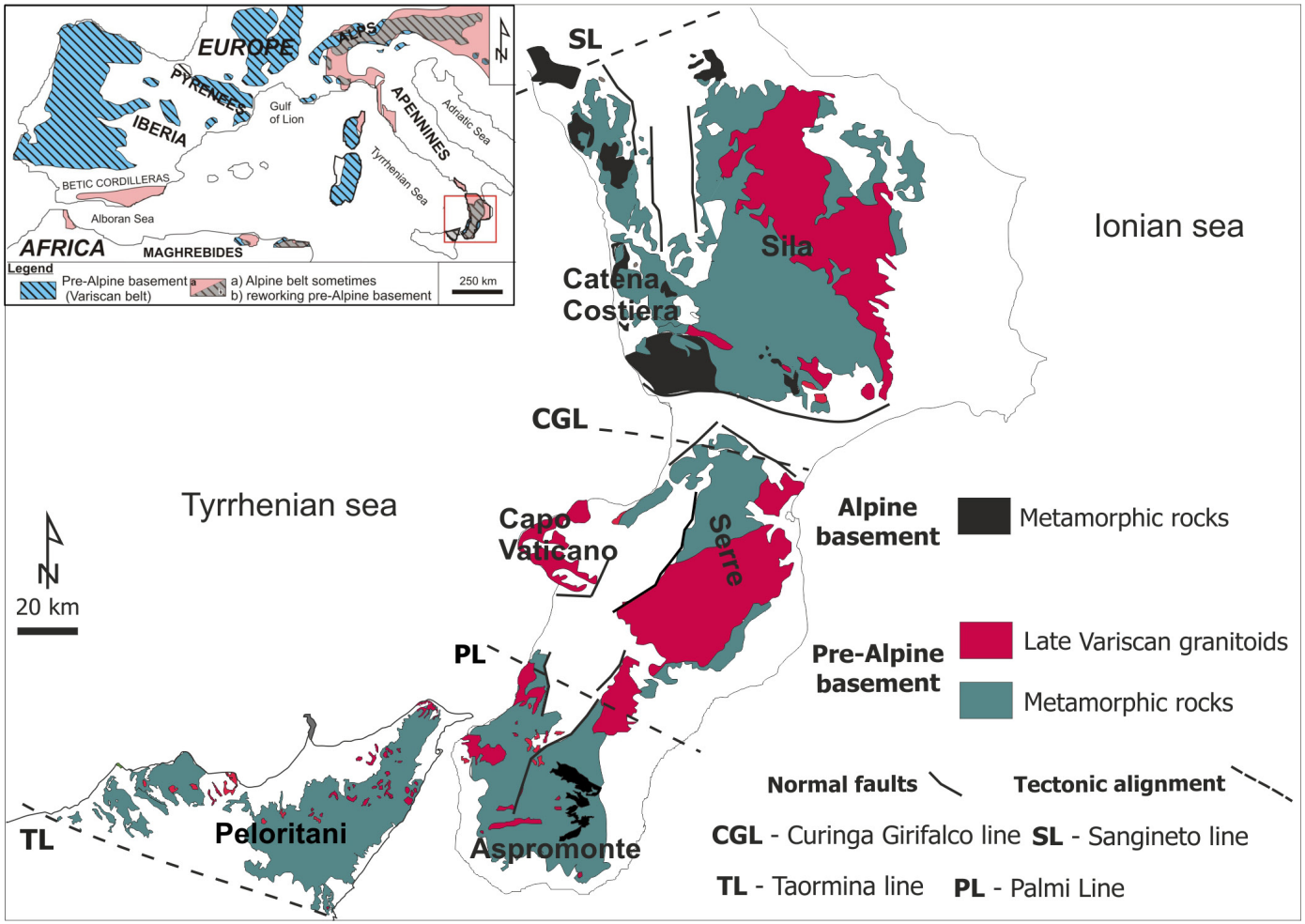

Fig. 1 - Distribution of Alpine and pre-Alpine (Variscan and/or pre-Variscan) basement rocks in the Calabria–Peloritani Orogen and main tectonic alignments (modified after Angì et al., 2010). The inset shows the present-day distribution of the Alpine and pre-Alpine basements in Western Europe with CPO locations (modified after Cirrincione et al., 2015).

https://doi.org/10.3301/GFT.2024.09

and Stampfli, 2008) that, with neighbouring areas such as Sardinia, Corsica, West Carpathians and much of the Alpine basement, were part of the future south Variscan terranes. These peri-Gondwana-derived terranes were located at the northern Paleotethys margin, while domains such as Armorica, Saxothuringia and Bohemia faced to the north the Rheic Ocean (e.g., Domeier and Torsvik, 2014; von Raumer et al., 2013). The end of subduction under the Galatian superterrane was marked at ~ 340–330 Ma by the intrusion of Mg-K-rich magmatic bodies likely related to slab break-off (vaugnerites–durbachites; von Raumer et al., 2013, 2014); these rocks, absent in the CPO, are scattered throughout western Europe. The sequential closure of the Rheic and Paleotethys oceans resulted in the final collision among Gondwana, peri-Gondwanan terranes and Laurussia, leading to formation of Pangea at ~ 300 Ma. Extensive crustal melting and granitoid magmatism recorded throughout the south Variscan terranes at 320–280 Ma are considered to have developed as a result of the change from a compressional to a transtensional/transpressional regime, associated to a complex pattern of strike-slip shear zones, collectively known as East Varisican Shear Zone and locally coupled with significant crustal thinning and asthenosphere upwelling (e.g., Corsini and Rolland, 2009; Carosi et al., 2012; von Raumer et al., 2013; Padovano et al., 2014). According to reconstructions by Padovano et al. (2012, 2014), the CPO was also involved in the activity of the East Variscan Shear Zone (Fig. 2).

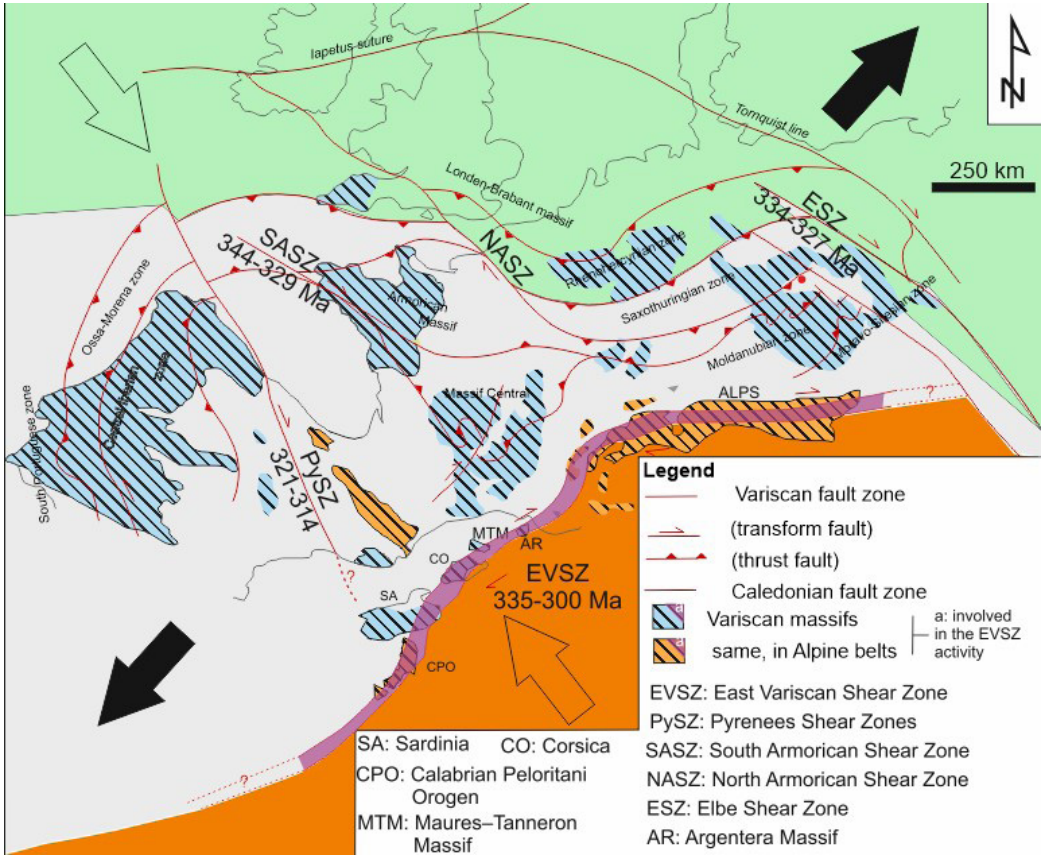

Fig. 2 - Western Mediterranean strike-slip kinematic pattern in the Late Carboniferous–early Permian (modified after Ortolano et al., 2022, and references therein). Green: Laurussia; gray: Gondwana-derived microplates; orange: Gondwana. Transparent arrow: main contractional stress axis; black arrow: main extensional stress axis.

The latest stages of the Variscan Orogeny were also marked in the CPO by widespread crustal melting and voluminous granitoid magmatism. After generation of small weakly peraluminous trondhjemite plutons, which crop out exclusively in southern Calabria (Aspromonte Massif) and northeastern Sicily (Peloritani Mountains), at ~ 310 Ma (Fiannacca et al., 2008, 2020), and strongly peraluminous leucogranodiorite-leucogranite plutons, scattered throughout the CPO (D'Amico et al., 1982; Rottura et al., 1993; Caggianelli et al., 2003; Fiannacca et al., 2019), at ~ 300 Ma (Graessner et al., 2000; Fiannacca et al., 2008), the bulk of late Variscan magmatism gave rise to the composite Serre and Sila batholiths in southern and northern Calabria, respectively (Rottura

https://doi.org/10.3301/GFT.2024.09

et al., 1990, 1991; Ayuso et al., 1994; Caggianelli et al., 1994, 2003; Fornelli et al., 1994; Langone et al., 2014; Fiannacca et al., 2015, 2017; Russo et al., 2023).

Late Variscan magmatism in the CPO ended with extensive dyke magmatism producing swarms of medium- to high-K calc-alkaline felsic to intermediate dykes (Festa et al., 2010; Romano et al., 2011), intruding both the granitoids and their upper crustal metamorphic host rocks. These subvolcanic rocks represent the transition from a late-orogenic to a post-orogenic geodynamic environment, associated with the early breakup of Pangea and subsequent opening of the Tethyan Ocean, which is documented, in turn, by sodic-alkaline and tholeiitic Triassic basalts from northern Calabria (Barca et al., 2010) and central-western Sicily (Cirrincione et al., 2014, 2016). The pre-Alpine rocks from the CPO were then locally affected by Alpine metamorphism, which reworked pre-existing metamorphic rocks, or produced mono-metamorphic Alpine rocks, the latter mostly exposed in the Catena Costiera and Aspromonte Massif; other areas such as the Serre Massif and the Capo Vaticano Promontory in southern Calabria were largely unaffected by Alpine metamorphic overprints (Cirrincione et al., 2015 and references therein).

The cross-section of continental crust in southern Calabria

The central part of the CPO, in southern Calabria (Fig. 3) stands out for the presence of a nearly complete and continuous cross-section of late Paleozoic continental crust including metamorphic and magmatic Variscan rocks equilibrated, or emplaced, at paleodepths between ~ 33 and ~ 6 km. Despite intermediate-seated portions of the crustal section cropping out also in the Capo Vaticano Promontory and the Palmi-Bagnara area, the most complete exposure is in the Serre Massif.

The Variscan crustal section is now exposed due to Cenozoic tectonics, responsible for its exhumation and tilting of about 40° to the SE (e.g., Thomson 1994; Festa et al. 2003). During meso-Alpine tectonic stages, the Serre lower crust units were eradicated and thrusted along the Curinga–Girifalco Line over the mylonitic Castagna Unit (Fig. 3) that represents, in turn, a reworked deep-to-intermediate portion of late Variscan continental crust (e.g., Ortolano et al., 2020a; Brandt & Schenk, 2020; Festa et al., 2020, 2022; Tursi et al., 2021).

It is worth mentioning that a similar, but less complete, late Paleozoic crustal section is also exposed in northern Calabria, in the Sila Massif (Fig. 1), with the deepest lower crustal rocks equilibrated at ~ 0.6 GPa (Graessner and Schenk, 2001; Cirrincione et al., 2015, and references therein).

In the Serre Massif, from the northwest to the southeast, it is possible to distinguish three portions, broadly representative of the lower, middle and upper crust, respectively. All the metamorphic rocks and some of the late Variscan granitoids show a compositional layering plunging to SE and dipping about 40°, which is roughly the general dip of the whole crustal section exposed in the massif.

The lower crust

The 7–8 km thick lower crustal portion, exposed in the northern part of the Serre Massif, is represented by a ~ 3 km-thick Granulite Unit (aka Granulite-Pyriclasite Unit, after Schenk, 1980, 1984), made up of felsic and mafic granulites, including basal layered metagabbros and

https://doi.org/10.3301/GFT.2024.09

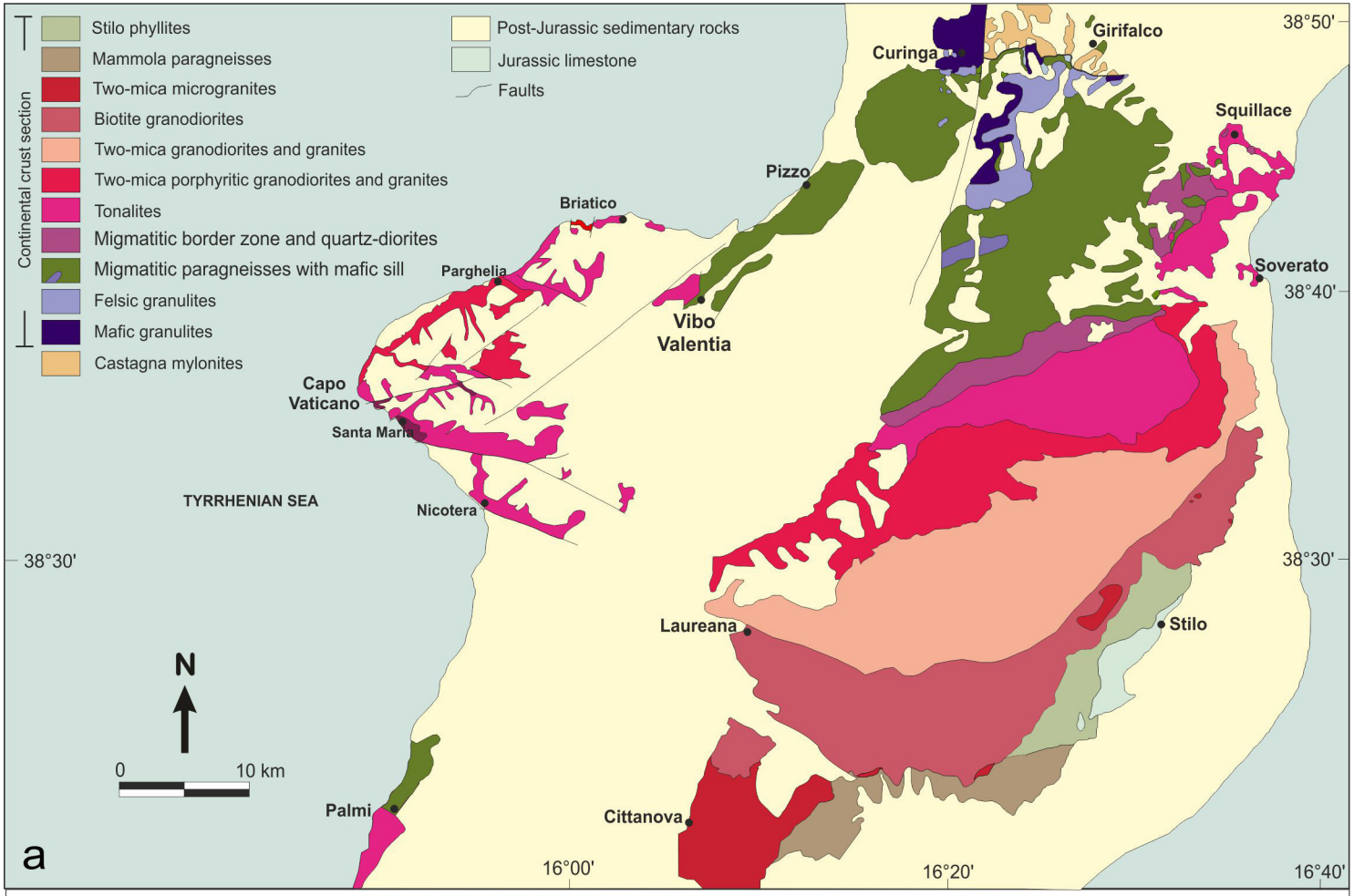

ultramafic rocks (spinel peridotites, pyroxenites, and hornblendites), and minor fine-grained metapelites and metacarbonates. These are overlain by a Migmatite Metapelite Unit (aka Metapelite Unit, Schenk, 1980, 1984) of 5–6 km overall thickness, dominated by migmatitic paragneisses with minor felsic granulites, widespread intercalated metabasites up to some hundreds of metres thick and rare marbles. Cm- to dm-thick leucosomes of dominant dioritic composition occur in the metabasic rocks; leucosomes may be isoclinally folded or discordant to the main foliation. Concordant and discordant leucosomes also occur in the metasediment-derived felsic granulites and metapelitic migmatites. Tonalitic–trondhjemitic dykes, dm- to m-thick, locally intrude the metagabbro complex (Rizzo et

Fig. 3 - (a) Geological sketch-map of Serre Massif, Capo Vaticano Promontory and Palmi-Bagnara area in southern Calabria, with distribution of the main metamorphic and plutonic rock types (modified after Russo, 2023, and references therein); (b) schematic geological section through the Serre Massif (after Fiannacca et al., 2015, and references therein).

https://doi.org/10.3301/GFT.2024.09

al., 2005), while a quartz monzogabbro-monzodiorite dyke with a thickness of ~ 250 m occurs in the overlying Migmatite Metapelite Unit (Schenk, 1984, Fornelli et al., 2011).

The mafic granulites from the base of the crustal section experienced multi-stage dehydration–decompression, passing from peak values of at least 1.1 GPa at 900 °C to ~ 0.7–0.8 GPa at 650–700 °C (Acquafredda et al., 2008; Fornelli et al., 2012, and references therein). Fig. 4a illustrates the P-T-t path proposed by Fornelli et al. (2018), based on previous thermobarometric and geochronological data from the same research team (Acquafredda et al., 2008; Fornelli et al., 2011, 2012, 2014; Duchene et al., 2013). The authors place the granulite metamorphic peak of 1.1 GPa and ~ 900 °C at ~ 347–340 Ma, with the peak assemblage consisting of garnet, clinopyroxene and orthopyroxene. Decompression at 0.8–0.9 GPa and 850 °C would be documented by Opx-Pl ± Am coronae formed between Cpx and Grt at 323–318 Ma; further decompression and cooling down to 0.7–0.8 GPa and 650–750 °C would have started at ~ 300 Ma and ended at ~ 280 Ma, producing Cpx-Pl-Am-Bt symplectic coronae around garnet porphyroblasts.

Phase equilibrium thermodynamic modelling of migmatitic metapelites from the base of the Migmatite Metapelite Unit by Festa et al. (2024) suggests that peak P-T conditions of 0.97 GPa and 800-840 °C, respectively, were achieved by isobaric heating starting at ~ 700 °C; according to the same authors a minimum of 30 vol% melt was extracted from the metapelites during the above heating event.

Finally, according to Fornelli et al. (2012) (Fig. 4b), the metapelites from the top of the Migmatite Metapelite Unit, experienced amphibolite facies metamorphism with thickening-related peak P conditions up to 0.9 GPa at ~ 650 °C, likely occurring earlier than 320 Ma, followed by nearly isobaric heating for about 20 Ma, up to peak T conditions of ~ 700 °C. The thermal peak at ~ 300 Ma was followed by slow exhumation, with the end of the Variscan decompression estimated at about 270 Ma, at T of ~ 600 °C. In agreement with the above results, both peak pressure and temperature values are considered to increase progressively from the top to the bottom of the crustal section, as confirmed by the regular development of mineral assemblages consistent with gradually deeper and hotter conditions (e.g., Schenk, 1984).

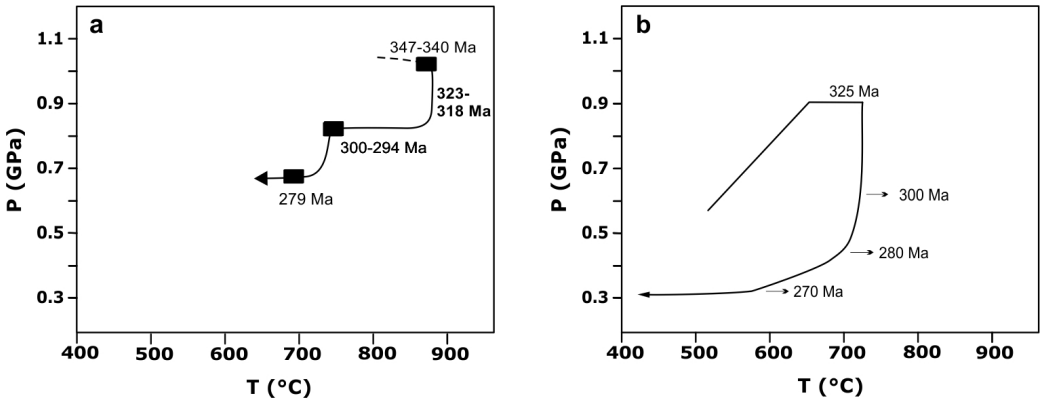

Fig. 4 - P-T paths for lower crustal rocks of the Serre Massif. (a) Metagabbros from the base of the crustal section (redrawn after Fornelli et al., 2018, and references therein); (b) metapelites from the top of the lower crustal section (redrawn after Fornelli et al., 2012, and references therein).

The Serre Batholith

The intermediate portion of the crustal section consists of the late Variscan plutonic rocks of the Serre Batholith (Rottura et al., 1990, 1991; Del Moro et al., 1994; Fornelli et al., 1994; Caggianelli et al., 2000; Fiannacca et al., 2015), with an overall thickness of ~ 13 km. An entire

https://doi.org/10.3301/GFT.2024.09

cross-section of the batholith, from floor to roof, is exposed in the Serre Massif (e.g., Russo et al., 2023), while only the deepest and deep-intermediate granitoid units crop out in the Palmi-Bagnara area and the Capo Vaticano Promontory, respectively.

Although the Serre plutonic rocks are collectively referred to as mid-crustal granitoids, they were emplaced at depths between ~ 23 and 6 km (~ 0.65 to 0.17 GPa; Caggianelli et al., 1997). Specifically, strongly to weakly foliated tonalites and minor quartz diorite were first intruded at deep structural levels, producing a migmatitic border zone in the lower crustal metapelitic host rocks (Rottura et al., 1990; Clarke and Rottura, 1994). Russo et al. (2023) grouped the tonalites and minor quartz diorites of the Serre Massif in two separate granitoid units, namely Amphibole-Biotite Tonalites (ABT) and Biotite Tonalites (BT), noting that both granitoids can occur at the batholith floor but, where present, the ABT lie beneath the BT; the same authors also mapped the distribution in the Serre Massif of the more and less foliated ABT and BT granitoids (Fig. 5).

Apart from the presence or absence of amphibole (hornblende ± cummingtonite; e.g., Rottura et al., 1990, 1991; Lombardo, 2020), more common in the ABT quartz diorites than in the tonalites, the typical mineral assemblage in both ABT and BT is Pl + Qtz + Bt + Ep + Aln + Spn + Ilm + Ap + Zrc (mineral abbreviations after Whitney and Evans, 2010).

Swarms of variably flattened and elongated mafic microgranular enclaves (MME) with quartz dioritic, quartz monzodioritic and tonalitic composition, commonly occur in both ABT and BT, being more abundant in the deeper levels of the units. They are typically decimetric in size, but MMEs up to more than 1 metre in size, locally occur.

The overlying deep-intermediate level granitoids are predominantly porphyritic two-mica granodiorites and monzogranites (PMBG) (Rottura et al., 1991; Del Moro et al.,1994; Fiannacca et al. 2015; Lombardo et al., 2020; Russo et al., 2023), characterised by K-feldspar megacrysts up to ~ 12 cm long.

The uppermost granitoids, representing the shallowest intrusions (Fornelli et al., 1994; Fiannacca et al., 2015, 2021; Russo et al., 2023) and cropping out exclusively in the Serre Massif, are two-mica equigranular granodiorites and granites (MBG), passing upward to biotite ± amphibole weakly peraluminous granodiorites (BG). These dominantly unfoliated granodiorites were the last granitoids to emplace, producing contact aureoles in the low- to medium-grade metamorphic host rocks of the upper crust (e.g., Angì et al., 2010; Festa et al., 2013, 2018).

Typical mineral assemblages are:

Qtz + Pl + Kfs + Bt + Ms + Ilm + Ap + Zrc + Mnz ± Sill ± Grt ± Crd	in the PMBG
Qtz + Pl + Kfs + Bt + Ms + Ap + Ilm + Zrc + Mnz	in the MBG
Qtz + Pl + Kfs + Bt ± Am + Ilm + Ap + Zrc + Aln + Spn + Ep	in the BG

MME up to ~ 50 cm in size only occur in the BG, with a typical rounded shape and quartz monzodioritic or tonalitic composition. BG also contain cm-size metabasic and rarer metapelitic enclaves, whereas only the latter occur in the two-mica granitoids. Fornelli (1994) considered the occurrence of the different types of enclaves, together with their petrographic and mineral chemical features as possible evidence of melting of heterogeneous crust or mixing between mantle- and crust-derived magmas, with the second hypothesis deemed more likely. PMBG show

https://doi.org/10.3301/GFT.2024.09

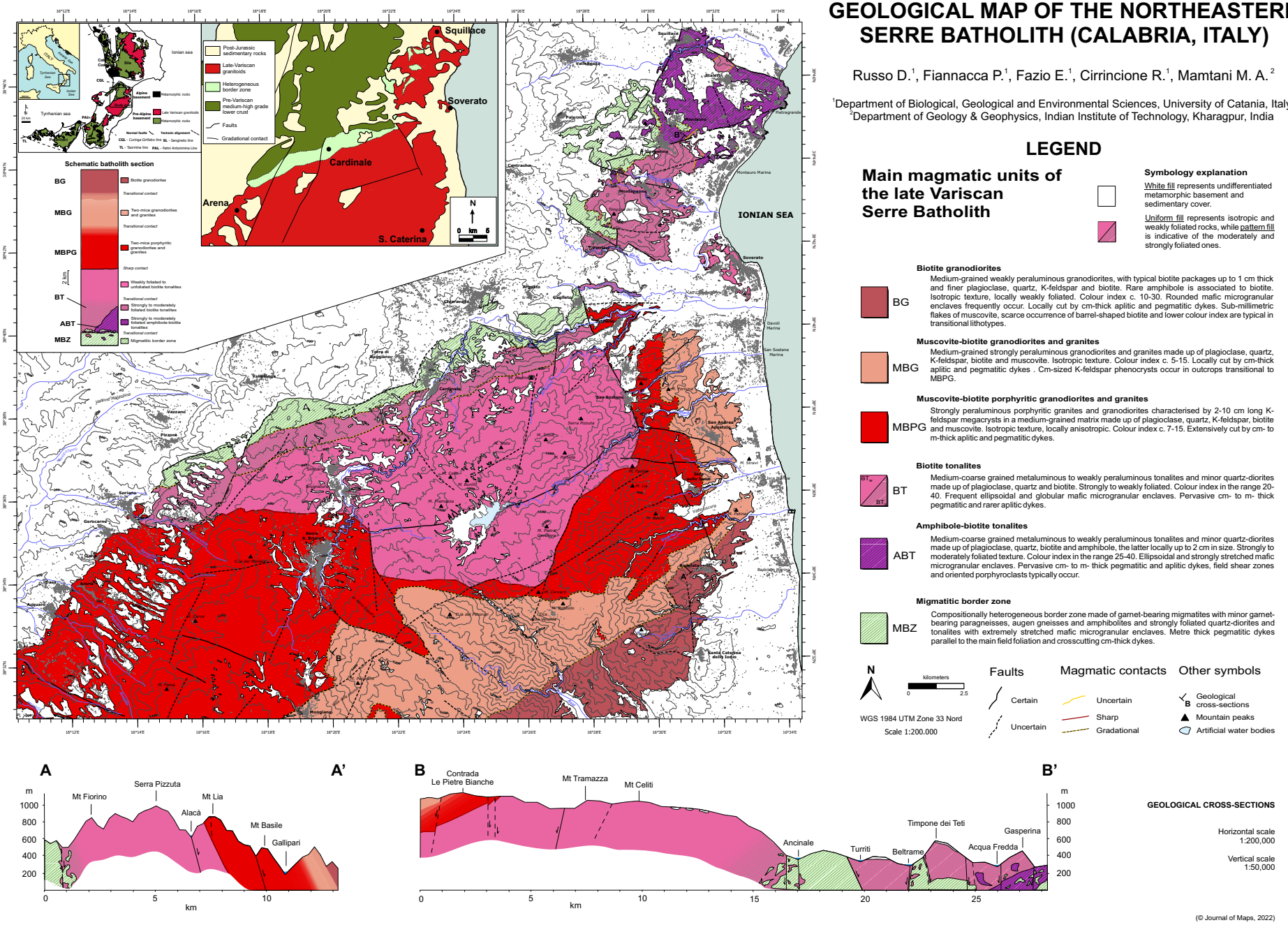

Fig. 5 - Geological map of the north-eastern Serre Batholith (after Russo et al., 2023).

https://doi.org/10.3301/GFT.2024.09

intrusive contacts with the underlying BT, with outcrops from the Capo Vaticano Promontory illustrating outstandingly the interaction between the granodioritic-granitic magma and the solidifying tonalitic mush.

On the other hand, Russo et al. (2023) report gradational contacts between the PMBG and the overlying MBG, as well as between the MBG and the overlying BG, resulting in the formation of transitional rocks over bands wide up to 500 m for the PMBG-MBG transition, and up to 1.5 km for the MBG-BG transition. A detailed description of the field, petrographic and general microstructural features of the granitoids from the Serre Massif is provided in Russo et al. (2023), while an outline of the above features is given in Figs. 6-10.

Zircon SHRIMP U-Pb and isotope oxygen investigations by Fiannacca et al. (2017, and references therein), aimed at constraining the construction ages and mechanisms of the different levels of the batholith, indicate ~ 297 Ma for the emplacement of the deep-seated quartz diorites-tonalites, ~ 295 for the upper-intermediate strongly peraluminous granodiorites and granites and, finally, ~ 292 Ma for the upper crustal granodiorites. These results indicate that the Serre Batholith may have developed over a relatively short time of about 5 Ma and, anyway, not greater than 9 Ma.

Microstructural studies on the Serre Batholith granitoids (Acquafredda et al., 1995; Caggianelli et al., 1997, 2000; Fiannacca et al., 2021) have documented that all the granitoid rocks experienced deformation

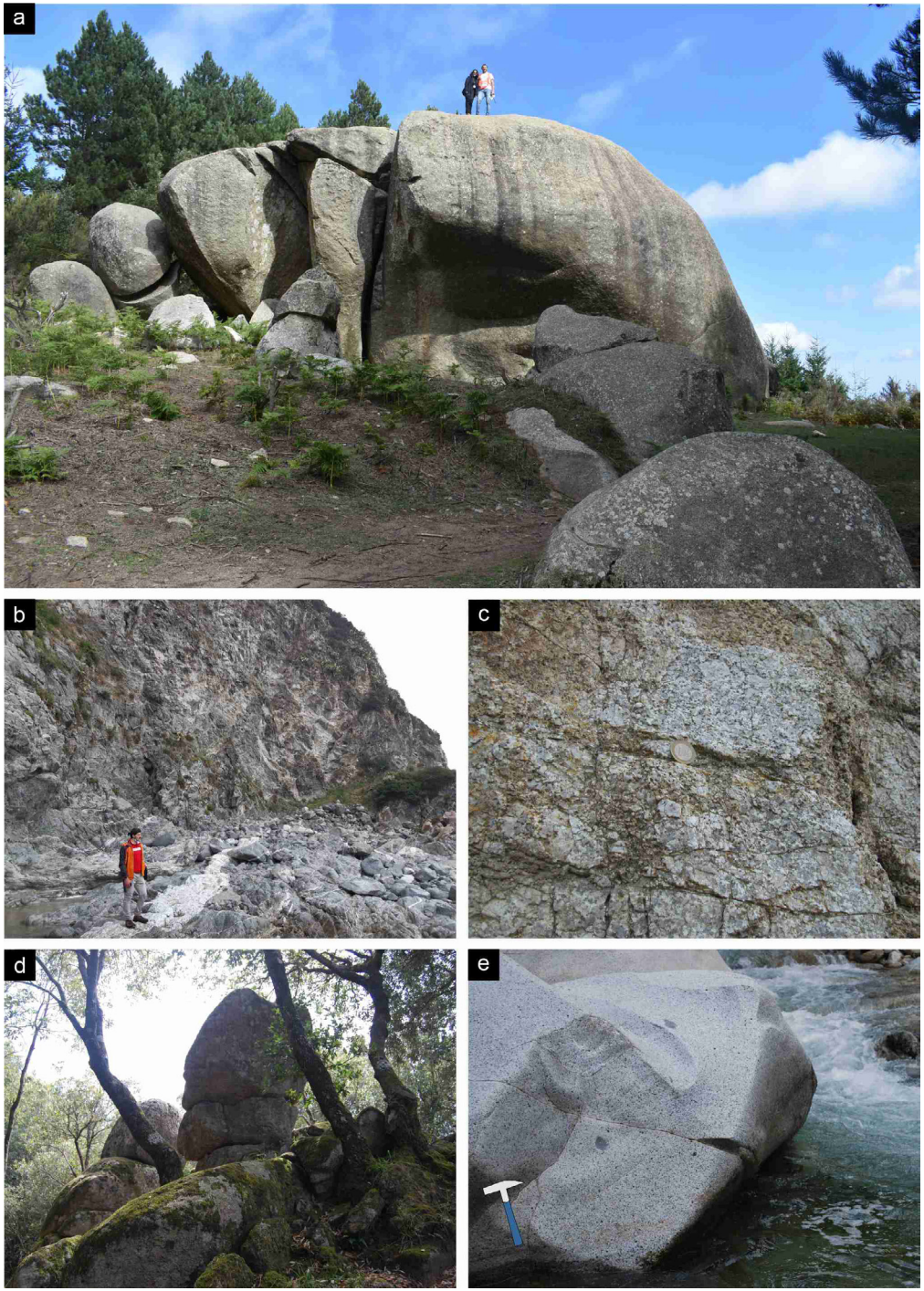

Fig. 6 - Selected granitoid outcrops from different levels of the north-eastern Serre Batholith (after Russo et al., 2023). (a) Monolith of deep-seated biotite tonalites (BT). (b) Cliff and pavement outcrop of amphibole-biotite tonalites (ABT) from the batholith floor, pervasively intruded by swarms of dm-to m-thick pegmatite dykes. (c) Outcrop of porphyritic two-mica granodiorites and granites (PMBG) from the deep-intermediate levels, with K-feldspar megacrysts up to 3 cm long. (d) Tors of equigranular two-mica granodiorites and granites (MBG) from the intermediate-upper crustal levels. (e) Riverbank exposure of biotite granodiorites (BG) from the batholith roof.

https://doi.org/10.3301/GFT.2024.09

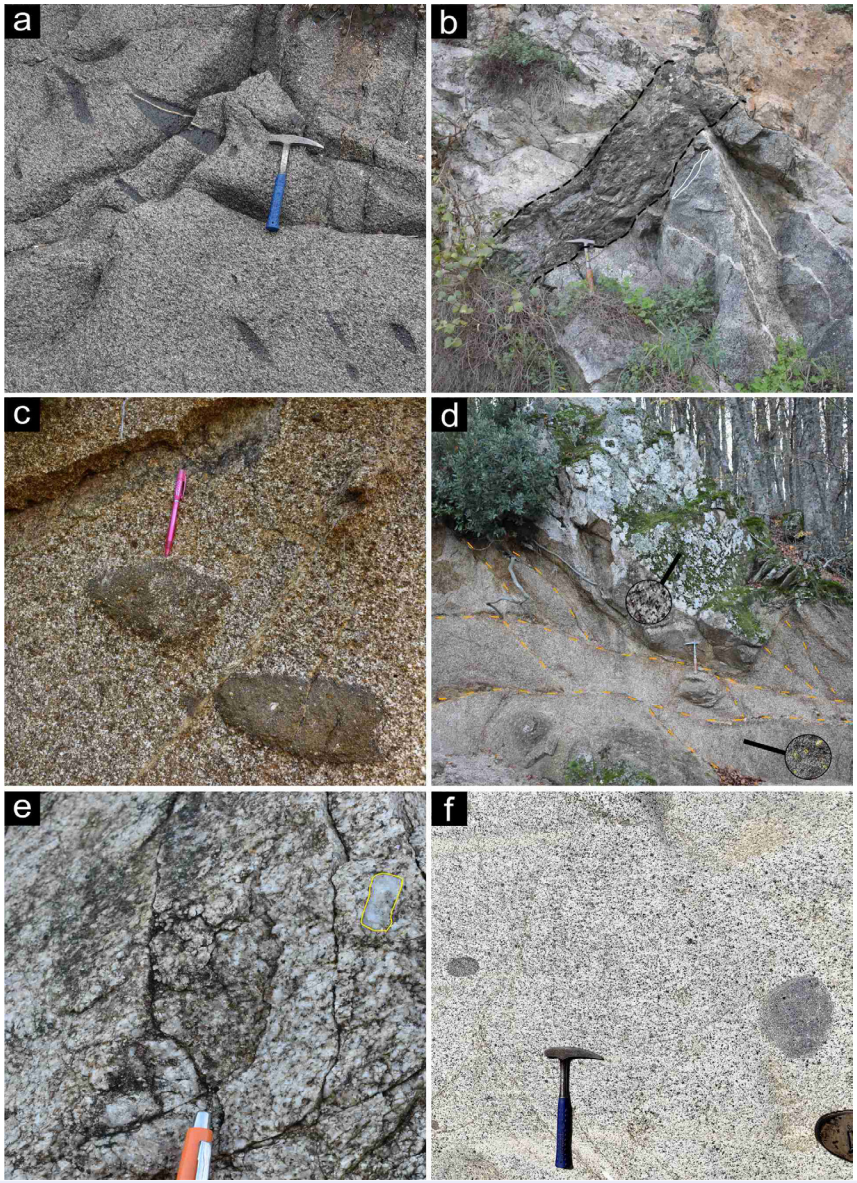

Fig. 7 - Outcrop-scale features of granitoids from north-eastern Serre Batholith (after Russo et al., 2023). (a) Swarm of stretched mafic microgranular enclaves in ABT. (b) ABT cut by discordant aplitic dykelets and 30 cm-thick shear zone parallel to tonalite foliation, also marked by flattened enclaves. (c) Slightly flattened mafic microgranular enclaves in unfoliated BT. (d) three-metre-sized tonalite block within PMBG from the BT-PMBG transition zone. PMBGs are crossed by a narrow shear zone system. (e) Outcrop of transitional MBG from the PMBG-MBG transition zone. (f) Globular MMEs in BG.

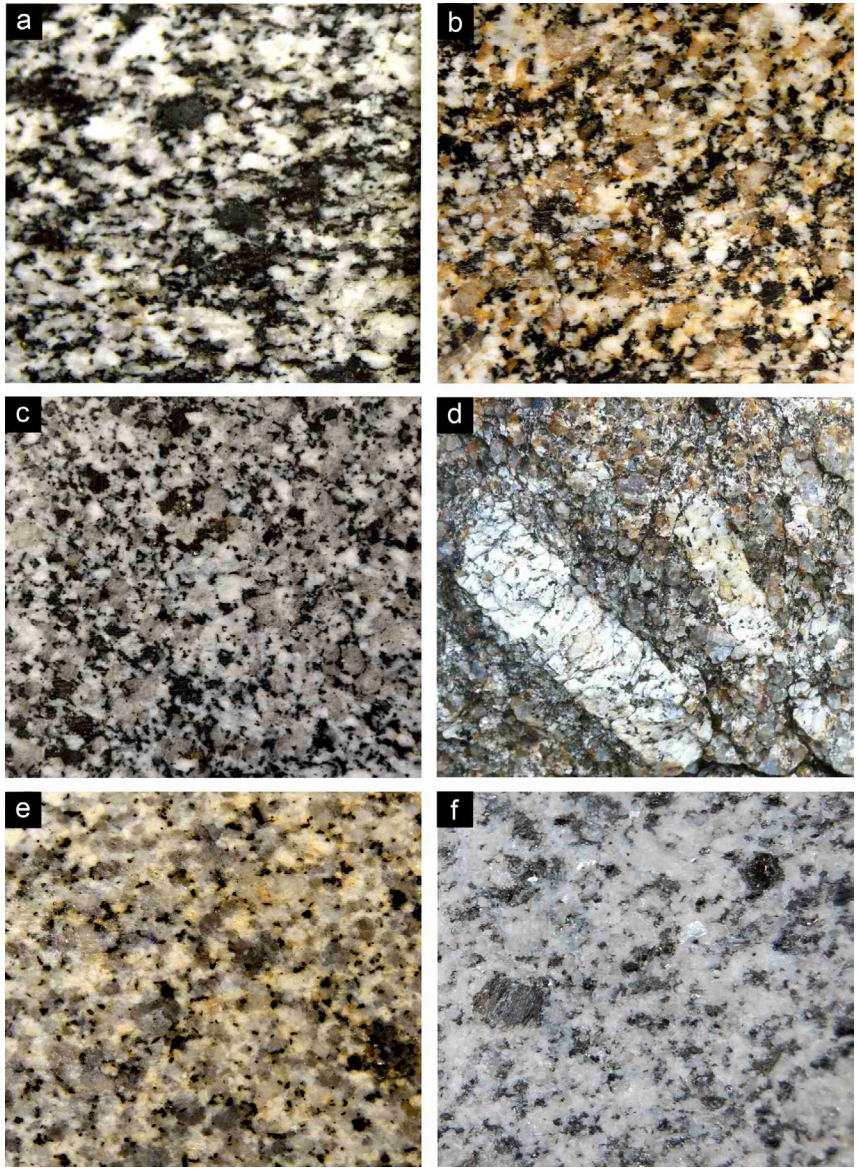

Fig. 8 - Mesoscopic comparison of floor (a) to roof (f) granitoids from the north-eastern Serre Batholith (after Russo et al., 2023). (a) Strongly foliated ABT. (b) Weakly foliated BT. (c) Unfoliated BT. (d) Roughly iso-oriented K-feldspar megacrysts in PMBG. (e) Unfoliated MBG. (f) Unfoliated BG. The long side measures 6 cm in all photos.

https://doi.org/10.3301/GFT.2024.09

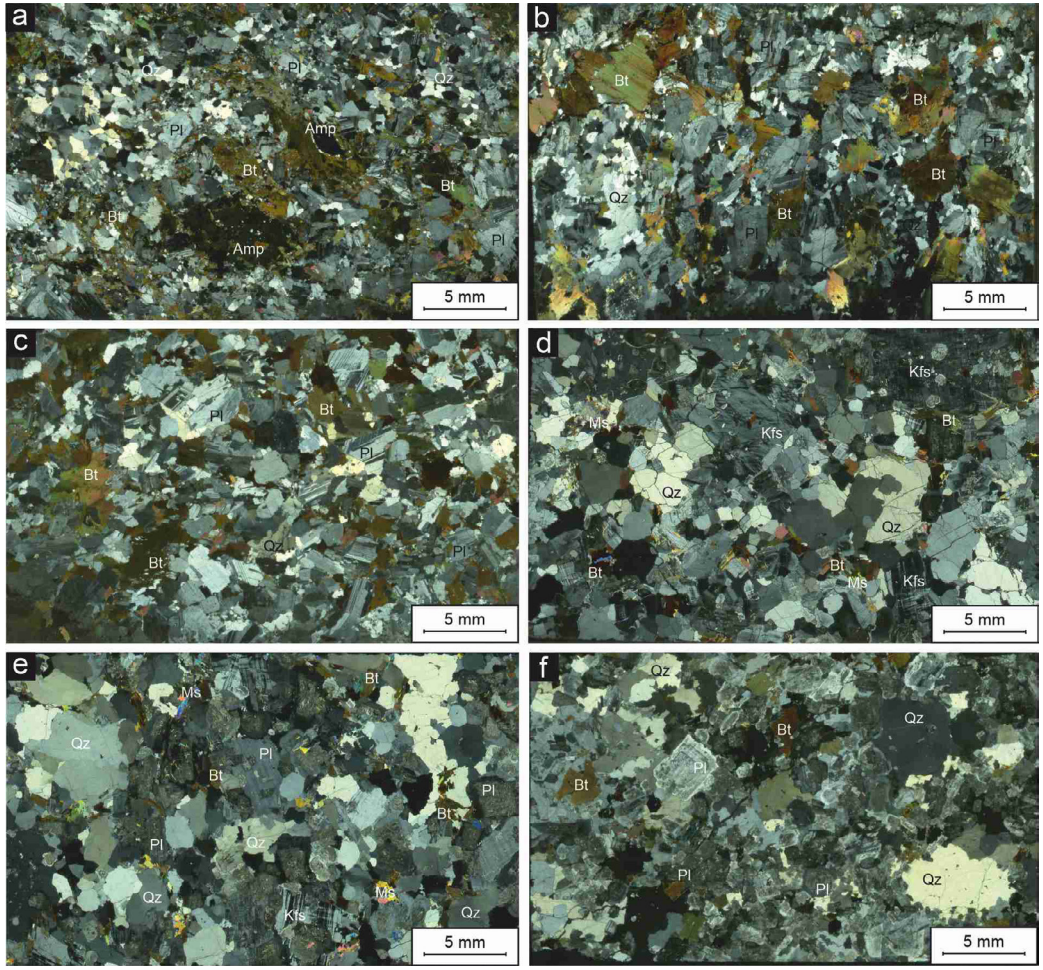

▲ Fig. 9 -Microscopic (crossed polar) comparison of floor (a) to roof (f) granitoids from the northeastern Serre Batholith (after Russo et al., 2023). (a) Strongly foliated ABT. (b) Moderately foliated BT. (c) Weakly foliated BT. (d) Unfoliated PMBG matrix. (e) Unfoliated MBG. (f) Unfoliated BG.

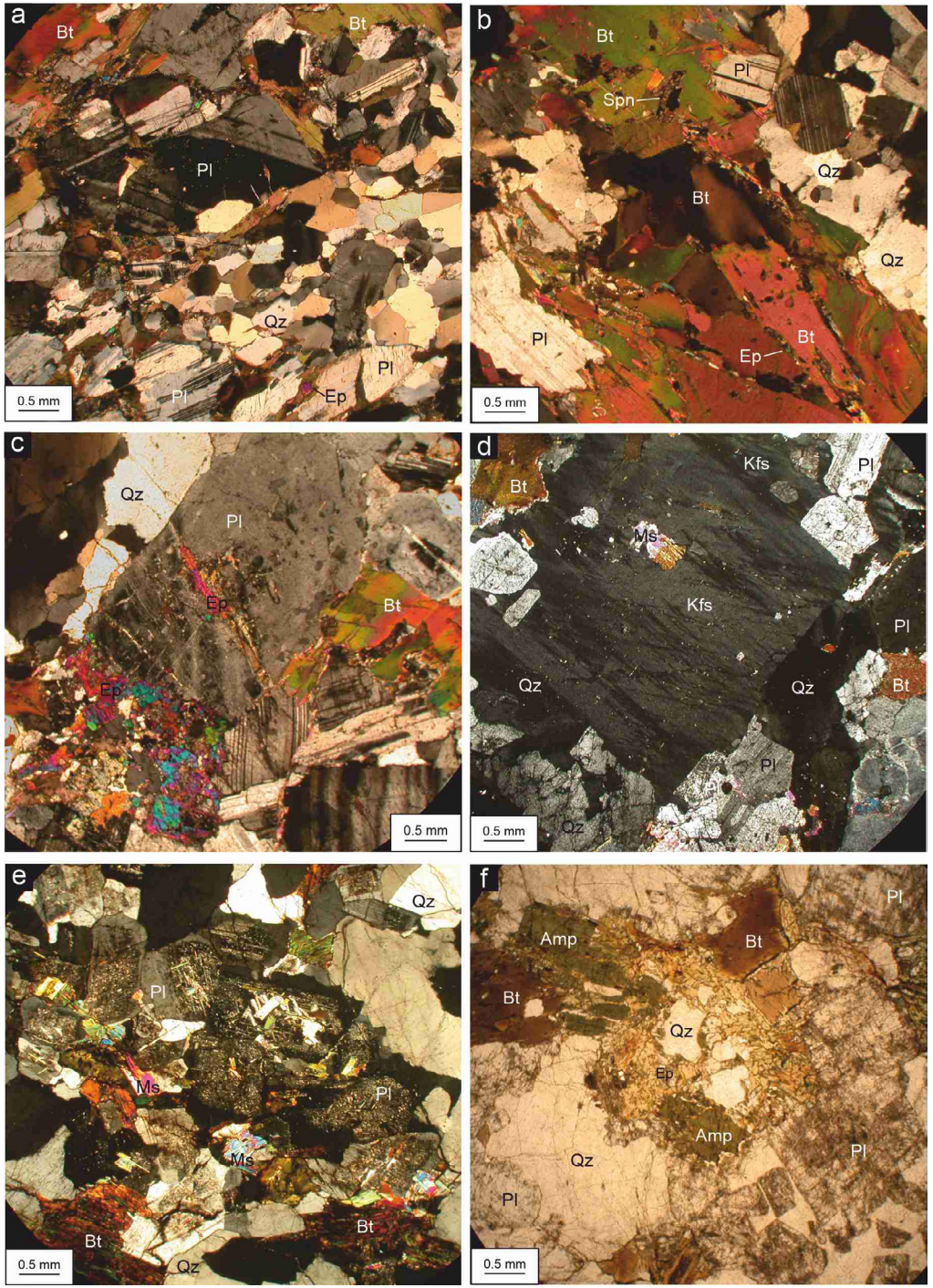

▶ Fig. 10 - Selected representative petrographic features of floor to roof granitoids from north-eastern Serre Batholith (after Russo et al., 2023). (crossed polar except Fig 5f). (a) Oriented fabric defined by alignment of subhedral plagioclase crystals, polygonal quartz aggregates and stretched biotite plates in ABT. (b) Iso-oriented biotite and plagioclase in foliated BT. (c) Submagmatic fracture filled with biotite and epidote in plagioclase from foliated BT. (d) Euhedral microcline from the medium-fine grained matrix of PMBG. (e) Two-mica assemblage in MBG. (f) Partially replaced amphibole in BG.

https://doi.org/10.3301/GFT.2024.09

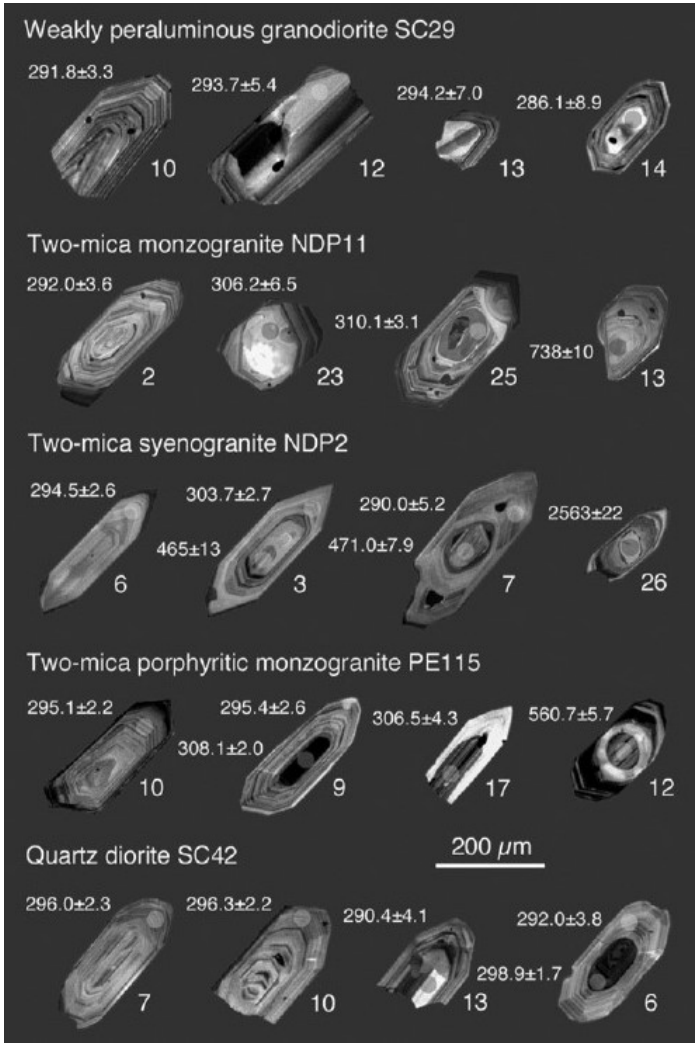

Fig. 11 - Cathodoluminescence images of representative zircon crystals from the main granitoid units of the Serre Batholith. Uncertainties in the spot dates is 1σ (after Fiannacca et al., 2017).

at decreasing temperatures from submagmatic to low-temperature subsolidus conditions; in particular, Fiannacca et al. (2021) showed that even the shallower, younger and apparently isotropic MBG and BG, exhibit widespread deformation microstructures. In addition, despite the deformation experienced by the shallow-seated granitoids resulted only very locally in the development of an oriented fabric at the meso/microscale, AMS (Anisotropy of Magnetic Susceptibility) investigations by Fiannacca et al. (2021) indicate that both MBG and BG rocks are characterised by an internal magnetic fabric; this, in association with the local occurrence of field and microstructural evidence for shear-related deformation, might support the idea that the emplacement of the shallow-seated Serre granitoids was influenced by shear zone activity, in a likely waning stage.

Magma emplacement along ductile shear zones in a likely extensional regime (Rottura et al., 1990; Caggianelli et al., 2007; Angì et al., 2010) has long been envisaged for the Serre Batholith granitoids, also based on the strong oriented fabric in the deepest and oldest magmatic units (ABT-BT). In more detail, Angì et al. (2010) proposed that the present-day upper crustal host paragneiss rocks of the BG (Mammola paragneisses, Fig. 3), after achieving baric peak conditions of 0.9 GPa during collision-related thickening, were quickly exhumed through a shear zone operating in a mainly extensional regime (more details in the following "Upper crust section"). Furthermore, as suggested by Rottura et al. (1990) and Langone et al. (2014) and confirmed in more detail by Fiannacca et al. (2017), the construction of the batholith took place via a mechanism of overaccretion. Specifically, according to the latter authors, partial melting conditions were reached, at different times, in specific lower crustal sources, which generated magmas whose emplacement depth was then strongly influenced by the presence of the previously intruded granitoid bodies.

In fact, an origin by exclusive intracrustal melting of pre-existing continental crust has been proposed by Fiannacca et al. (2015) for all the main granitoid units, partly similar to Rottura et al. (1990) and Del Moro et al. (1994), and differing from other previous interpretations invoking a possible origin by contamination and/or mixing of mantle-derived magmas with crustal components (e.g., Rottura et al., 1991; Del Moro et al., 1994; Fornelli et al., 1994). In more detail, Rottura et al. (1991), tentatively propose that the strongly peraluminous porphyritic granitoids (PMBG) from Capo Vaticano Promontory derived from mixing between two distinct felsic melts, one of crustal origin and the other derived from tonalitic magma through fractional crystallisation or assimilation-fractional crystallisation; the

https://doi.org/10.3301/GFT.2024.09

tonalites, in turn, were possibly produced by interaction of mantle-derived magmas with large volumes of crustal material similar to the PMBG. The same authors conclude by highlighting the difficulty of working out simple petrogenetic models accounting for all petrological, isotopic and geochemical data of the CVP granitoids. Del Moro et al. (1994), indicate that the origin of strongly peraluminous K-feldspar megacryst granitoids from the Serre Massif could be explained either with a complex history of deep crustal modification of a mantle-derived magma or by partial melting of a compositionally heterogeneous deep crust. Finally, Fornelli et al. (1994) suggested for the MBG and BG an origin by contamination and/or mixing of mantle-derived magmas with crustal components; the evolution from the more mafic BAG to the BMG would have occurred by combined mixing and fractional crystallisation. A comprehensive review of the geochemical features of the Serre granitoids and of the previous petrogenetic interpretations is reported in Fiannacca et al. (2015). The main results of the above study are synthetically reported in the following. As already mentioned, the Serre Batholith displays a wide diversity, ranging from quartz diorites and very rare quartz gabbros to tonalites, granodiorites and monzogranites, with minor syenogranites and including a distinct group of leucotonalites, characterised by high Q values in the following Fig. 12. All rock types crop out in the Serre Massif, while MBG and BG are absent in the Capo Vaticano Promontory, where only the deep-intermediate levels of the batholith are exposed.

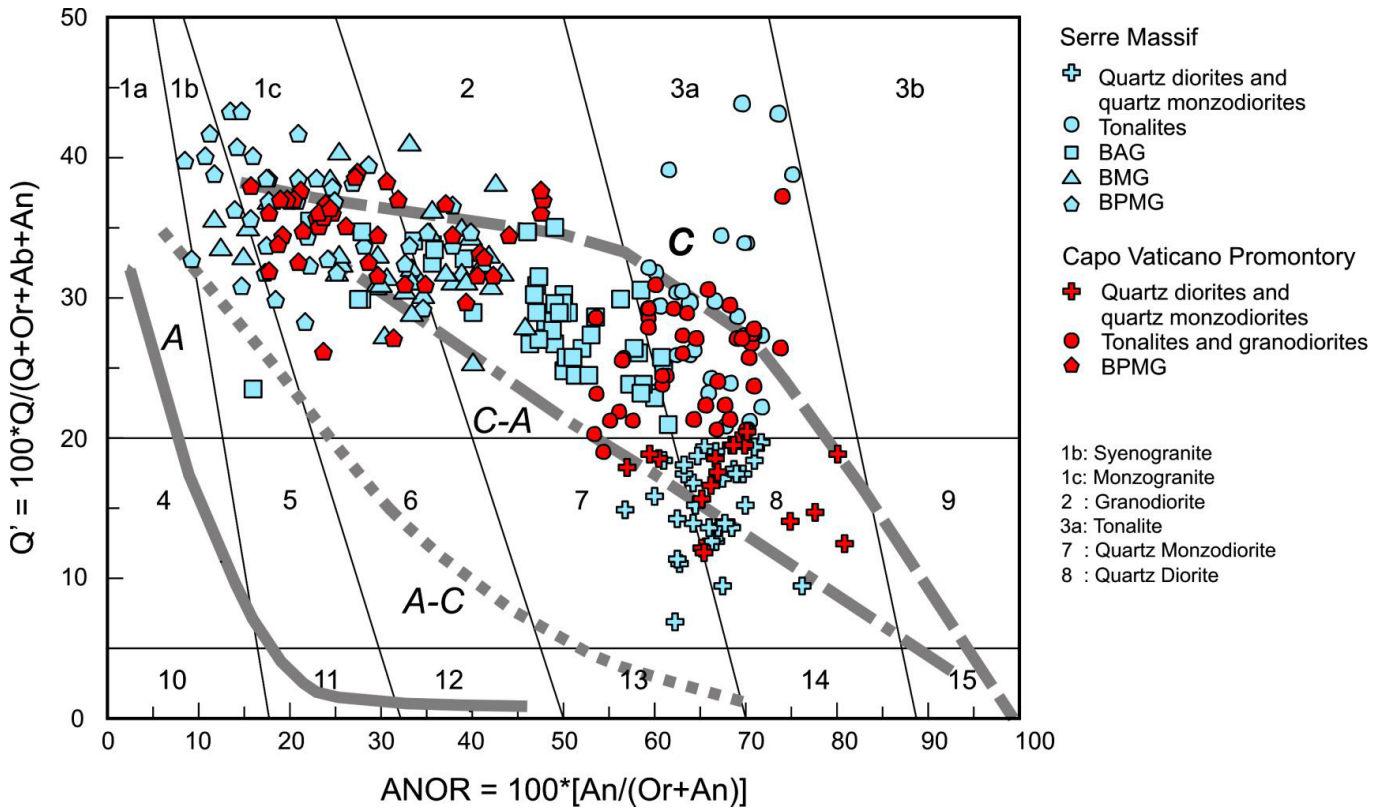

Fig. 12 - Q'-ANOR classification (after Streckeisen and Le Maitre, 1979) for the Serre Batholith granitoids. Compositional trends are from Whalen and Frost (2013). Series: C, calcic; C-A, calc-alkalic; A-C, alkali-calcic; A, alkalic. Sources of geochemical data are reported in Fiannacca et al. (2015).

The Serre Batholith granitoids are dominantly magnesian and calcic to calc-alkalic, with only some of the more evolved PMBG and MBG samples from the Serre Massif showing a ferroan calc-alkalic to alkali-calcic composition (Fig. 13). Comparison with typical examples of granitoid suites indicates a strong general similarity with Cordilleran granitoids. No specific information in terms of affinity of the Serre Batholith rocks with I- and S-type granites (Chappell and White, 1974, 2001) emerges from the Fe-

https://doi.org/10.3301/GFT.2024.09

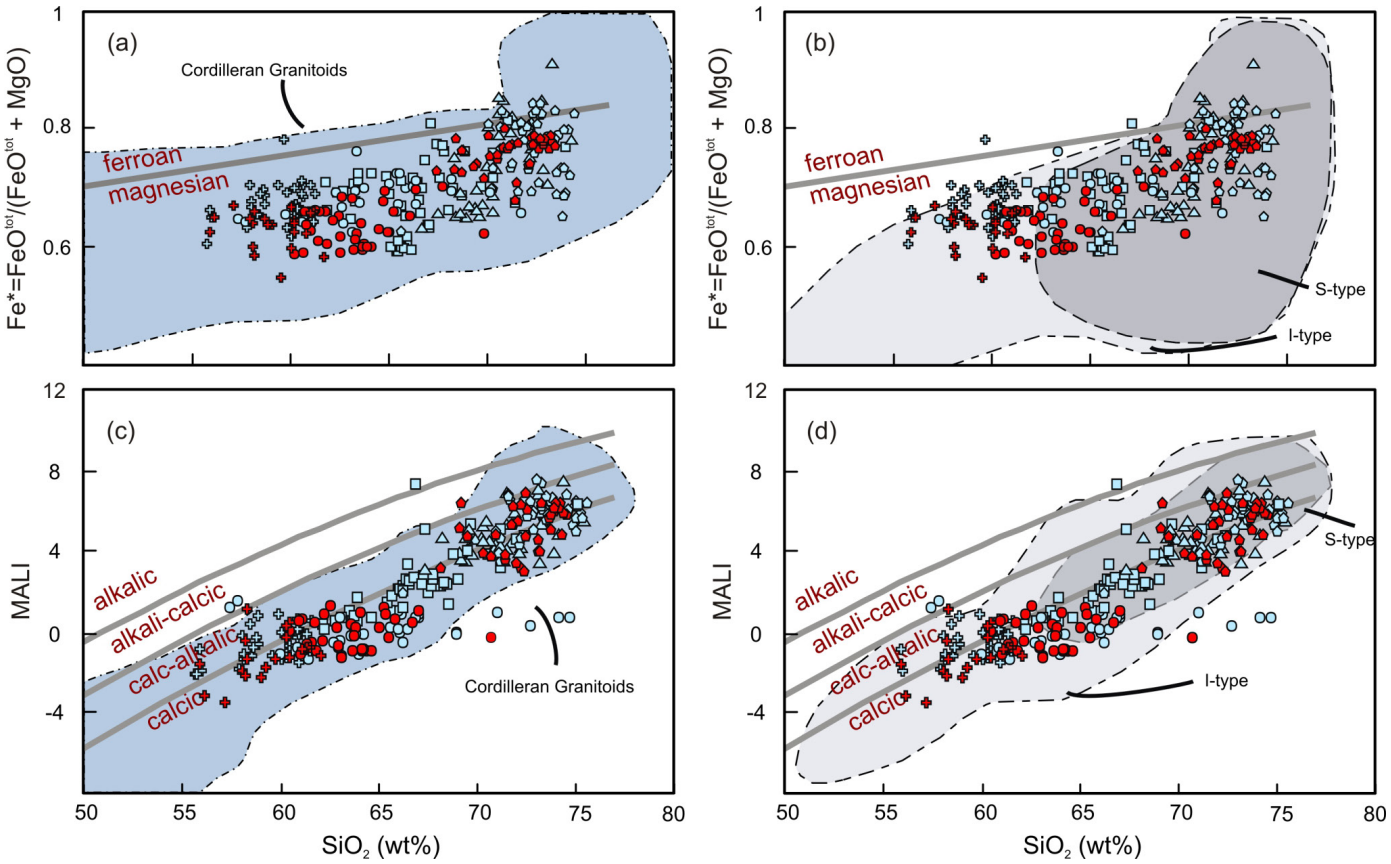

Fig. 13 - Classification of the Serre Batholith granitoids according to Frost et al. (2001), and Frost and Frost (2008), after Fiannacca et al. (2015). (a, b) $FeO_{tot}/(FeO_{tot}+MgO)$ vs. SiO2 diagram and (c, d) Na_2O+K_2O-CaO vs. SiO_2 diagram. Fields of Cordilleran and I-S type granites are from Frost et al. (2001). Symbols as in Fig. 12.

number and MALI vs. SiO_2 diagrams, since the granitoids with SiO_2> 63 wt. % plot in a field where both granite types overlap; on the other hand, Fig. 13 illustrates the basic assumption that rocks with SiO_2 < 63 wt. %, including all the quartz diorites and many tonalites, cannot be S-types except for some garnet- or biotite-rich cumulates (Chappell and White, 2001).

Quartz diorites and tonalites are metaluminous to weakly peraluminous, while granodiorites and granites are weakly to strongly peraluminous, with the two-mica porphyritic granitoids being the only population with a marked strongly peraluminous character (ASI > 1.1).

According to Fiannacca et al. (2015), major, trace element and Sr-Nd isotopic compositions are consistent with a dominant crustal origin of the Serre Batholith. In particular, initial $^{87}Sr/^{86}Sr$ ratios ≥0.710 and εNd values lower than –6 for the great majority of the granitoids indicate the involvement of old crustal components (Fig. 14a). In addition, the vertical εNd array observed in the εNd vs. $(^{87}Sr/^{86}Sr)_i$ diagram is difficult to reconcile with mixing processes between mantle and crustal magmas, which should generate curved trends. Furthermore, no variation trends linking enriched mantle compositions to the plutonic rocks in terms of $(^{87}Sr/^{86}Sr)_i$ and εNd vs. elements such as SiO_2, CaO and MgO + FeO_T can be observed (Fig. 14). Even the Sr-Nd isotopic features of mafic rocks such as the quartz diorites match those of the basement beneath the batholith, being particularly similar to those of the mafic granulites. Some possible mixing trend is only observed for the central Serre granitoids (Fornelli et al., 1994), whose εNd values become progressively more negative from the less silicic BAG to the more silicic BMG. On the other hand, Fiannacca et al. (2016a) documented that plagioclase disequilibrium features indicative of magma mixings, such as resorption surfaces,

https://doi.org/10.3301/GFT.2024.09

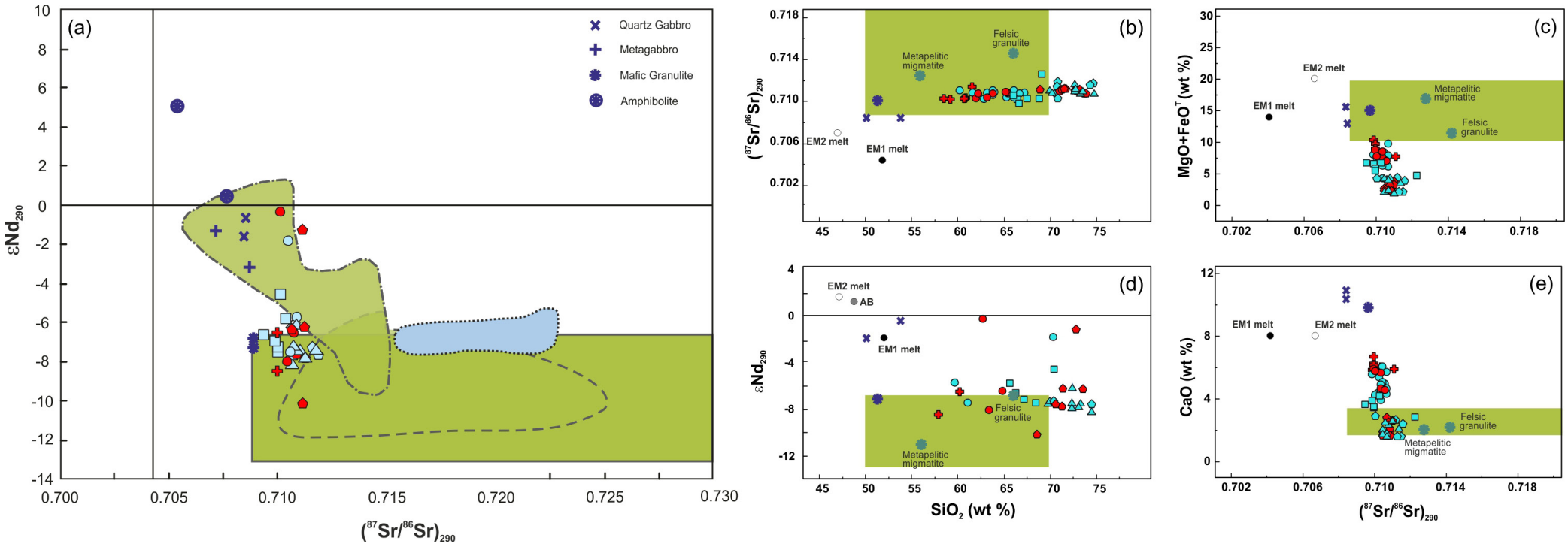

Fig. 14 - Sr-Nd isotopic features of the Serre Batholith, modified after Fiannacca et al. (2015), with the sources of all the plotted data reported in the same article. (a) εNd_{290} vs. $(^{87}Sr/^{88}Sr)_{290}$ diagram for the studied granitoids and CPO basement rocks; (b) Isotope-element correlation diagrams. Compositional range of Serre metasedimentary lower crust and average compositions of lower crustal metaigneous and metasedimentary rocks after Caggianelli et al. (1991). Compositions of enriched mantle EM1 and EM2 and average continental alkali basalt (AB) after Clemens et al. (2009). Symbols as in Fig. 12.

patchy zoning and reverse zoning are exclusive of the BMG proximal to the BG, in line with the gradational contact between the two magmatic units described in detail by Russo et al. (2023); in both BMG and BG far from the contact, plagioclase with equilibrium microstructures and distinct compositions associated no or weak normal zoning, suggests an independent origin and an undisturbed crystallisation in closed magmatic systems.

A dominant origin from the assembling of several batches of magmas with specific compositions derived by fluid-absent melting of different crustal sources is therefore proposed by Fiannacca et al. (2015, and references therein), as also supported by the different trends displayed by the different granitoid units shown in Fig. 15. According to the above authors, quartz diorites and tonalites (ABT-BT) derived from metabasaltic magma sources, whereas metagraywackes with various mafic and pelitic contents have been considered the most likely sources of strongly peraluminous granodiorites and granites (MBG) and weakly peraluminous granodiorites (BG). Actually, the latter granodiorites have compositions consistent with derivation from both mafic-intermediate metaigneous sources, or immature greywackes deposited after

https://doi.org/10.3301/GFT.2024.09

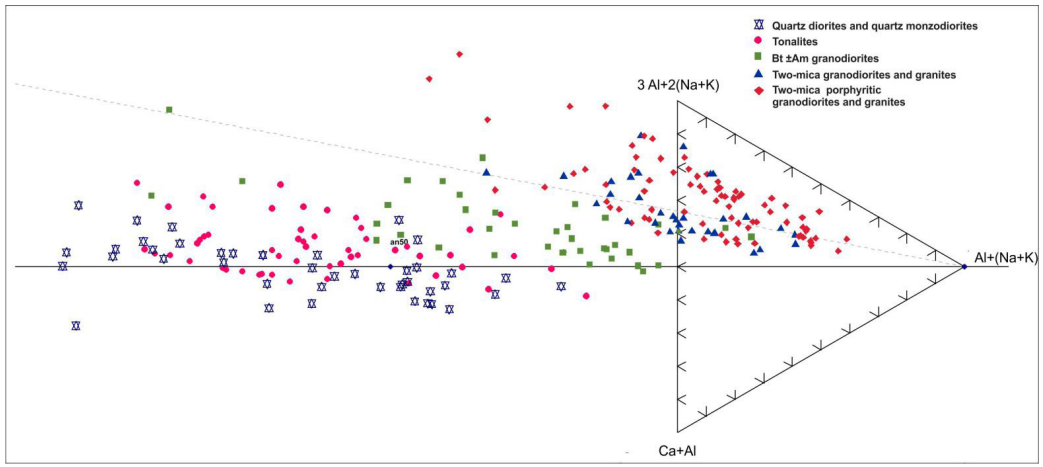

Fig. 15 - Compositions of the different granitoid rocks from the Serre Batholith projected from biotite onto the Ca+Al–3Al+2(Na+K)–Al+(Na+K) plane (after Moyen et al., 2017, and references therein). Different slopes in the trends correspond to different crustal source rocks.

the rapid dismantling of those igneous rocks. Two-mica porphyritic granites (PMBG) are the only rock types which appear to represent pure crustal melts, resulting from the melting of mafic pelitic sources. The other granitoid compositions are too silica-poor and MgO + FeO_t rich to represent pure melts, and are likely to include other components, such as solid restitic/peritectic phases entrained from the magma source, or cumulus phases.

Despite it cannot be totally excluded that some of the more mafic granitoids may have had a mantle derivation, totally obscured by intense processes of crustal contamination, results from Fiannacca et al. (2015) suggest that mantle-derived magmas did not play a direct dominant role in the geochemical diversity of the Serre Batholith granitoids. According to the same authors, post-collisional granitoid magmatism in southern Calabria is likely not to have been associated with the generation of new continental crust, but with dominant intracrustal differentiation of pre-existing continental crust. For more details or alternative views, the readers are referred to the cited literature in this manuscript and in Fiannacca et al. (2015).

The upper crust

The uppermost crustal portion, exposed in the southern part of the Serre Massif, consists of two different metamorphic units that were tectonically juxtaposed along a low-angle surface before being intruded by the granitoids of the Serre Batholith (e.g., Colonna et al., 1973; Angì et al., 2010; Festa et al., 2013, 2018; Tursi et al., 2020): a lower-grade hanging wall unit and a higher-grade footwall unit. The Stilo Phyllite Unit, i.e., the hanging wall, consists of low greenschist–facies phyllites with minor marbles, quartzites and metavolcanic levels with protolith ages up to early Carboniferous (e.g., Acquafredda et al., 1994; Navas-Parejo et al., 2009). The Mammola Paragneiss Unit, i.e., the footwall, comprises dominant lower amphibolite-facies paragneisses and subordinate leucocratic gneisses and amphibolites. The upper crustal rocks are locally intruded by late- to post-Variscan felsic to mafic dykes (Romano et al., 2011, and references therein). According to Angì et al. (2010), Mammola paragneisses were involved in collision-related crustal thickening together with the lower crustal metapelitic migmatites reaching peak P–T conditions of 0.9 GPa at 530 °C (Fig. 16), but they were then detached from the lower-crustal metapelites before achieving thermal equilibrium and rapidly uplifted to upper crustal levels (up to ~ 0.3 GPa at 470 °C) along a major extensional shear zone that also assisted the emplacement of the granitoids.

https://doi.org/10.3301/GFT.2024.09

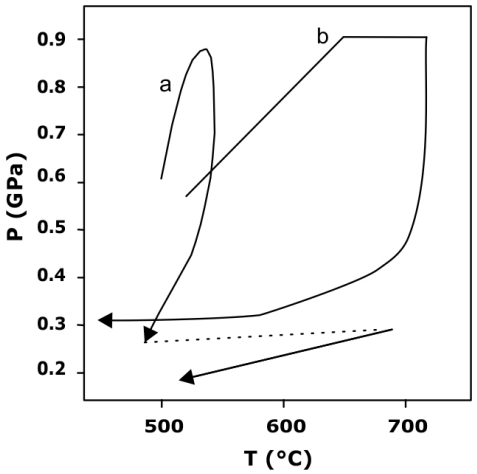

Fig. 16 - P-T path for the upper crustal Mammola paragneisses (a; redrawn after Angì et al., 2010), compared with the P-T path for the migmatitic paragneisses from the top of the lower crust (b, redrawn after Fornelli et al., 2012).

In this framework, Fiannacca et al. (2017) proposed that the Mammola paragneisses acted as the continuously uplifted lid of the Serre Batholith, accommodating the emplacement of the newly arriving magmas for most or all its accretion history. This interpretation would be supported by the matching of the decreasing pressures in the Mammola paragneisses with the progressively younger intrusion ages of the granitoids emplaced at progressively lower depths. During the last stages of batholith construction and concurrent waning stages of the shear zone activity, the Bt±Am granodiorites from the batholith roof were emplaced, suturing the tectonic contact between the two metamorphic units and producing late- to post-tectonic thermal metamorphism, as well as contractional deformation in the host rocks (Angì et al., 2010; Festa et al., 2013; 2018; Ortolano et al., 2022). In particular, according to Festa et al. (2013, 2018), the contractional events occurred in relation to the last growth increments of the Serre Batholith, producing a recumbent isoclinal syncline of regional extent. Thermal metamorphism is documented by static crystallisation of different porphyroblastic phases, based on rock composition and distance from the granitoids; for the Mammola paragneisses, a metamorphic peak at ~ 0.3 GPa and 685 °C was obtained by Angì et al. (2010) for the thermal metamorphism, followed by final exhumation and cooling to 0.15 GPa and T=500 °C (Fig. 16). Tursi et al. (2020) obtained a comparable P–T path, with cooling and exhumation from the orogenic metamorphic peak at ~ 0.9 GPa and 585 °C, to ~ 0.3 GPa and 440–470 °C, and subsequent thermal metamorphic cycle as in Angì et al. (2010). Tursi et al. (2020) propose that mylonitisation occurred already during the prograde evolution to deep-crustal conditions and continued during subsequent exhumation and final juxtaposition to the upper crustal Stilo–Pazzano phyllites. Furthermore, the above authors interpreted the obtained P-T path, including the difference in peak temperature between the Mammola paragneisses and the similarly deep-seated migmatitic metapelites, as due to the location of the Mammola unit in a Palaeotethys–Gondwana subduction complex, while both migmatitic metapelites and Stilo phyllites would have been part of the Laurussia upper plate. Finally, Fornelli et al. (2020) suggest that, in the same geodynamic context, the Stilo-Pazzano phyllites, i.e., the former sedimentary cover of the Palaeotethys and Gondwana passive margin, were tectonically accreted to Laurussia.

https://doi.org/10.3301/GFT.2024.09

DAY 1

THE DEEP VARISCAN CRUST

The most complete cross-section of the Calabrian lower continental crust is exposed in the northwestern sector of the Serre Massif, over an area of more than 400 km^2, and with an estimated thickness of ~ 7-8 km (Schenk, 1984).
We will start our field trip from the deepest part of the exposed crustal section, at the Turrino Quarry near Curinga, where metagabbros of debated protolith age and origin, equilibrated at a depth of ~ 35 km, crop out. Metagabbros are part of a Granulite Unit, ~ 3 km thick, mainly composed by felsic and mafic granulites with minor metacarbonates.
The next stop will be at one of the better-preserved outcrops of felsic granulites. We will then move upward to the overlying Migmatite Metapelite Unit, ~ 4 km thick, visiting two typical migmatite outcrops from the the top of the lower crustal sequence.

Stop 1.1 - Metagabbro from the bottom of the crustal section

Coordinates: Lat. 38°49'22" N, Long. 16°17'47" E
Location: Turrino quarry, Curinga

Turrino quarry (Fig. 17) provides the best exposure of the layered metagabbro complex forming the base of the lower crustal section. The thickness of the metagabbro complex exposed in the quarry is ~ 160 m. It is worth highlighting that the actual thickness of the whole metagabbro body is unknown, since the base of the crustal section is in tectonic contact with the underlying mylonitic Castagna Unit, so the exposed metagabbro might only represent the top of a much thicker body. The host rock at the metagabbro roof consists of felsic granulites of metasedimentary derivation, which can be locally observed as xenoliths, especially in the upper part of the quarry. The metagabbro complex, which also includes boudinaged layers and lenses of pyroxenites and peridotites, is locally intruded by coarse-grained to pegmatitic dykes with large biotite and minor garnet or pyroxene.
The main rock is a medium-coarse-grained two-pyroxene metagabbro (Fig. 18a-c; Fig. 19), commonly containing also green and brown amphibole; other varieties may also include biotite, K-feldspar and garnet, with compositions varying accordingly. The presence of garnet only in lighter-coloured rocks (Fig. 18b) from the upper part of the exposed sequence, where the garnet-bearing felsic granulites are more abundant, has been considered by Caggianelli et al. (2013) as evidence of contamination of the gabbroic magma by assimilation of the host metasedimentary rocks. The gabbro is usually well layered, with layers ranging in thickness from 1 cm to ~ 1 m (Fig. 18b-e); plagioclase-rich types, with plagioclase content up to ~ 80 % vol. and layering marked by pyroxene aggregates ± amphibole, dominate.

https://doi.org/10.3301/GFT.2024.09

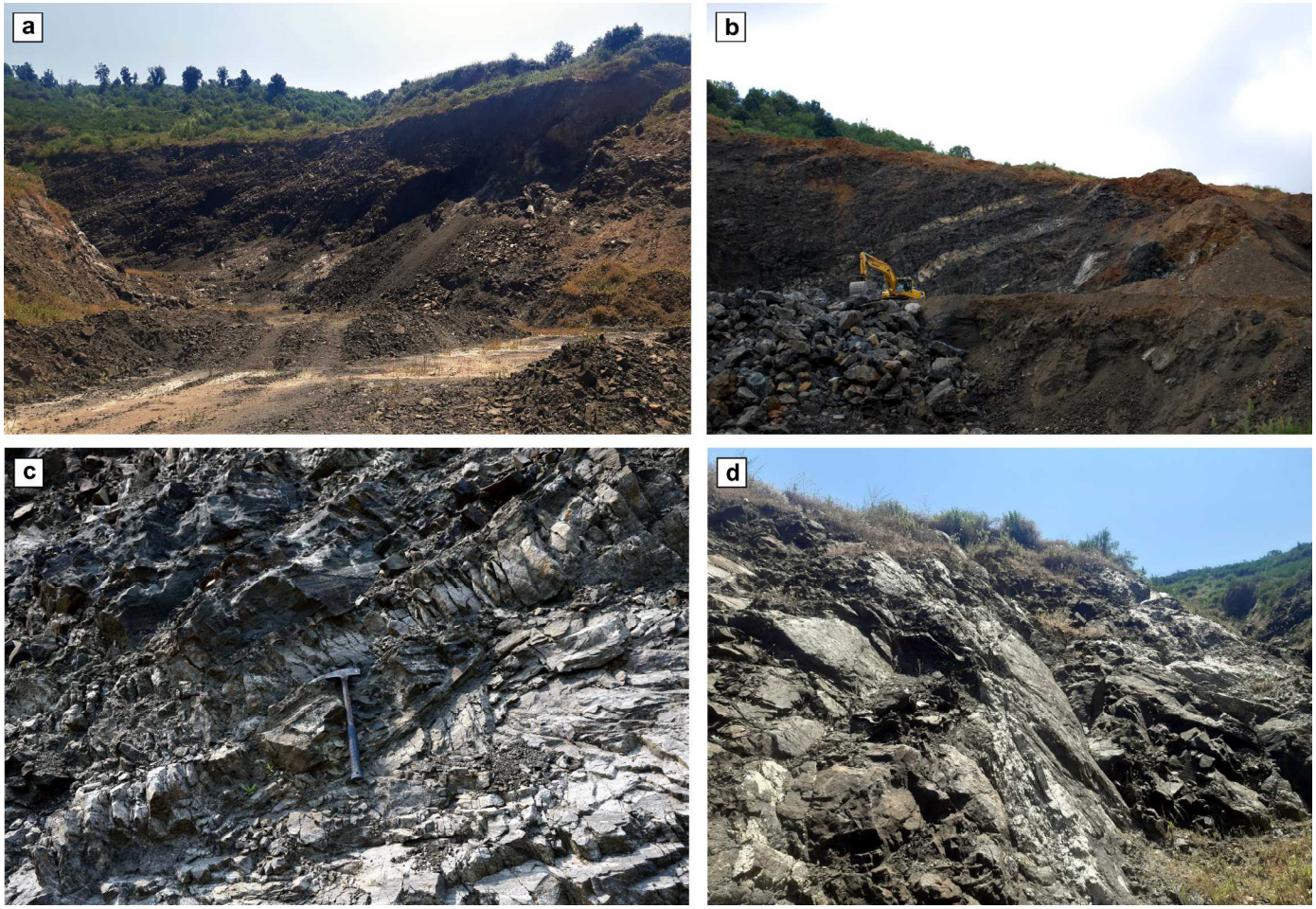

Fig. 17 - Views at different scales of the Turrino Quarry. (a) Panoramic view of the quarry face, looking south-west; (b) subhorizontal discordant pegmatitic dykes of metric thickness; (c) outcrop view of the layered metagabbro; (d) decimetre-thick pegmatites cutting the metagabbro foliation.

Metasedimentary felsic granulites are typically more massive and garnet rich (Fig. 18f). Orthopyroxene- or sillimanite-bearing types can occur, together with garnet, plagioclase and quartz, which are always present in all felsic granulite types; K-feldspar and biotite can be either present or absent in both orthopyroxene- or sillimanite-bearing granulites.

As already mentioned, a strong similarity between the crustal section exposed in southern Calabria and the Ivrea Zone has long been proposed (Moresi et al., 1978; Schenk, 1980, 1981); in this framework, analogies between the Ivrea Mafic Complex and the Serre metagabbro have been highlighted by Moresi et al. (1978). Though, a main difference is that a Permian age in the range of ~ 292-282 Ma has been indicated as the emplacement age of the Mafic Unit in the lower crust, coeval with granitoid magmatism in the middle-upper crust (Peressini et al., 2007; Klotzli et al., 2014; Karakas et al., 2019). In fact, metagabbros from the base of the Serre crustal section have long been considered the latest Neoproterozoic layered mafic intrusions, metamorphosed under granulite facies during the Variscan Orogeny. Nevertheless, such proposed age of the magmatic protolith was based on a single zircon intercept age of 553±27 Ma of a single zircon grain (Schenk, 1990), and on the dates of two zircon cores dated at 584±24 Ma (Micheletti et al., 2008) and 574±18 Ma (Fornelli et al. 2011), while several other zircon cores from the same samples gave dates ranging from 744±20 to 278±12 Ma. These measurements do not appear unambiguously constrain the emplacement age of the gabbroic protoliths. Different

https://doi.org/10.3301/GFT.2024.09

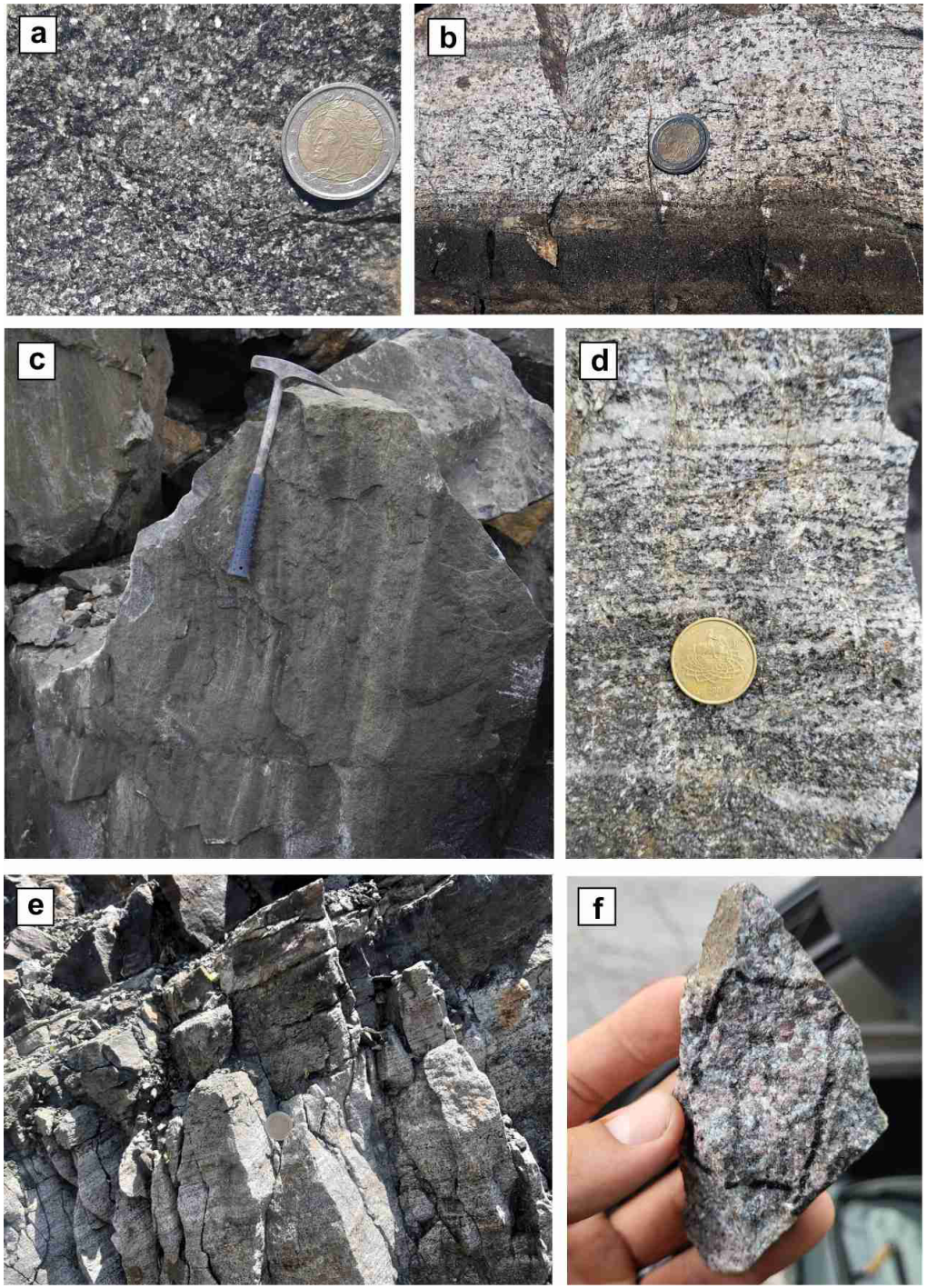

ages for the gabbro protolith have different implications on the role of mafic components in the formation of the Serre Batholith, since the metagabbro might either represent old mafic crust undergoing partial melting and forming I-type, geodynamically unrelated granitoids, or late Paleozoic mantle-derived mafic magmas, possibly mixing with coeval crustal melts, or triggering partial melting as underplated magmas at the base of the crust.

Two metagabbro samples from the Turrino quarry were studied by Fiannacca et al. (2016b) (Fig. 20). Most of the zircon grains appear to be either metamorphic or older grains with metamorphic rims. SHRIMP U-Pb dates on zircon cores gave a wide range from ~ 3.2 Ga to ~ 320 Ma, reflecting the incorporation of detrital zircon due to the assimilation of the metasedimentary host rock during the emplacement of gabbroic magma. The majority of the older cores yield ~ 720–450 Ma, with the youngest cluster at ~ 450 Ma possibly placing an upper limit on the age of magmatism. Metamorphic zircon, providing a maximum age for the metamorphism of ~ 313 Ma, is characterised by high $\delta^{18}O$ values (9.3–10.6‰), indicating its crystallisation in the presence of sediment-derived fluids, consistent with metasediment assimilation documented by detrital zircon and field observations. Older zircon cores have lower $\delta^{18}O$ values (6.1–9.2‰), of which only three are <7.5‰, giving no evidence for primary zircon crystallised from a mantle-derived magma. Instead, all the oxygen isotopes have a strong sediment signature, consistent with the large amount of detrital zircon in the sample. Zircon data suggest that prolonged residence of the sediment-contaminated mafic magma in the deep crust has largely

Fig. 18 - Field features of deep crustal rocks from Turrino Quarry. (a) typical metagabbro sample; (b-e) examples of layering developed in the metagabbro complex; (f) garnet-rich felsic granulite from the overlying host metasedimentary unit.

https://doi.org/10.3301/GFT.2024.09

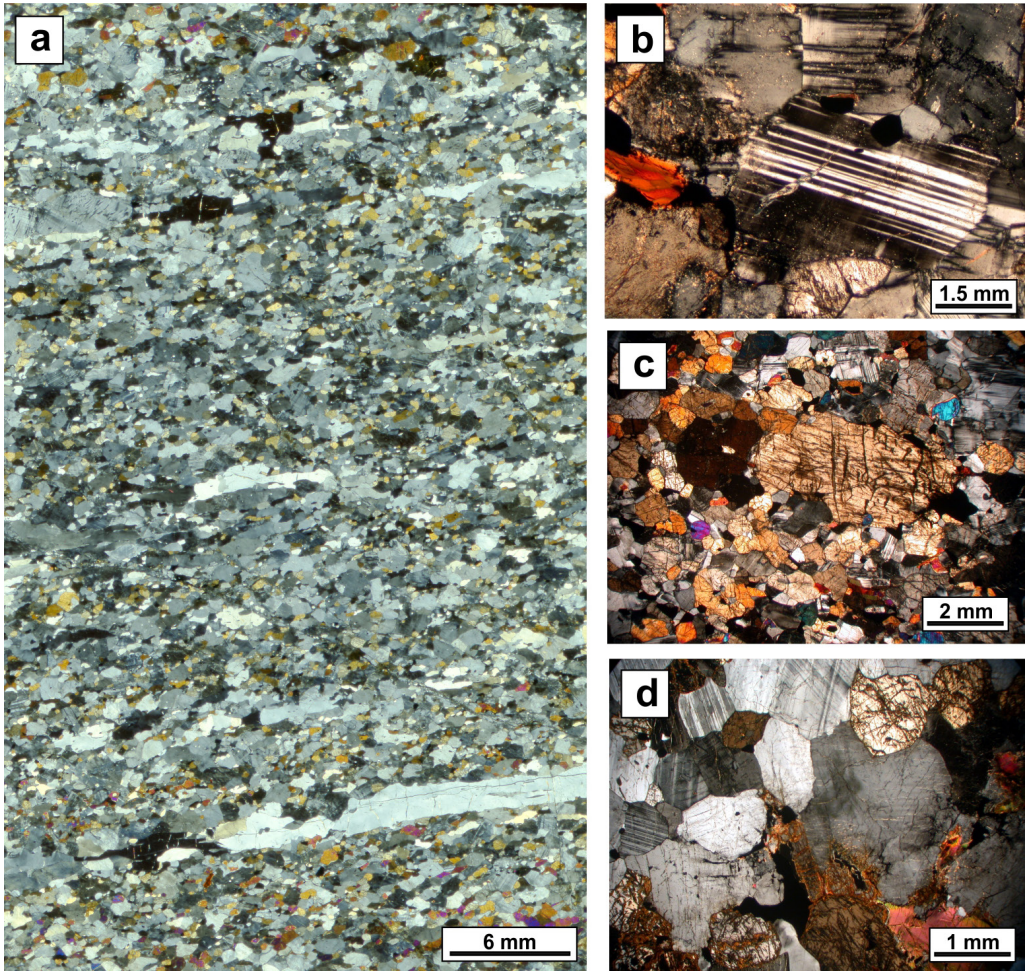

▲ Fig. 19 - Thin-section features of the metagabbros. (a) Thin section scan of a garnet-bearing two-pyroxene metagabbro showing a well-developed anisotropy; (b-c) microdomains showing respectively plagioclase and pyroxene individuals with relic magmatic shape; (d) plagioclase forming triple junctions in a poligonal granoblastic microdomain.

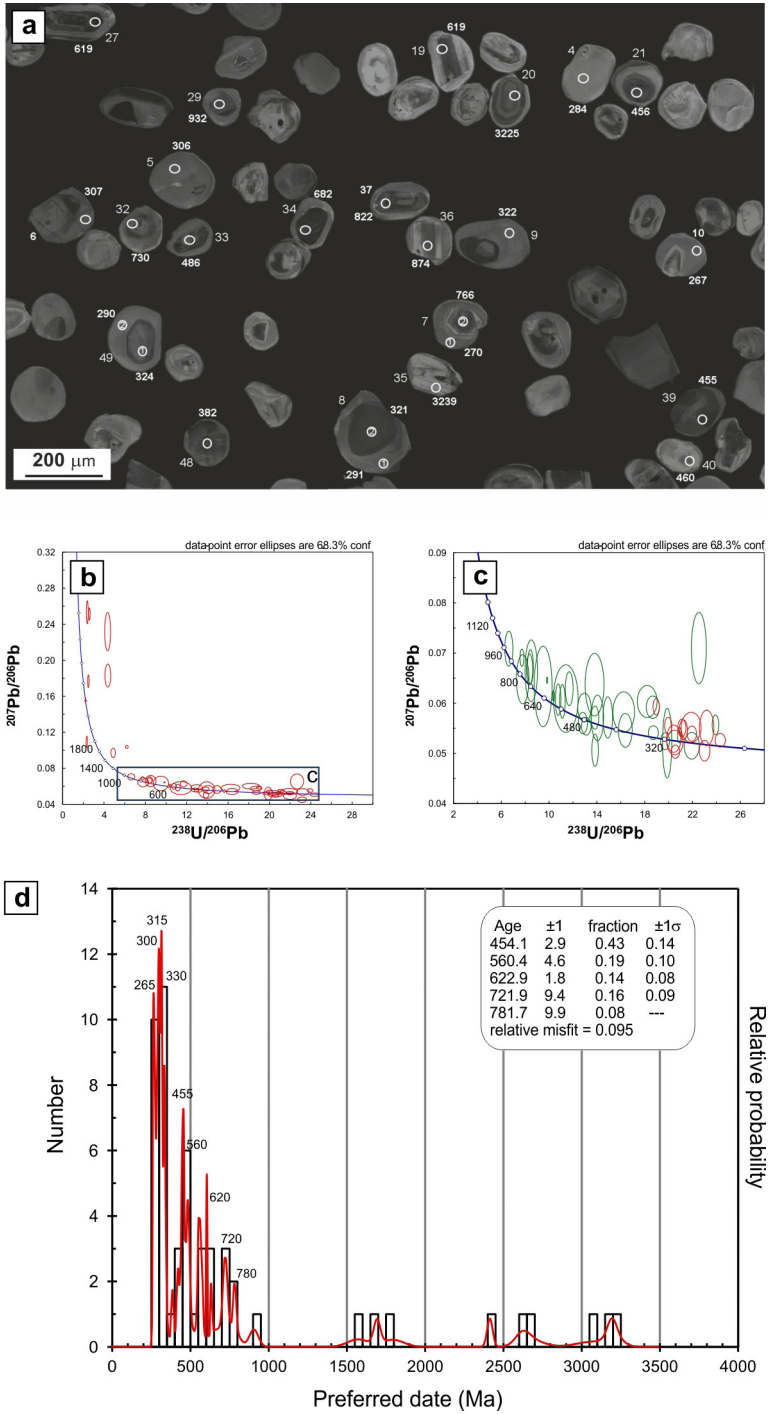

▶ Fig. 20 - Geochronological data for metagabbro sample SC-45 (Fiannacca et al., 2016b). (a) Cathodoluminescence images of sectioned zircon grains showing textural features, analytical spots and obtained dates for some of the dated zircon grains; (b) U-Pb analyses showing a wide range of dates from ~ 3.2 Ga to ~ 270 Ma ; (c) zoom of (b) for dates < 1 Ga. Green: cores, red: overgrowths or grains with no core ; d) relative probability distributions of the zircon ages (in Ma), with the cluster at ~ 450 Ma possibly representing the youngest detrital zircon population.

https://doi.org/10.3301/GFT.2024.09

modified the zircon $\delta^{18}O$ and many U-Pb dates, making it hard to determine the gabbro emplacement age. Nevertheless, if the ~450 Ma zircon age is that of detrital zircon, the gabbro magmatism must be younger than that age.
As said, the zircon rims of the metagabbro rims show no evidence of being magmatic, possibly a consequence of prolonged residence at a high deep crustal temperature in a fluid/melt-rich environment. A sample from the felsic granulite host rock was also analysed by Fiannacca et al. (2016b), in the attempt of getting constrains on the intrusion age of the gabbro by determining the maximum deposition age of the host metasediments. Nevertheless, it is to be highlighted that a large amount of the spots analysed by Fiannacca et al. (2016b) in both the metagabbros and the metasedimentary rocks were isotopically heterogeneous, resulting in very large uncertainties and several discordant analyses.

Stop 1.2 - Felsic granulites

Coordinates: Lat. 38°47'50" N, Long. 16°14'10" E
Location: Country road cut, Francavilla Angitola

Medium-fine-grained granulites made of Pl + Qtz + Grt ± Opx ± Bt ± Sill ± Kfs are rock types typical of the felsic granulites from the Granulite Unit, while metasedimentary rocks with Bt progressively more abundant upward in the section occur in the overlying Migmatite Metapelite Unit. A main feature of the felsic granulites is their lower Al contents compared to the metapelitic migmatites (i.e., average 14.72 wt. % vs. 18.73 wt. %, and up to 30.05 wt. % in garnet-sillimanite rich metapelites), reported by Caggianelli et al. (1991) and considered by the same authors to reflect a derivation of the felsic granulites from arenites and arenite-pelite mixtures. Pelite-rich levels were anyway certainly also present in the deepest part of the granulite unit, as documented by the occurrence of sillimanite-rich granulites in the Turrino quarry.
Rocks from Stop 1.2 (Fig. 21) consist of medium-fine-grained felsic granulites with a slighly dominantly anhydrous mafic assemblage, despite having relatively large amounts of biotite that locally define a poor relic schistosity. The granulites are migmatitic, with mm- to cm-thick concordant leucosomes; they are also extensively cut by cm- to dm-thick discordant leucosomes.
Even if not well visible in this outcrop, concordant leucosomes are folded, with the axial plane parallel to the schistosity plane, suggesting anatectic conditions preceding or coeval with the deformational event that produced the (at least) S_2 schistosity surface, which represents the field foliation in the lower crustal metasediments (e.g., Schenk, 1984; Acquafredda et al., 2006). Melting also occurred after the deformation, producing discordant leucosomes.
Despite some of the granitoid melt produced during granulite-facies melting crystallised in situ, the felsic granulites are typical restitic rocks due to the extraction of up to ~ 40 vol. % of felsic magma (Caggianelli et al., 1991; Fornelli et al., 2002), then forming part of the Serre Batholith S-type granites, at ~ 295 Ma (Fiannacca et al., 2015, 2017).
The felsic granulites from this outcrop (Fig. 22a-b) are dominantly granoblastic, with an assemblage consisting of quartz, plagioclase, garnet and biotite, the latter in slightly lesser amounts than garnet, and with minor K-feldspar, sillimanite and opaques. A faint foliation is

https://doi.org/10.3301/GFT.2024.09

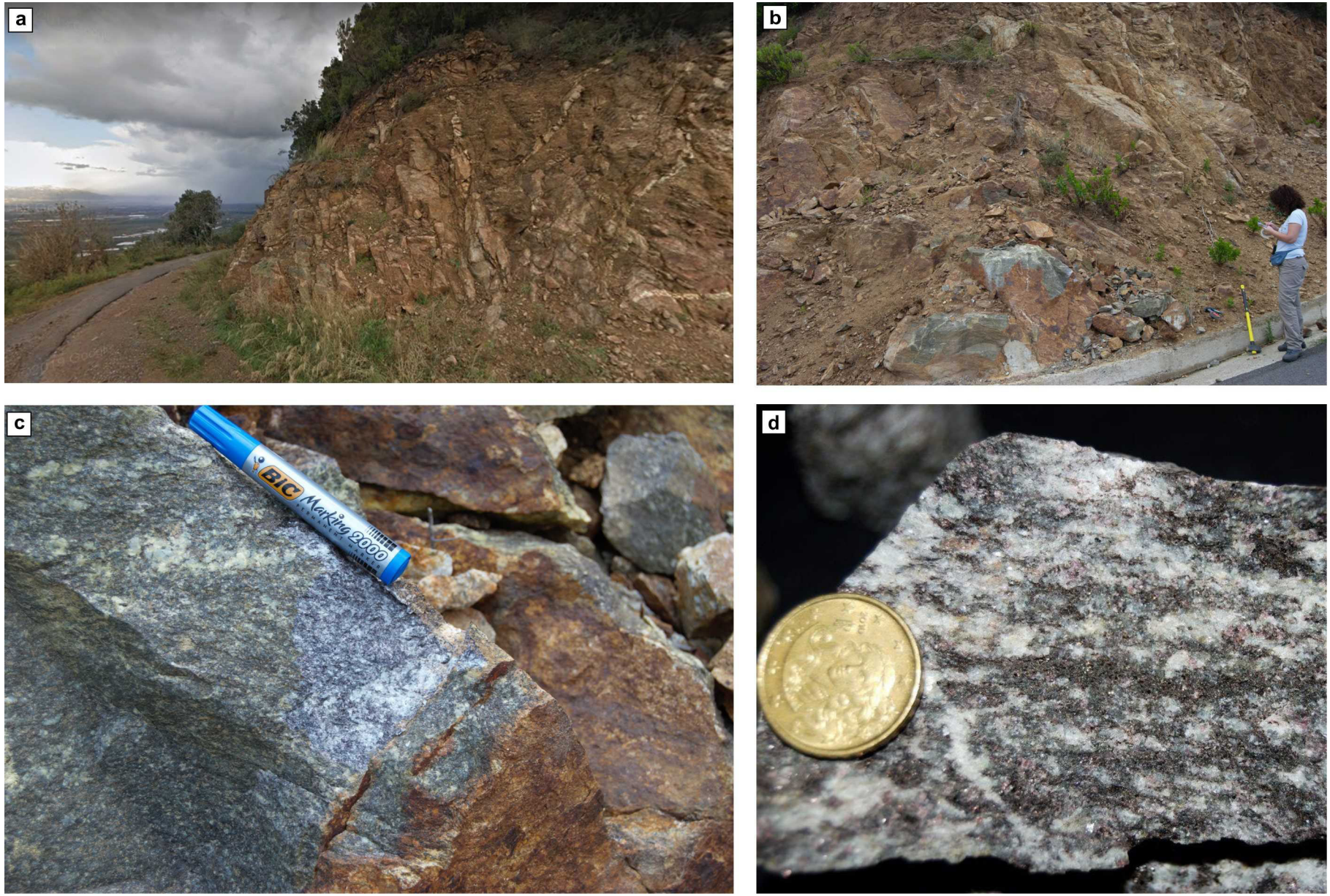

Fig. 21 - Outcrop appearance of the felsic granulites, with heavy alteration evident in (a) and (b) and fresh samples in (c and d). The structure of the rocks in this outcrop ranges from dominantly granofelsic (c) to gneissic, with a poor schistosity defined by Grt- and Bt-rich melanosomes (d). A network of leucocratic dykes is visible in (a).

https://doi.org/10.3301/GFT.2024.09

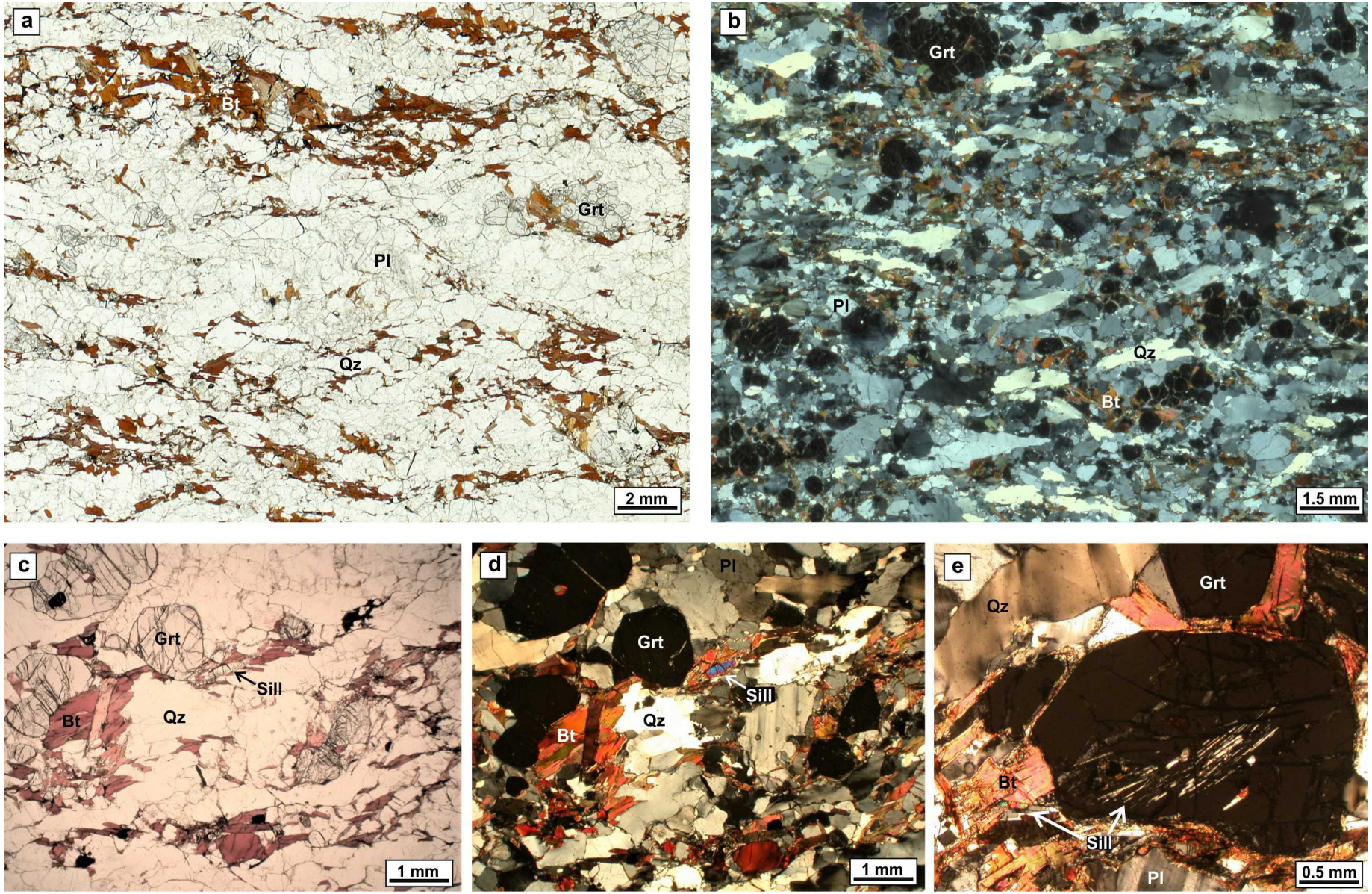

Fig. 22 - Petrographic and microstructural features of felsic granulites at Stop 1.2. (a) Thin section of felsic granulite showing a gneissic structure defined by alternance of leucosomes with mm- to submillimetre-thick melanosomes (parallel polar); (b) same of (a) under crossed polar, better highlighting the presence and distribution of the garnet in the rock; (c-d) parallel and crossed polar microphotographs of the same microdomain showing a sillimanite crystal subparallel to the main foliation; quartz with well-developed chessboard pattern is visible in the upper right; (e) microdomain with sillimanite occurring both as inclusions in garnet and the rock matrix.

https://doi.org/10.3301/GFT.2024.09

defined by alternating leucocratic layers, only containing quartz and feldspar, and darker layers also containing concentrations of garnet together with biotite, in aggregates or isolated corroded plats, and rarer sillimanite pryms (Fig. 22c-d). Some relic sillimanite can also occur in garnet (Fig. 22e). The rock shows evidence for both static textural readjustment at high temperatures and deformation at high to moderate temperature; the best examples are provided by quartz, that can exhibit either polygonal texture, or chessboard to undulose extinction in elongated and, sometimes, s-shaped crystals (Fig. 22b, d-e). Replacement microstructures indicative of high-temperature back reactions in the presence of melt, such as biotite-sillimanite replacing garnet, are not observed; only fine-grained myrmekites, deriving from supra- or subsolidus replacement of former K-feldspar, rarely occur in the leucosomes, suggesting that the melt was able to leave the source before the system cooled significantly. Finally, all the minerals appear unaffected by medium to low-temperature alteration leading to the formation of secondary phases.

As earlier reported, previous attempts to date the granulitic rocks from the Serre lower crust have not provided conclusive results so far. Deposition ages of ~ 400 Ma and ~ 596-649 Ma have been tentatively suggested for the arenite-pelite protoliths of the felsic granulites by Fiannacca et al. (2016b) and Fornelli et al. (2020), respectively. As for the metamorphic ages, all the authors agree that the main metamorphism experienced by the Serre lower crust was Variscan, climaxing at ~ 300 Ma. Micheletti et al. (2008) report several events of crystallisation, dissolution and recrystallisation affecting the zircon from the felsic granulites, possibly ranging from the Ordovician to the Triassic.

The preliminary study by Fiannacca et al. (2016b) also suggested that prolonged residence under lower crustal conditions of the studied felsic granulite samples resulted in significant migration and clumping of the radiogenic Pb in the analysed zircon cores, despite metamorphic conditions being in the range of common granulite-facies metamorphism (<900 °C). This detected Pb mobility makes it complicated obtaining reliable ages for the deep crustal Serre granulites, also including the suggested younger deposition age of the metasediments protoliths.

Stop 1.3 - Garnet-rich metapelitic migmatites

Coordinates: Lat. 38°43'03" N, Long. 16°08'05" E
Location: Vibo Marina Beach

Migmatitic paragneisses are the dominant rock type of the Serre lower crust, forming most of the Migmatite Metapelite Unit. These rocks were named "kinzigites" in the past (e.g., Novarese, 1931; Borsi et al., 1976; Paglionico et al., 1982), like the similar rocks from the Kinzigite Formation of the Ivrea Zone (e.g., Redler et al., 2012). The Serre migmatitic paragneisses are mainly Grt-Sill-Bt metapelitic metatexites with a well-defined migmatitic layering marked by aligned biotite and sillimanite and mm- to dm-thick concordant leucosomes of granitic or trondhjemitic composition; less common discordant leucosomes also occur; similar, but sillimanite-free or poor metatexites, likely derived from greywacke protoliths (e.g., Fornelli et al., 2002), are also widespread. The trondhjemitic and granitic leucosomes have been considered as the result of multi-stage melting at progressively higher temperatures and lower pressure producing first trondhjemitic melt, under water-

https://doi.org/10.3301/GFT.2024.09

fluxed conditions, and then granitic melt under fluid-absent conditions (Fornelli et al., 2002). A similar multi-stage melting process has been also documented for migmatites of the Peloritani Mountains (southernmost CPO), but developing entirely at upper amphibolite facies conditions, with only incipient biotite breakdown (Fiannacca and Cirrincione, 2020). On the contrary, the abundance of large peritectic garnet formed by Bt-dehydration melting, and of prismatic mm-to cm-sized sillimanite crystals (e.g., Schmid and Wood, 1976) attest to widespread melting at granulite facies conditions in the Serre lower crust.

As in the underlying Granulite Unit, structural and compositional variations are also recorded in the Migmatite Metapelite Unit, with migmatitic paragneisses being more massive and containing larger amounts of garnet, cordierite and prismatic sillimanite in the deeper levels of the unit. In parallel, all the mafic phases (also including biotite) are progressively Mg-richer downward in the section (Schenk, 1989). Kyanite has been also reported, as being more abundant and coarser towards the uppermost levels (Acquafredda et al., 2006); according to those authors, the assemblage before partial melting likely consisted of Grt–Bt–Ms–Ky–Pl–Qtz–Ilm.

The P-T path reconstructed by Acquafredda et al. (2006), based on textural relationships, conventional thermobarometry and Thermocalc computations, would indicate a prograde evolution with initial P-T increase within the stability field of kyanite until the P-peak at ~ 0.8 GPa and ~ 600 °C, followed by progressive heating up to T>700 °C at slightly decreasing pressure, during which melting of metapelites took place, mostly at expenses of plagioclase and muscovite. Partial melting continued through reaction Bt + Sill + Qtz + Pl = Grt + Kfs + melt, during subsequent decompression.

According to recent work by Festa et al. (2024), melting in the deepest levels of the unit occurred during isobaric heating, at an average peak pressure of 0.97 GPa, from ~ 700 °C to 800-840 °C.

Leucosomes from the Migmatite Metapelite Unit amount to ~ 30-40 vol%, locally form larger bodies in areas close to the batholith and decrease in abundance to 10-20% towards the deeper levels (e.g., Caggianelli et al., 1991). According to Fornelli et al. (2002), trondhjemitic leucosomes prevail, but the shallower and deeper paragneisses experienced extraction of ~ 32 vol% and ~ 40 vol% of granitic melts, respectively. The most depleted metapelites, rich in garnet and sillimanite, would represent the residue after partial melting leading to a loss of ~ 60 vol. % of total melt (~ 10 vol. % formed by water-present melting and ~ 50 vol. % by mica-dehydration melting), with the highest values in the deepest levels of the unit.

The stop is located along the beach just northeast of Vibo Marina tourist harbour (Fig. 23).

The migmatitic layering is here marked by mm- to dm-thick concordant leucosomes, separated by melanosomes consisting of varying amounts of biotite, sillimanite and large garnet porphyroblasts (Fig. 23a-d). Grain size ranges from medium to coarse in both melanosomes and leucosomes. Migmatites were affected by deformation after the melting event producing the migmatitic layering, as documented by widespread folded leucosomes (Fig. 23b-c) and flattened porphyroblasts of peritectic garnet (Fig. 23d). The main foliation is at least an S_2 schistosity, in addition flattened and stretched garnet porphyroblasts would suggest a subsequent mylonitic foliation locally developed parallel to S_2. In this outcrop, the migmatites are intruded by a ~ 2 m-thick granitoid body with a Pl + Qz + Bt + Grt assemblage (Fig. 23e-f);

https://doi.org/10.3301/GFT.2024.09

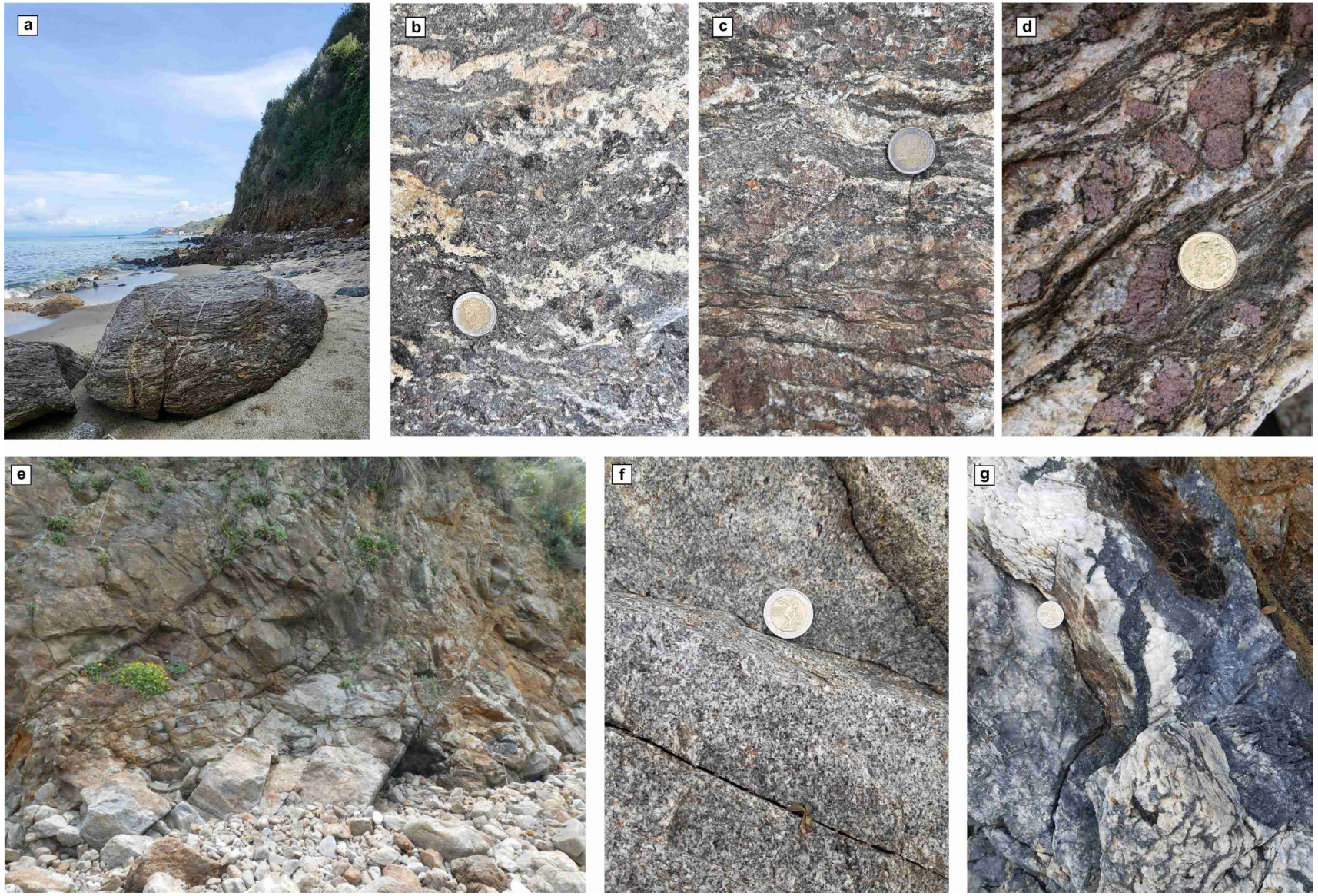

Fig. 23 - Field features of the migmatites at Vibo Marina. (a) View of Vibo Marina beach, with migmatites exposed as boulders (in the foreground), as well as in cliff and pavement outcrops (in the background); (b-d) details of the migmatitic foliation marked by the alternance of concordant leucosomes and melanosomes of various thickness consisting of biotite, sillimanite and large garnet porphyroblasts. Syn- to post-migmatisation deformation is documented by folded leucosomes (b-c) and flattened porphyroblasts of peritectic garnet (d); (e) outcrop view with the migmatites intruded by felsic dykes and a larger light-couloured granitoid body; (f) close-up view of the granitoid body; (g) pegmatitic dyke with large biotite plate (in the central-upper part of the image) and deformation highlighted by the blackish colour of quartz. Fig. 23d from Cirrincione et al. (2015).

https://doi.org/10.3301/GFT.2024.09

the grain size is medium-coarse, but a pegmatitic edge is developed at the contact with the host rock. All the rocks are cut by cm- to m-thick discordant dykes. Larger dykes are pegmatitic (Fig. 23g) and affected by deformation as shown by widespread blackish quartz. The whole outcrop is strongly tectonised, with all rock types displaced by several faults.

The mineral assemblage is Pl + Qz + Grt + Bt + Sill + Op ± Kfs ± Crd (Fig. 24a). Melanosomes are Grt-Bt-Sill rich, with well-developed prismatic sillimanite (Fig. 24b). Leucosomes are dominated by plagioclase and quartz, but widespread myrmekites attest to the former crystallisation

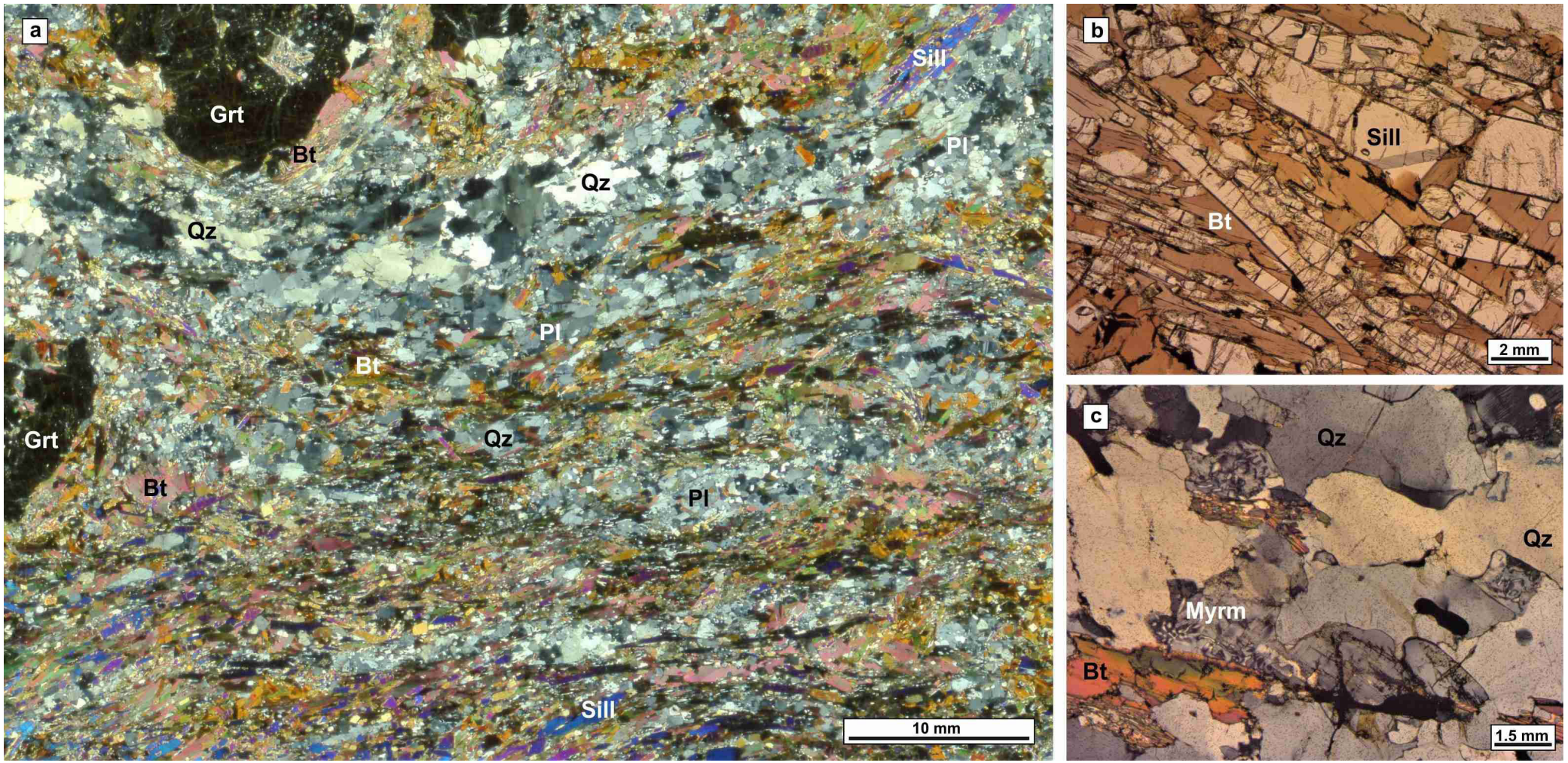

Fig. 24 - Petrographic and microstructural features of garnet-rich migmatitic paragneisses from Vibo Marina. (a) Thin section scan showing the main foliation given by alternance of leucosomes and Bt-Sill-rich melanosomes; (b) close-up of a Bt-Sill-rich microdomain; (c) myrmekites partly to totally replacing K-feldspar in leucosome.

https://doi.org/10.3301/GFT.2024.09

of K-feldspar (Fig. 24c). In thin section, deformation after migmatisation is well documented by quartz exhibiting a range of deformation microstructure from high- to low-temperature. In particular, a mylonitic fabric paralleling the S_2 schistosity is locally marked by elongated quartz grains.

Stop 1.4 - Metapelitic migmatites from the top of the lower crust

Coordinates: Lat. 38°40'15'' N, Long. 16°06'46'' E
Location: southern entrance of Tangenziale Est, Stefanaconi

Migmatites from Stefanaconi are rock types of representative of the top of the lower crustal section, coming from a level ~ 600 m higher than the migmatites from Vibo Marina. They consist in strongly foliated metatexites with mm- to cm-thick leucosomes with dominant trondhjemitic composition.
Compared with the migmatites from the deeper levels, the Stefanaconi migmatitic paragneisses are considered as not having been affected by significant melt extraction, with their overall major and trace element composition similar to common shales largely reflecting the compositions of the pre-migmatitic protoliths (Fornelli et al., 2004). This has been ascribed to the P-T melting conditions in the uppermost migmatites only allowing H_2O fluxed-melting that produced small amounts of trondhjemitic melts that mostly crystallised "in situ".
This interpretation is supported by the general low amounts of sillimanite in the Stefanaconi paragneisses that, coupled with the trondhjemitic composition of the leucosomes, could also be a consequence of the melting conditions. In fact, like the other Calabrian lower crustal metasedimentary rocks, Stefanaconi paragneisses lack primary muscovite, totally consumed by the partial melting reactions, so that the scarcity of peritectic sillimanite together with the dominant tronhjemitic composition of the leucosomes could support exclusive congruent melting of muscovite at relatively high pressure under water-fluxed conditions (e.g., Fiannacca and Cirrincione, 2020, and references therein).
Stop 1.4 is of particular interest because the works for the realisation of a freeway (Tangenziale Est of Vibo Valentia) have created an outstanding continuous outcrop of ~270 m in length and ~ 12-14 m in height (Fig. 25).
This outcrop allows the observation of the relationships between partial melting, melt segregation and melt transfer in a deep crustal anatectic zone. In fact, in addition to concordant mm- to cm-thick leucosomes, the outcrop is crossed by an intricate network of anastomosing leucocratic dykes, mostly up to a few dm-thick, which diverge and merge without truncations, isolating variously sized migmatite portions (Fig. 25 a-b). Curiously, two types of discordant leucocratic dykes occur, i.e., discordant leucosomes and neptunian dykes, with the latter sometimes associated with the leucosomes. Finally, sets of larger dykes, with straight edges and up to ~ 2 m-thick, also occur (Fig. 25c).
All the dykes appear to have intruded the migmatitic paragneisses after a deformational event producing isoclinal folds in the leucosomes (Fig. 25d); on the other hand, no migration of the leucosome melts is observed along the axial planes of these folds, as typical for syn-anatectic folding where melt migration and subsequent efficient extraction are focused toward the hinge zones of anticlines (e.g., Cruden and Weinberg, 2018).

https://doi.org/10.3301/GFT.2024.09

Fig. 25 - (a-c) Outcrop views of the migmatitic paragneisses, with intricate networks of leucocratic dykes and, in (c) larger dykes, with straight edges; (d) hand sample showing the migmatitic layering and relic fold hinges.

https://doi.org/10.3301/GFT.2024.09

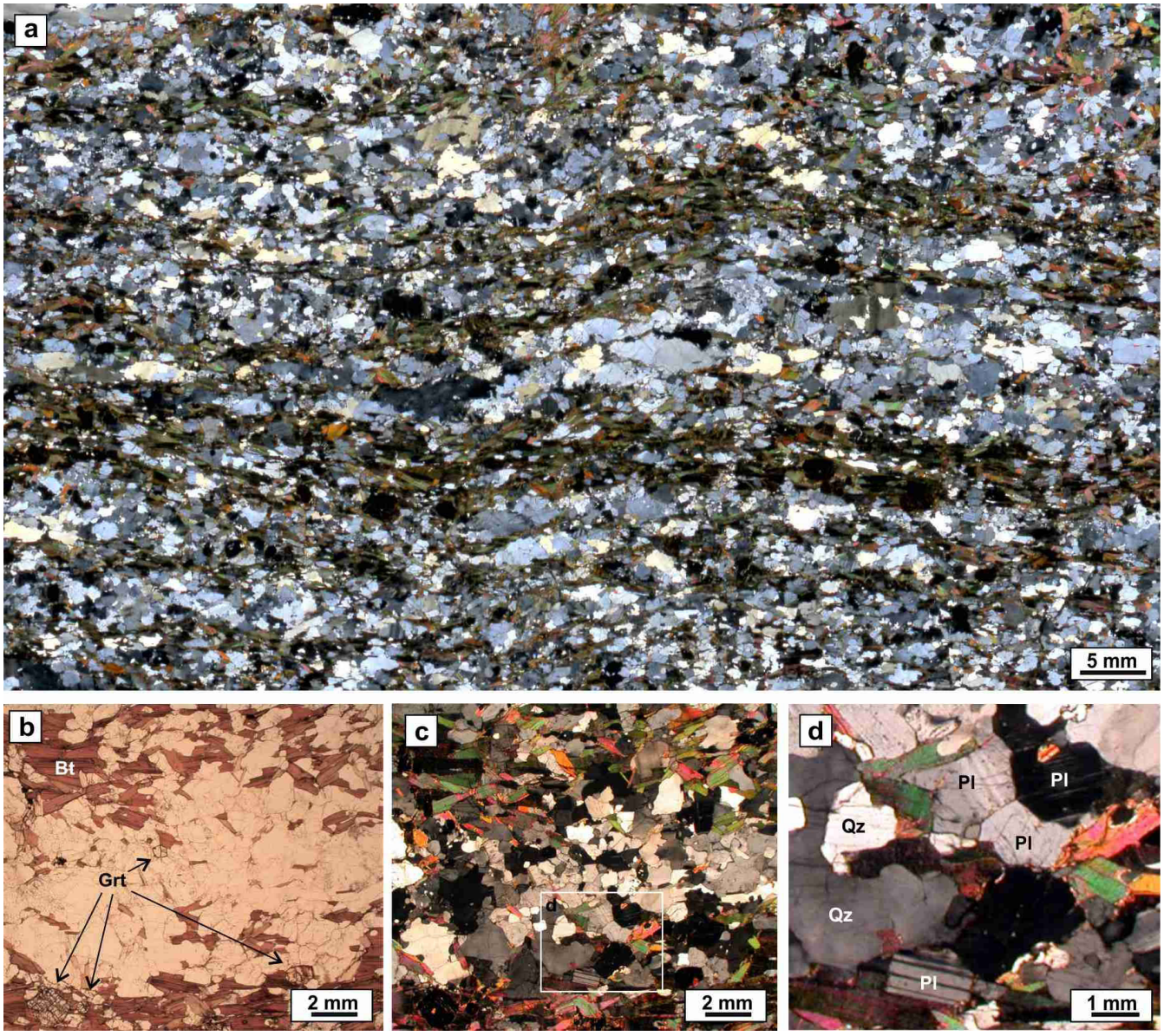

Fig. 26 - Petrographic features of Stefanaconi paragneisses. (a) Thin-section scan showing the migmatitic foliation with Grt-Bt rich melanosomes and Pl-Qtz rich leucosomes; (b) parallel and (c) crossed polar zoomed view of leucosome with garnet and biotite of mesosome derivation; (d) zoom of (c) showing twinned plagioclase with magmatic habit together with recrystallised plagioclase grains forming polygonal aggregates. Large quartz crystals are also visible.

In thin section (Fig. 26), Stefanaconi paragneisses show medium-grained mesosomes-melanosomes formed by dominant biotite, with abundant garnet and minor plagioclase and quartz; the latter two phases represent ~ 95% vol. of the leucosomes, with little amounts of biotite likely deriving from entrainment from the mesosomes-melanosomes rather than crystallisation from the melt (e.g., Fornelli et al., 2002). Leucosomes are medium-coarse-grained and slightly inequigranular for the presence of larger deformed quartz with undulose or, more rarely, chessboard extinction. Both quartz and plagioclase are mostly anhedral, but some euhedral plagioclase with tabular shape and polysynthetic twinning parallel to elongation, as typical for plagioclase crystallizing freely from melt also occur. In addition, plagioclase does not form a compact framework of euhedral touching crystals, but it is often in contact with large quartz crystals, suggesting that leucosomes reflect direct crystallisation from a trondhjemitic melt rather than accumulation of early-formed phases. Finally, evidence for static crystallisation at relatively high temperatures is provided by microdomains with granoblastic polygonal texture.

https://doi.org/10.3301/GFT.2024.09

DAY 2

FROM THE TOP OF THE LOWER CRUST TO THE DEEPEST GRANITOIDS OF THE SERRE BATHOLITH

The stops of Day 2 are entirely located in the Capo Vaticano Promontory (CVP, Fig. 3), a structural high developed along the Tyrrhenian coast and separated from the central Serre Massif by the Miocene-Pleistocene Mesima graben. The basement in the CVP area is also dismembered by systems of Quaternary normal faults with a NE-SW and WNW-ESE trend, associated with a fast uplift of the area (e.g., Tortorici et al., 2003).
In the CVP, the uppermost levels of the Migmatite Metapelite Unit and the deep-intermediate portion of the Serre Batholith crop out discontinuously beneath a terrigenous and carbonate cover (Burton, 1971). The metamorphic rocks, mostly consisting of migmatitic paragneisses, crop out in the northeastern and southwestern parts of the CVP (Maccarrone et al., 1983; Clarke and Rottura, 1994; Fornelli et al., 2002, 2004).
In particular, in the latter area, intrusion of earliest and deepest granitoids of the Serre Batholith (i.e., tonalites and quartz diorites from the ABT-BT units), triggered extensive further partial melting in the host paragneisses producing a migmatitic border zone (Rottura et al., 1990; Clarke and Rottura, 1994).
The CVP granitoids crop out over an area of ~ 270 km^2 and consist of strongly to weakly foliated tonalites and minor quartz diorites, accounting for ~ 65% of the exposed magmatic rocks, and weakly to non-foliated porphyritic granodiorites, with minor granites (~35%). In particular, the ABT-BT, forming the floor of the batholith, crop out in the northern and southern sectors of the CVP, while the overlying strongly peraluminous porphyritic granodiorites and granites (PMBG) are exposed in the central sector.
Tonalites are composed of plagioclase, quartz and biotite, with varying small amounts of hornblende, and scarce interstitial K-feldspar only in the most evolved tonalites. Apatite, allanite (often rimmed by epidote), ilmenite, zircon and titanite are the main accessory phases. Quartz diorites are the typical plutonic rocks in the migmatitic border zone. As earlier highlighted by Clarke and Rottura (1994), two different types of quartz diorites, plagioclase- and biotite-rich, respectively, occur in the southwestern CVP. The first type is dominant and consists of cumulus plagioclase ($An_{47–57}$; ~ 64 vol.%) with interstitial biotite, quartz, amphibole (hornblende and cummingtonite) and accessories; the second type occurs as dm- to m-sized bodies within the tonalites and consists mainly of cumulus biotite (up to 45 vol.%) and plagioclase ($An_{46–60}$; ~ 40 vol.%), with minor quartz and cummingtonite–hornblende intergrowths. The plagioclase-rich quartz diorites contain cm- to m-sized metapelitic enclaves; in addition, large garnet crystals are widespread in the CVP quartz diorites, particularly close to the metapelitic enclaves, and have been interpreted as peritectic phases produced by partial melting of the enclosed metasedimentary rocks (Clarke and Rottura, 1994).
Mafic microgranular enclaves diffusely occur in both tonalites and quartz diorites. They typically consist of porphyritic quartz diorites and tonalites, with ~ 2 mm-sized phenocrysts of plagioclase and biotite (2-5 % vol.) ± amphibole in a fine-grained matrix made up of the same minerals plus quartz and accessories. The MME are variably flattened and elongated, in accordance with the degree of deformation in the host rocks.

https://doi.org/10.3301/GFT.2024.09

Syn-tectonic tonalites-quartz diorites were intruded at ~ 302-297 Ma into the lower crustal gneisses (Fiannacca et al., 2017; Lombardo, 2020; Lombardo et al., 2023), triggering partial melting of country rocks (Clarke and Rottura et al, 1994), while weakly foliated to unfoliated two-mica granodiorites and granites were intruded later (~ 296-295 Ma; Fiannacca et al., 2017), at a shallower level. Based on Al-in-hornblende barometric estimates (Caggianelli et al., 1997) CVP tonalites-quartz diorites were emplaced at a depth of ~ 17-20 km (at Ioppolo, Santa Maria, Capo Vaticano), and greater than ~ 20 km (at Briatico).

The overlying PMBG are mainly medium coarse-grained porphyritic granodiorites and granites, with 1–12 cm-sized K-feldspar megacrysts, which intrude the tonalites in the central part of the CVP. The rocks consist of quartz, unzoned or weakly zoned plagioclase, microcline, Al-rich biotite (6–10 vol. %) and both primary and secondary muscovite (2–3 vol. %). Relatively large crystals of apatite, zircon, monazite and ilmenite represent common accessory phases; sillimanite and garnet are occasionally present. The PMBG lack MME but locally contains small metapelitic enclaves.

Recent geochemical modelling by Lombardo et al. (2020) confirmed the lack of genetic relationships between the ABT-BT and the PMBG (Fiannacca et al., 2015, and references therein) and suggested fractional crystallisation as the main process responsible for the compositional diversity from I-type quartz-diorite to leucotonalite in the ABT-BT and from S-type granodiorite to syenogranite in the PMBG.

The abundance of MME in the ABT-BT is not considered here as evidence for mixing with mantle-derived magmas and generation of hybrid host rocks granitoids apart from local hybridisation effects in the immediate surroundings of the enclaves, and within the enclaves themselves, as also testified by crystal transfer processes from the host tonalites to the enclaves.

Both ABT-BT and MME have a marked crustal isotopic signature, with recent Sr-Nd isotopic analyses on 16 new CVP samples (Lombardo, 2020; Lombardo et al., 2023) giving a restricted range of Sr_i ratios (recalculated at 300 Ma) of 0.7098–0.7102 and a wider range of εNd values from -5.88 to -7.43. Both compositional ranges are more restricted than those obtained by Rottura et al. (1991) on two tonalite and two quartz diorite samples, consisting of Sr_i ratios from 0.7095 to 0.7123, and highly variable εNd values from –0.3 to –10.1, though mostly lower than –6. Interestingly, the two MME samples analysed by Lombardo (2020) have εNd values among the most negative (-6.97 and -7.15). Hafnium isotopic compositions of magmatic zircon are also similar in both CVP tonalites, quartz diorites and MME, with dominant-negative εHf values, mostly spreading in the range - 4 to -15, a few less negative values and 4 spots (over 134) giving positive values (Lombardo, 2020; Lombardo et al., 2023). Isotopic data therefore mostly point to a dominant crustal contribution in the generation of the studied granitoids. This crustal contribution might be related to the assimilation of metasedimentary crust, widely documented in the granitoids from the batholith floor, which may have obscured the mantle isotopic signatures of the tonalitic magmas. On the other hand, a direct crustal origin is supported by a number of evidence, including the presence of isotopically and geochemically compatible potential metabasaltic source rocks in the Serre lower crust, and the documented temperatures exceeding 900 °C (Acquafredda et al., 2008), necessary to produce extensive melting of those mafic sources.

The first stop of the day will be at the cobble-boulder beach of Santa Maria, where each cobble/boulder is a 3D record of the interaction between the syn-tectonic quartz diorites-tonalites (~ 302-297 Ma) making up the floor of the batholith, and the underlying metapelitic

https://doi.org/10.3301/GFT.2024.09

migmatites. Emplacement of the granitoid magma triggered indeed further melting in the migmatites, producing peritectic garnet up ~ 5 cm large and anatectic melt variably interacting with the tonalites. Garnet is particularly outstanding in this outcrop, also forming the main mafic component in peculiar quartz dioritic rocks. We will walk to a cliff where the quartz diorites-tonalites crop out and display a variety of textures and compositions related to the interaction with the anatectic magma. MME of quartz dioritic-quartz monzodioritic composition locally occurs. The second stop of the morning will be at a slighly higher structural level of the granitoid unit, still made up of syn-tectonic tonalites, with swarms of elongated MME and cut by pegmatite dykes. The third stop, in the afternoon, will be at the Michelino Beach (Parghelia), where it is possible to observe striking mush-magma relationships between the tonalites and the overlying two-mica porphyritic granodiorites and granites (~ 296-295 Ma), which are the dominant rocks in the beach. The porphyritic granitoids contain K-feldspar megacrysts up to 12 cm long, locally showing flow and/or accumulation textures.

Stop 2.1 - Migmatitic Border zone

Coordinates: Lat. 38°36'45" N, Long. 15°50'34" E
Location: Santa Maria Beach, Ricadi

The migmatitic border zone (MBZ) represents a transition zone between the top of the metamorphic lower crustal section and the earliest and deepest emplaced granitoids of the Serre Batholith, i.e. the tonalites/quartz diorites of the ABT-BT units. The MBZ is characterised by: a) migmatitic paragneisses with evidence of high melting degrees; and, b) medium-coarse-grained granitoids including cm- to m-sized metapelitic enclaves, as well as large crystals of peritectic garnet. The latter, up to 5 cm in size, is mainly associated with the metapelitic enclaves, occurring in extremely varied amounts in cm- to m-sized leucosome patches (i.e., paragneiss-derived magma, PDM), but also present as isolated crystals in tonalites far away from the enclaves. This peculiar multiscale commixture of tonalites, metapelitic enclaves and associated garnet-bearing leucosomes, also locally documented in the northern Serre Massif, is the result of extensive partial melting of the metapelites as a consequence of the emplacement of the tonalitic magma into the lower crustal host rocks (Rottura et al., 1990; Clarke and Rottura, 1994; Russo et al., 2023).
Santa Maria Beach (Fig. 27a-e) is probably the best location in Calabria for exploring the interaction effects between tonalitic mushes and the underlying host metapelitic migmatites. The migmatites are here only exposed in boulders and cobbles along the beach, and typically consist of large volumes of garnet-bearing leucosomes and rounded metapelitic enclaves, the latter representing the residua after extensive melting of the host paragneisses (Fig. 27b). Mesosome-leucosome-garnet proportions are anyway very variable, giving place to a number of rocks with different structures and compositions (Fig. 27c-e). The tonalites also occur as boulders and cobbles, but they also make up a large cliff outcrop (Fig. 27a), where it is possible to observe that the granitoids locally enclose mafic microgranular enclaves up to ~ 50 cm in size, and are then intruded by swarms of pegmatites and aplites.

https://doi.org/10.3301/GFT.2024.09

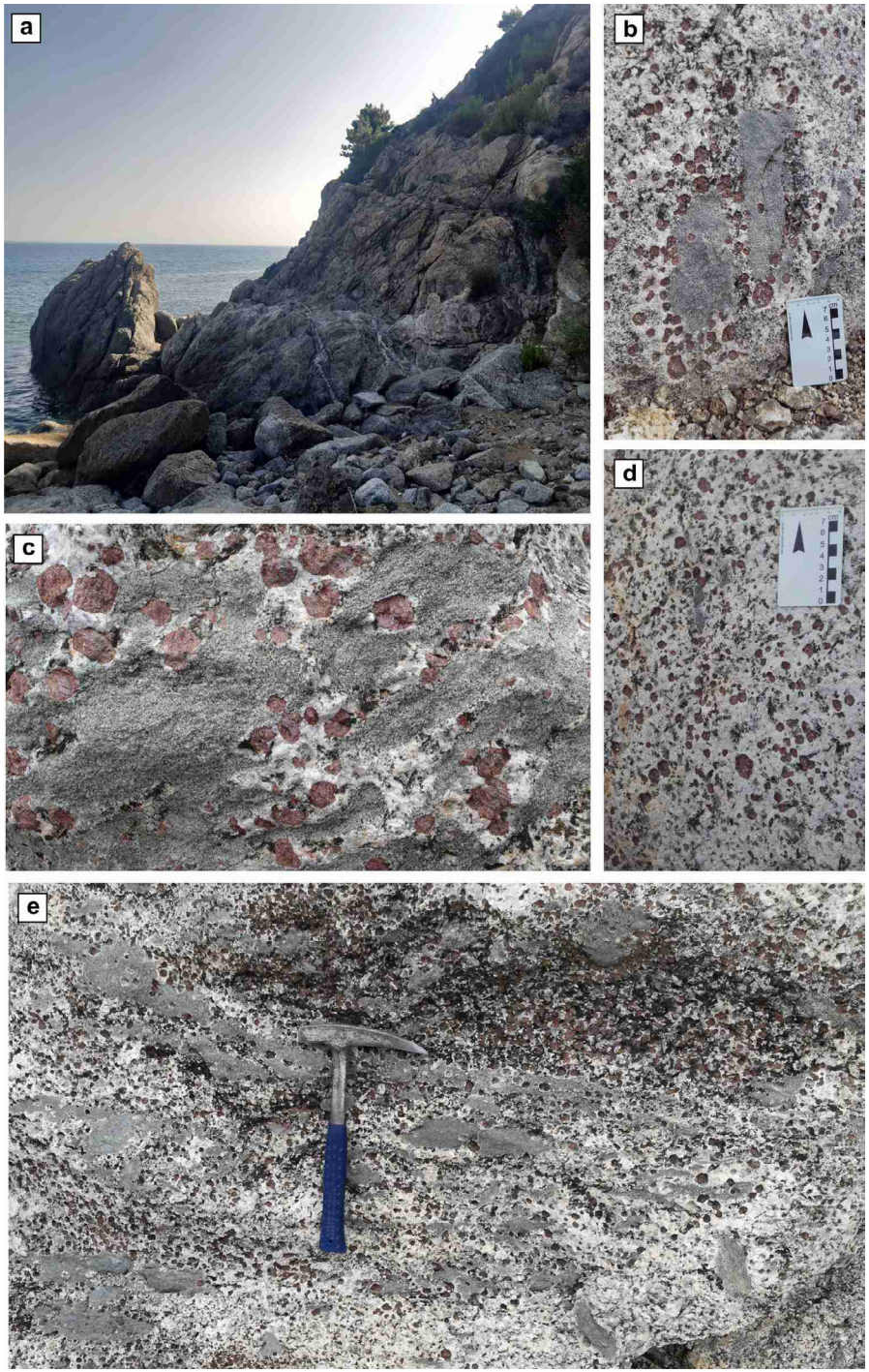

A closer observation shows that the tonalites are locally rich in garnet (Fig. 28a), clear evidence of the interaction between the tonalitic mush and the paragneiss-derived melt. In most outcrop of the MBZ, the occurrence of peritectic garnet is the only evidence for contamination by the S-type anatectic magma in apparently homogeneous tonalite. In other outcrops also this evidence can be erased, by back-reactions between the peritectic garnet and the tonalitic magma-producing biotite or biotite + hornblende at garnet expenses, as already documented in detail by Clarke and Rottura (1994). On the other hand, tonalites from Santa Maria outstandingly exhibit varying stages of interaction with the garnet-bearing or garnet-free anatectic magma. Early-stage infiltration of the anatectic magma through mushy tonalite might occur along irregular patches and channels (Fig. 28b-c), then forming an interconnected network of cm- to dm-wide channels (Fig. 28d). In some outcrops with high volumetric proportions of anatectic magma, peculiar hybrid rocks, characterised by pervasive mingling of PDM and tonalite, occur as the result of cm-scale disaggregation of the mushy tonalite in the anatectic S-type magma (Fig. 28e,f).

Thin sections of these hybrid rocks show that the fragments typically have a magmatic texture and a quartz dioritic or tonalitic composition, with dominant euhedral to subhedral tabular plagioclase, biotite, rare subhedral hornblende (Fig. 29a,b) and variable amounts of quartz; titanite and epidote locally occur as accessory phases; such textures and compositions are the same as the tonalites/quartz diorites from the main outcrop (Fig. 29c,d).

Finally, another peculiarity of the MBZ at Santa Maria is that also the leucosomes typically have quartz dioritic composition, being moslty formed by dominant euhedral to subhedral plagioclase with variable amounts of garnet,

Fig. 27 - Field appearance of tonalitic and migmatitic rocks from the MBZ at Santa Maria beach. (a) View of the cliff exposing the tonalites, here intruded by dm-thick pegmatitic dykes; (b-e) examples of migmatitic rocks showing an extremely variable appearance based on the various proportions and distribution of residual paragneiss (grey), leucosome (white) and garnet (red).

https://doi.org/10.3301/GFT.2024.09

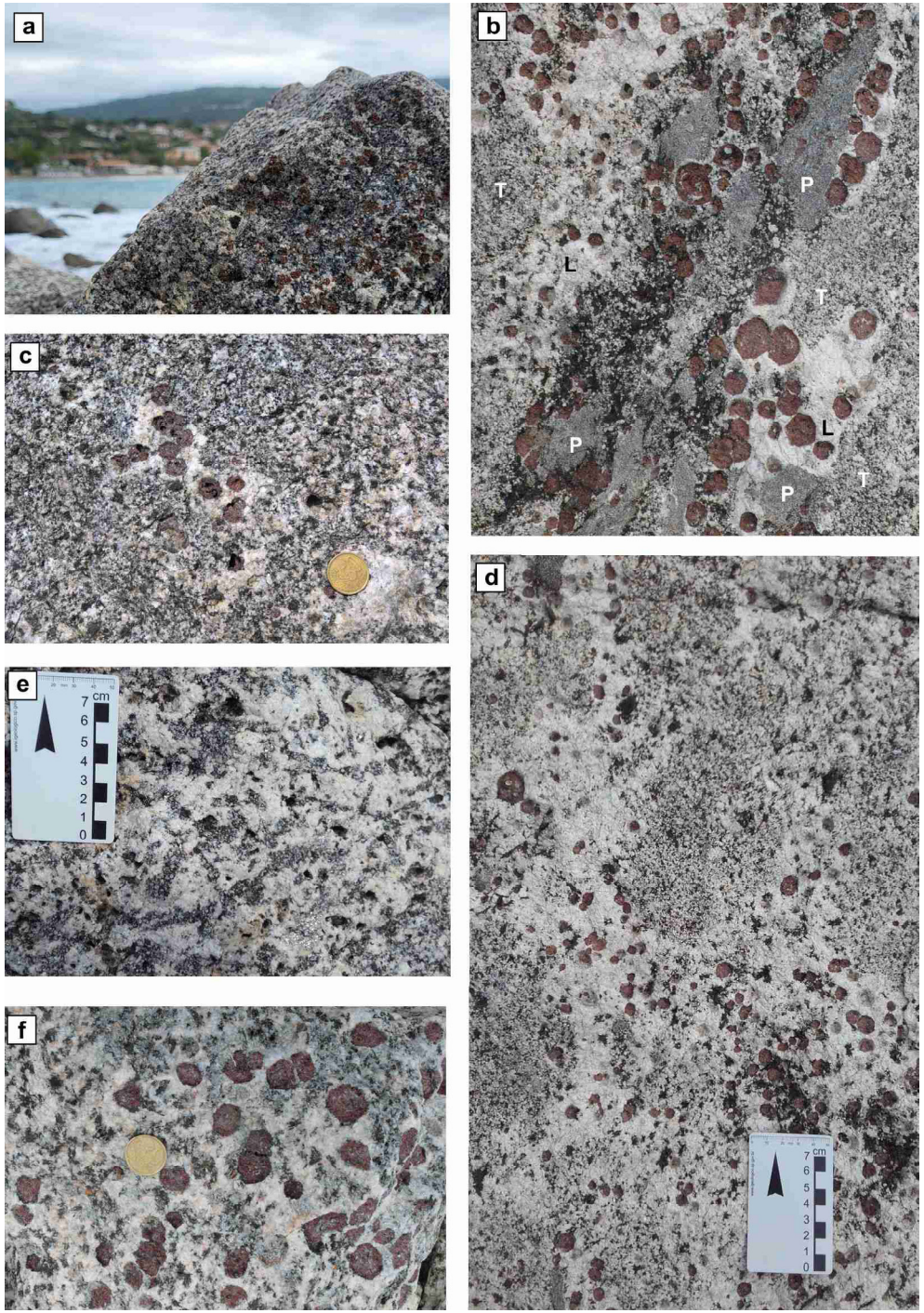

minor biotite and rare interstitial quartz (Fig. 29e,f). More in detail, composition ranges from leuco- to mela-quartz diorite, based on the highly variable amounts of garnet; some garnetites also occur locally. The lack of K-feldspar and the small amounts of quartz are at odds with the huge amounts of peritectic garnet, which attest to extensive incongruent melting of biotite that, in turn, should have led to the production of large amounts of granitic melt. Quartz diorite composition, together with the exhibited cumulitic texture, suggest that these peculiar anatectic S-type quartz-diorites are indeed cumulate rocks from which large amounts of granitic melt were extracted. Finally, it is worth highlighting that such locality is quite singular for the presence, in a very small area, of three different types of quartz diorites: I-type, S-type and hybrid.

Stop 2.2 - I-type tonalites with MME swarms and felsic dykes

Coordinates: Lat. 38°36'23" N, Long. 15°51'00" E
Location: Santa Maria, Scogli della Galea

The outcrop at Scogli della Galea (Figs. 30, 31), at the southern side of the Santa Maria beach, consists of strongly to moderately foliated tonalites and quartz diorites from the ABT unit with swarms of flattened and elongated mafic microgranular enclaves of dominant quartz dioritic composition, concordant with the host rock foliation. ABT are medium-coarse-grained and with a main assemblage consisting of plagioclase

Fig. 28 - Interaction between paragneiss-derived anatectic magma and tonalitic mushes at Santa Maria Beach. (a) Garnet-rich hybrid tonalite; (b-c) early-stage infiltration of the paragneiss-derived anatectic magma through mushy tonalite along irregular patches and channels; (d) interconnected network of cm- to dm-wide leucosome channels; (e, f) Grt-free and Grt-rich hybrid granitoids formed by pervasive mingling of mushy tonalite and anatectic magma.

https://doi.org/10.3301/GFT.2024.09

+ quartz + biotite + amphibole (cummingtonite-hornblende); accessory minerals are epidote, allanite, ilmenite, titanite, apatite and zircon. MME are made up of the same minerals, but typically with minor amounts of quartz and a finer grain size.

The MMEs are usually dm-sized, with larger enclaves up to ~ 1 m occurring locally. Contacts with the tonalitic host rocks vary from sharp to gradational, the latter due to partial assimilation of the MME in the tonalitic mush and formation of hybrid granitoids in cm-scale thick aureoles around the enclave (e.g., Fig. 30e).

Different generations of pegmatite-aplite dykes with thickness in the range of ~ 1-50 cm intrude both MME and host rocks (Fig. 31); contacts between the dykes and the host rocks are commonly sinuous suggesting intrusion of the dykes in a quite ductile environment.

As typical for the granitoids from the deeper level of the ABT and BT units, quartz diorite and tonalites from Scogli della Galea mostly exhibit a cumulate texture, while more evolved tonalites with rare interstitial Ms and Kfs crop out in the upper levels, close to the contact with the overlying two-mica porphyritic granodiorites and granites.

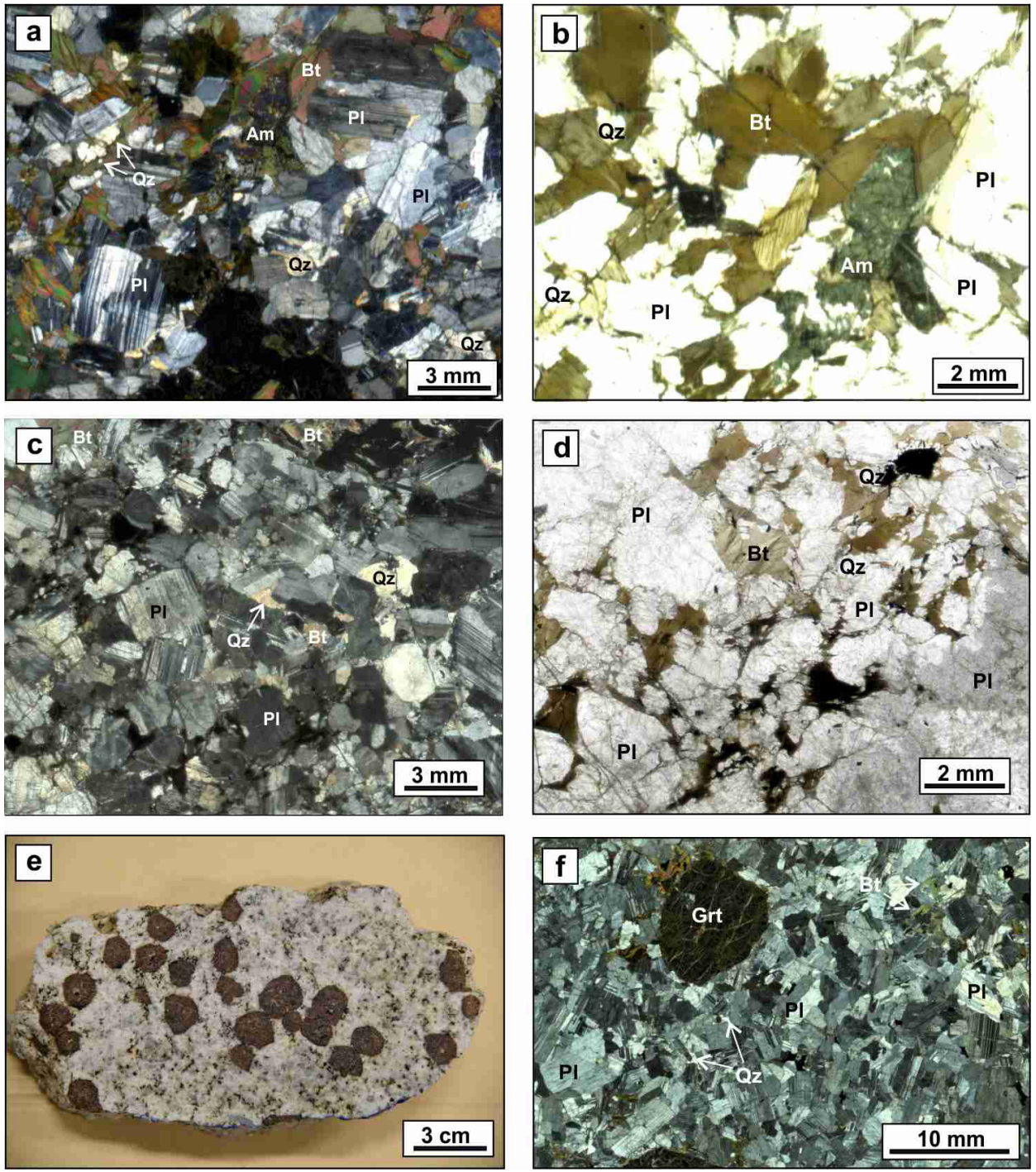

Fig. 29 - (a-b) Petrographic features of hybrid quartz diorites (under crossed and parallel polars, respectively) containing fragments of a pre-existing crystal mush disaggregated by the anatectic magma. The presence of hornblende indicates that such hybrid rocks derived by fragmentation of mushy tonalites; (c-d) petrographic features of the I-type tonalites from the main outcrop for comparison; (e-f) S-type quartz diorite at hand-sample and at microscopic scale, the latter showing adcumulate nature with minor interstitial quartz.

https://doi.org/10.3301/GFT.2024.09

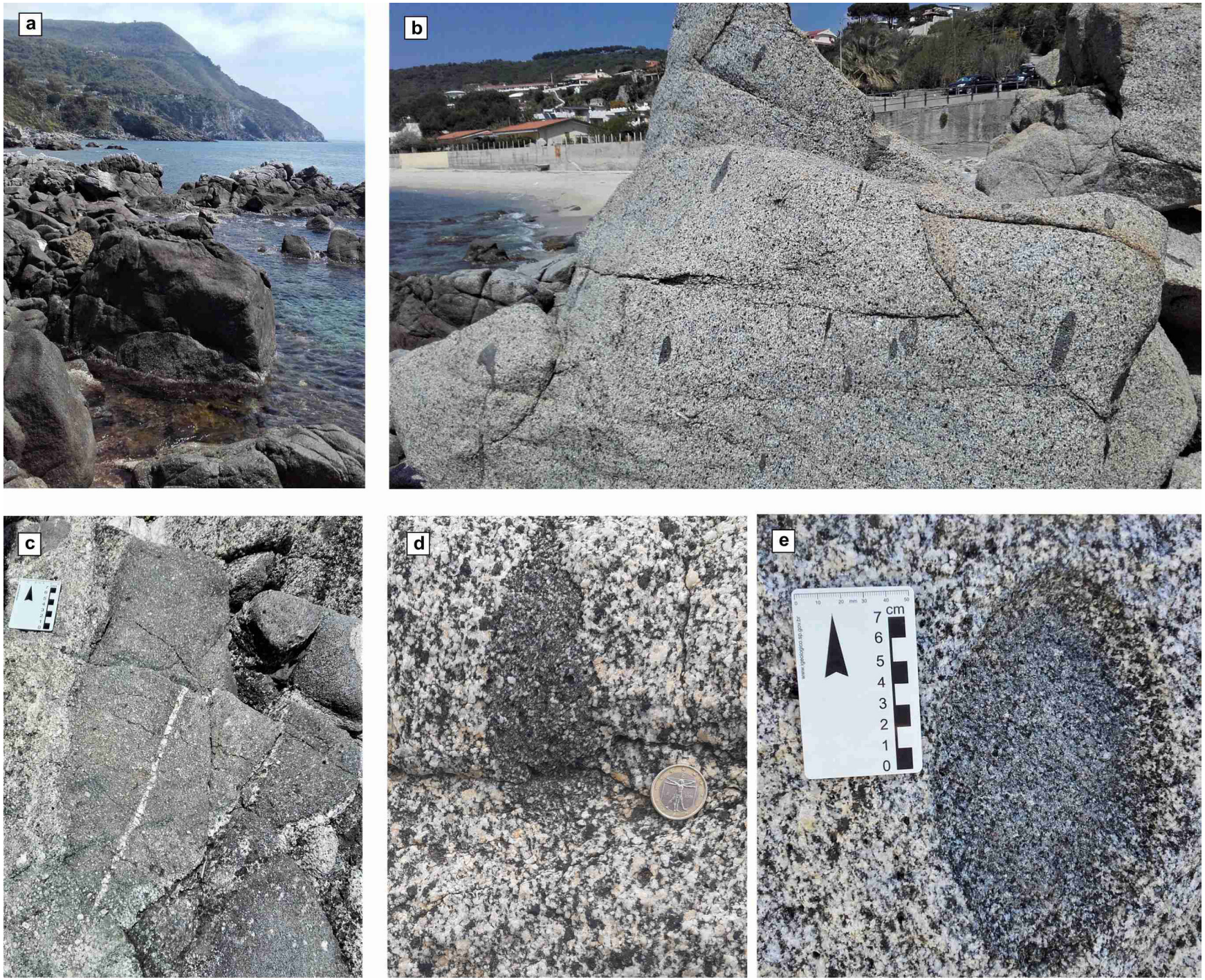

Fig. 30 - (a) Outcrop view of ABT quartz-diorites and tonalites at Scogli della Galea; (b) swarm of flattened MME, sub-vertically iso-oriented, in ABT; (c) portion of m-sized MME, cut by thin felsic dykes; (d) dm-sized MME with small plagioclase phenocrysts, likely transferred from the host tonalite; (e) dm-sized MME with a largely hybridised rim at the contact with the tonalitic magma.

https://doi.org/10.3301/GFT.2024.09

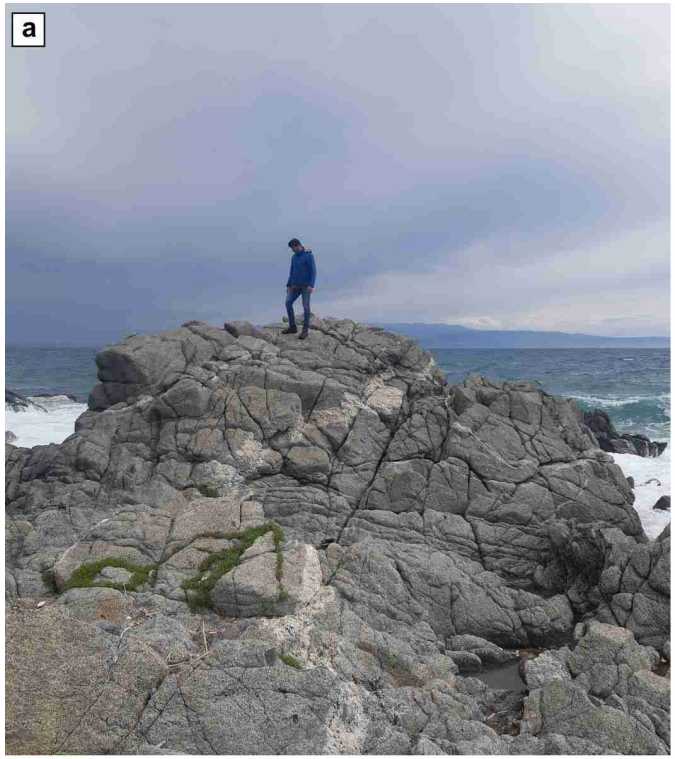

The typical ABT rock at Scogli della Galea is a medium-coarse-grained Am-bearing quartz diorite with an orthocumulate texture defined by a framework of early-formed plagioclase grains, and a marked anisotropy defined by the isorientation of hornblende, biotite and plagioclase (Fig. 32a-b). ABT consist of unzoned to weakly zoned euhedral to subhedral plagioclase (~ 55 vol. %), subhedral to anhedral biotite (~ 25 vol. %) in clots or single plats, anhedral quartz (~ 10 vol. %) and subhedral to anhedral amphibole (~ 10 vol. %). Colour index is in the range 25-40. The accessory phases consist of epidote, allanite, ilmenite, apatite and zircon. Biotite commonly occurs in association with hornblende with textural relationships suggesting that at least part of the biotite may have formed by late-magmatic replacement of the amphibole (Fig. 32c-d).

The MMEs (Fig. 32e,f) are commonly fine-medium-grained and porphyritic due to the presence of small plagioclase phenocrysts that may have been derived by crystal transfer from the host granitoid magma.

Fig. 31 - (a) ABT crossed by thick pegmatitic dyke; (b) interaction between cm-thick felsic dyke and elongated MME; (c) felsic dyke cutting and displacing two older dykes; (d) zoom of (c) showing detail of the displaced dykelet.

https://doi.org/10.3301/GFT.2024.09

Despite many CPO areas have been affected by Alpine deformation and shearing, the foliation in the granitoids of the ABT and BT units developed during solidification and cooling of the granitoid magmas. This is clearly demonstrated by the occurrence of late Variscan felsic dykes not sharing the same foliation of the magmatic host rocks (tonalites and MME), as well as by microstructural evidence of high-temperature deformation. In particular, the best evidence of high-temperature deformation is given by chessboard extinction in quartz and, especially, by the occurrence of submagmatic fractures in plagioclase and amphibole, indicating deformation at suprasolidus conditions. The tonalites-quartz diorites show anyway a dominant subsolidus fabric, acquired by deformation continuing at a progressively lower temperature, during slow cooling at the depth of the magmatic bodies.

Stop 2.3 - Two-mica porphyritic granodiorites and granites and underlying tonalites

Coordinates: Lat. 38°41'07" N, Long. 15°55'15" E
Location: Michelino Beach, Parghelia

Michelino Beach (Fig. 33) is not only unique because of the beauty of the beach, the sea and the landscape, but also because of the high number of outstanding field features of great geological relevance.

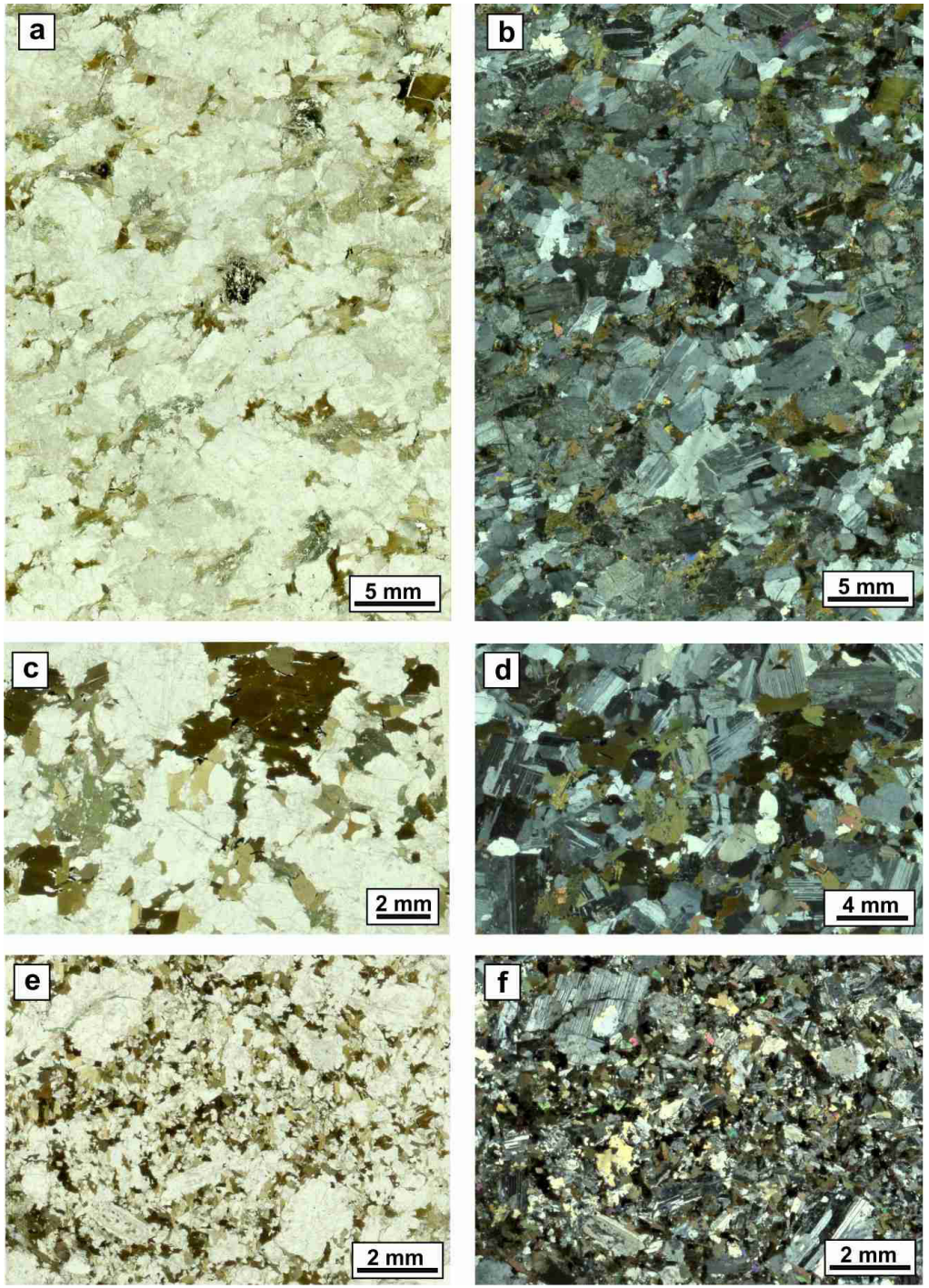

Fig. 32 - Petrographic and microstructural features of ABT (a-d) and enclosed MME (e-f). (a,b) Thin section scans showing a marked anisotropy, better visible under parallel polar in (a), and an orthocumulitic texture, visible under crossed polar in (b); (c-d) microdomains illustrating the typical ABT assemblage consisting of plagioclase, biotite, hornblende and quartz; (e-f) parallel and crossed polars view of an MME thin section with grain size typically finer than the host tonalite, apart from plagioclase phenocrysts likely entrained from the tonalite magma.

https://doi.org/10.3301/GFT.2024.09

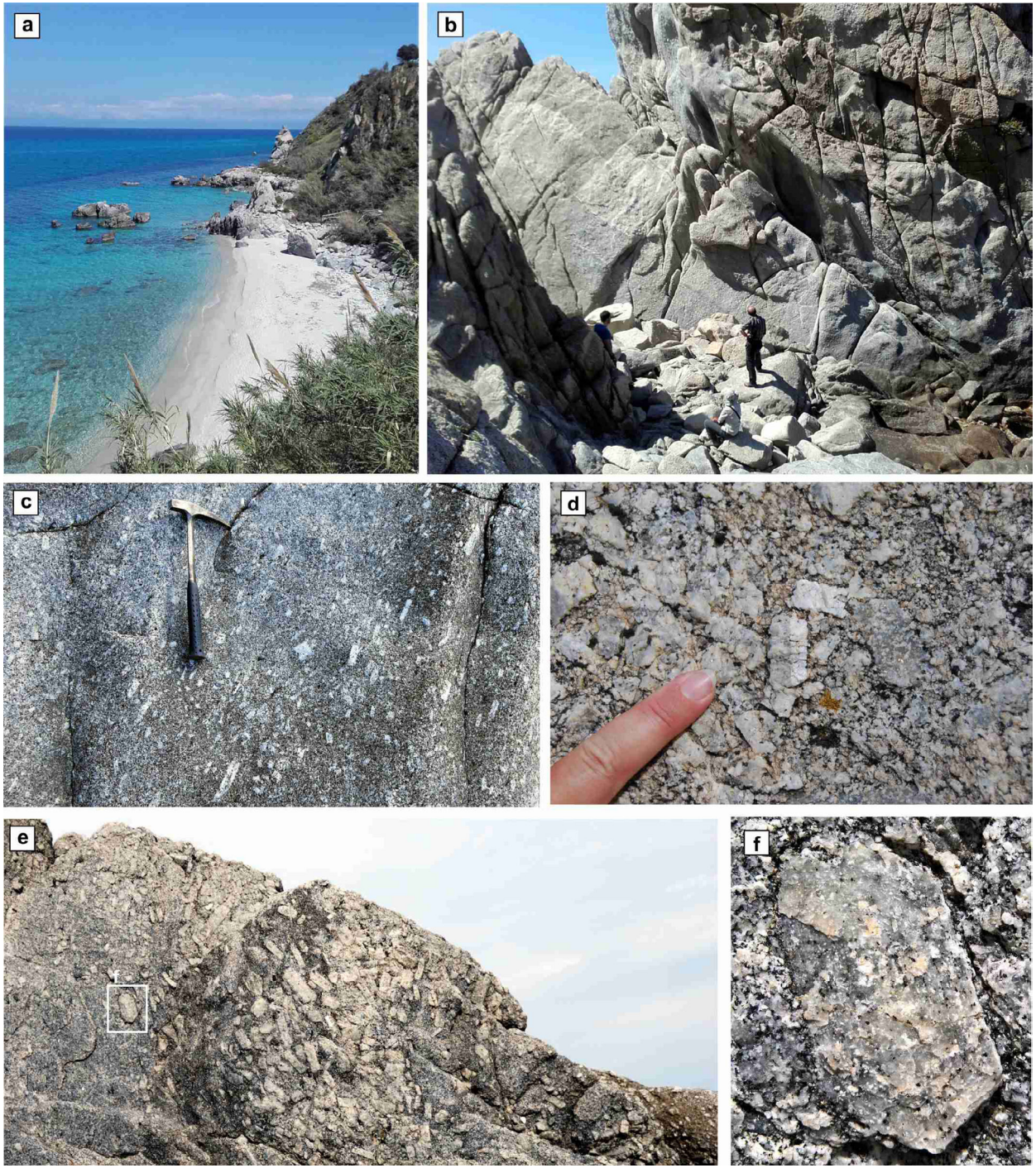

First, the beach hosts the largest accessible Calabrian exposure of fresh two-mica porphyritic granodiorites and granites (PMBG) that, in this area, exhibit variable large amounts of K-feldspar megacrysts ranging in size from 1 to ~ 12 cm.

K-feldspar megacrysts in granitic rocks have been traditionally defined as early grown in a predominantly molten system, below the rheological lockup threshold (~ 0.5 crystal fraction; e.g., Vernon and Paterson, 2008). Recent studies, starting from the observation that K-feldspar phenocrysts larger than 4 cm are exceedingly rare in compositionally similar volcanic rocks, have questioned this hypothesis (e.g., Johnson and Glazner, 2010; Glazner and Johnson, 2013). These studies ascribe the megacryst growth to late-stage textural coarsening caused by thermal cycling, that would remelt smaller crystals, providing material for the growth of more thermodynamically favorable larger crystals.

Michelino Beach is an ideal location to investigate the growth history of K-feldspar megacrysts and the rheology of megacryst-rich magmas. Field

Fig. 33 - (a) Panoramic view of Michelino Beach with granitic stack (Scoglio della Pizzuta) in the background; (b) lower part of the "Scoglio della Pizzuta"; (c) K-feldspar crystals aligned by magmatic flow; (d) accumulation of K-feldspar megacrysts, one of them with visible simple twinning; (e) other accumulation of K-feldspar megacrysts with box indicating the enlarged crystal in (f), exhibiting zoning and zonal arrangement of some biotite and plagioclase.

https://doi.org/10.3301/GFT.2024.09

observations highlight the presence of several relevant features such as flow structures given by megacryst alignment with no associated intracrystal deformation, mechanical accumulations, simple twinning and poikilitic texture with zonal arrangement of the included mineral phases (Fig. 33). All these features are diagnostic of relatively early crystallisation and growth of the megacrysts in a dominantly molten system, and some of them reflect free movement of the crystals in the magma, therefore indicating that K-feldspar can achieve their large final size below the rheological lockup threshold. A totally magmatic origin of the K-feldspar megacrysts from the adjacent Serre Massif was also proposed by Fornelli (1991), mostly based on the regular normal Ba zoning recorded in several analysed megacrysts.

PMBG at Michelino beach mostly contains large K-feldspar megacrysts, up to ~ 12 cm in size ("KA" type, after Cirrincione et al., 2013), even though a variety with rarer megacrysts, having a maximum length of 4 cm, locally occurs ("PA" type, after Cirrincione et al., 2013). In the KA PMBG (Figs. 34; 35a-d), poikilitic K-feldspar megacrysts are set in a medium- to coarse-grained matrix mainly composed of quartz, plagioclase, biotite, white mica and rare K-feldspar; magmatic white mica occurs both alone or surrounding biotite.

In the PA group (Fig. 35e-h), the matrix shows similar features except for slightly higher amounts of K-feldspar, minor amounts of biotite and for the local occurrence of fibrolitic sillimanite. K-feldspar from the megacrysts and the matrix is microcline in both KA and PA. Apatite, opaques, zircon, monazite and rare garnet occur as accessory phases in both PMBG types. The colour index is in the range of 15-21 and 8-13 in the KA and PA varieties, respectively.

Porphyritic granitoids from Parghelia were used in the antiquity as building material, and remnants of an ancient quarry of

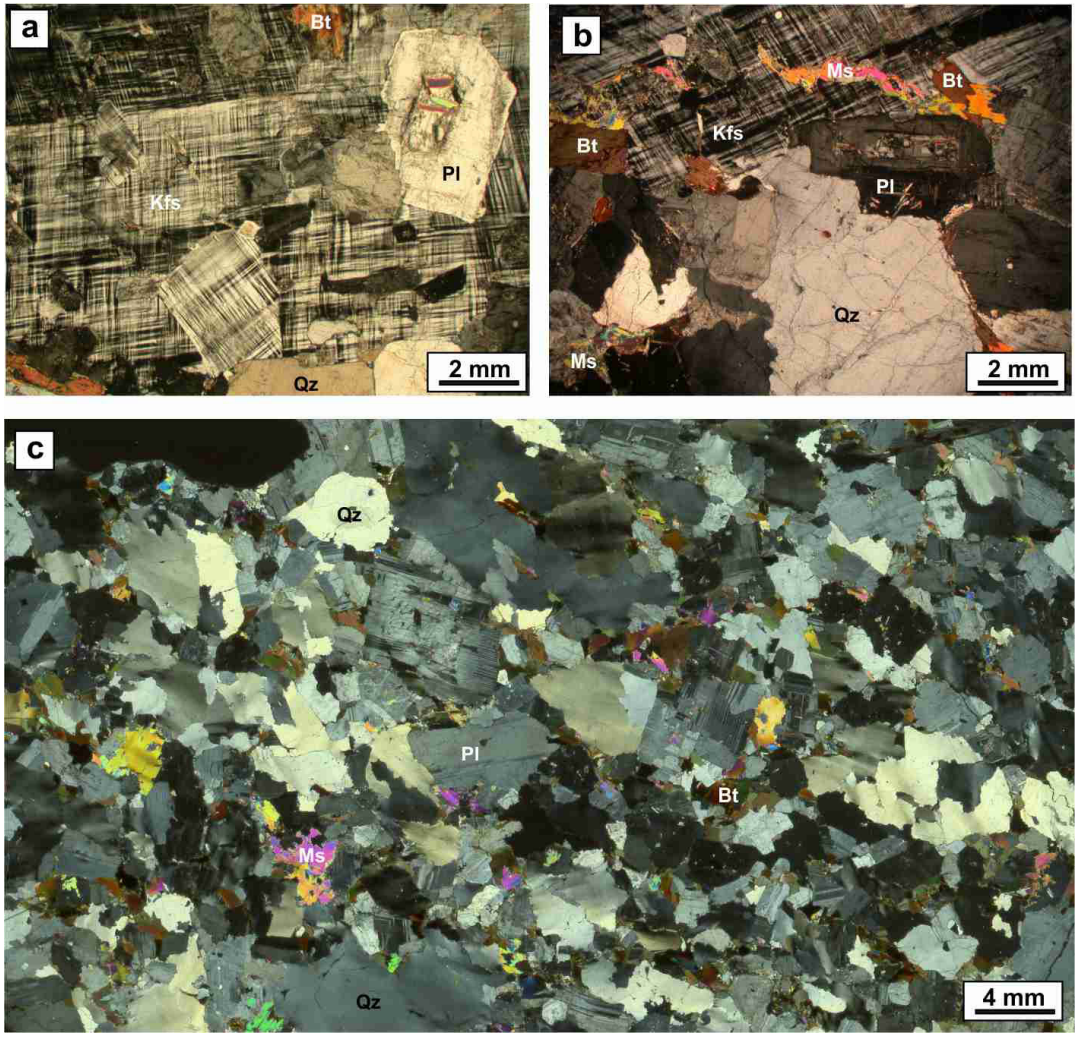

Fig. 34 - General petrographic features of KA PMBG. (a-b) portions of poikilitic microcline megacrysts with the inclusion of euhedral plagioclase and smaller microcline (a) as well as muscovite (b); (c) matrix with hypidiomorphic texture, absence of microcline and abundance of muscovite. Quartz exhibits a range of deformation microstructures, including a chessboard pattern developed at submagmatic conditions in the crystal in the upper centre of the image.

https://doi.org/10.3301/GFT.2024.09

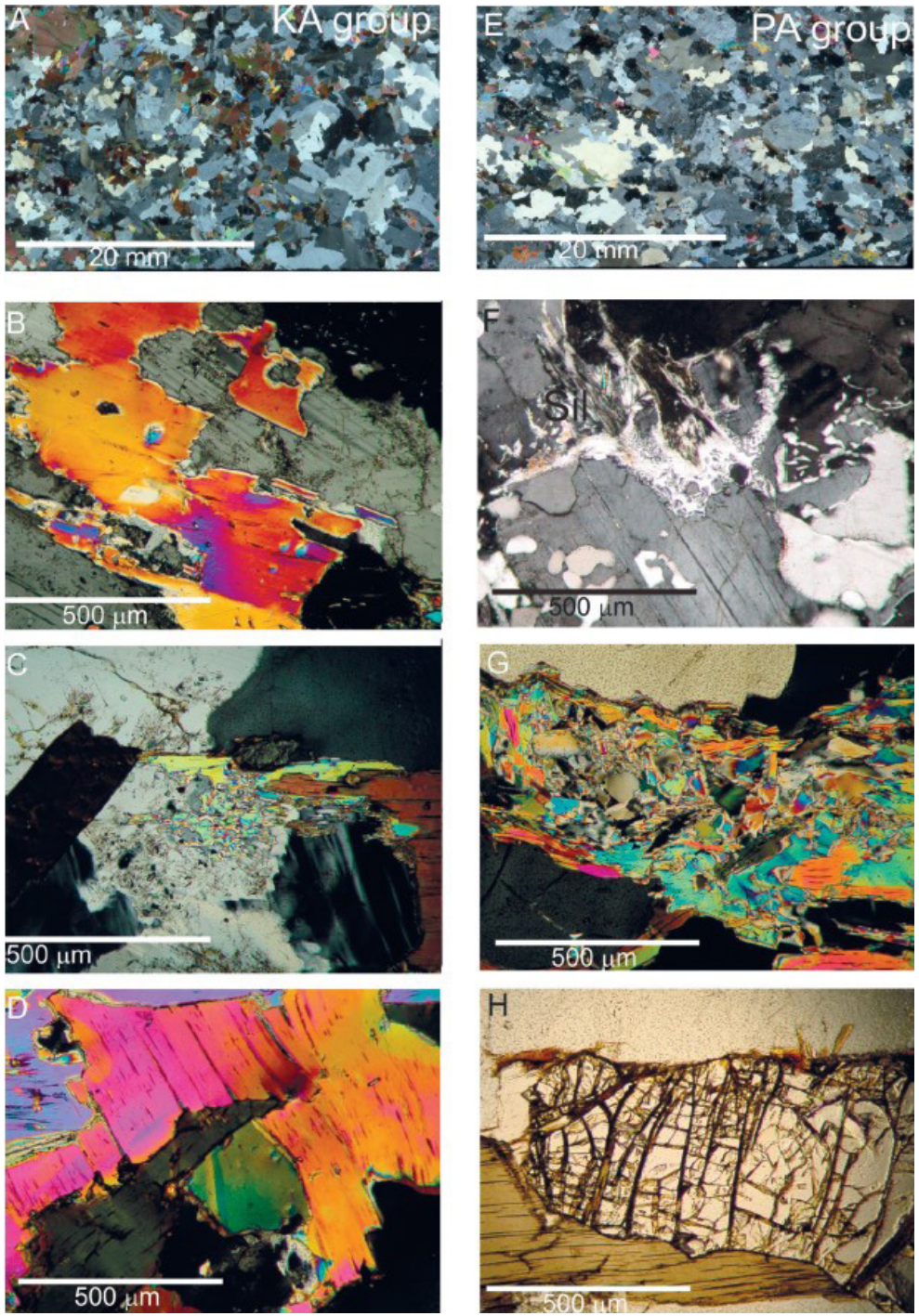

Roman age are indeed visible at Michelino beach (Cirrincione et al., 2013).

Michelino Beach is also one of the very rare places with well-exposed primary contacts between the PMBG and the host underlying tonalites (Fig. 36a), in this area belonging to the BT unit. Sharp intrusive contacts are visible at different locations on the beach; locally, the porphyritic granodioritic magma incorporated small rounded to angular blocks of tonalite (Fig. 36b), or displaced the mushy tonalite, disaggregating it in rounded blocks up to 1.5 metres in size (Fig. 36c). Compared to the interactions recorded at the base of the tonalite unit, such evidence indicates a more rigid state of the roof tonalites at the time of granodiorite emplacement, even though localised occurrence of small volumes of hybrid rocks attests to possible mixing between the granodioritic magma and the mushy tonalite. Finally, a filter-press mechanism is depicted by mechanical accumulation of K-feldspar megacrysts at a site where the granodioritic magma was intruding the mushy tonalite, but only the liquid part of the magma was able to pass through (Fig. 36d).

The BT in the Parghelia area (Fig. 3) are from the roof of the tonalitic unit and are typically represented by more felsic tonalites to minor leucotonalites. All the rock types are weakly foliated to unfoliated. Globular to weakly flattened cm- to m-sized mafic microgranular enclaves and pegmatitic-aplitic dykes are widespread in the BT unit. The tonalites (Fig. 37) exhibit a medium-coarse-grained texture, which is inequigranular for larger biotite and, especially, euhedral

Fig. 35 - Matrix features in PMBG from Michelino beach (after Cirrincione et al., 2013). KA variety (a-d); (a) matrix overview; (b) resorbed muscovite grain in association with plagioclase; (c) Muscovite overgrowing biotite rims; (d) Detail of mica aggregate. PA variety (e-h): (e) matrix overview; (f) fibrolitic sillimanite of restitic origin documenting muscovite breakdown; (g) fine-grained mica aggregate; (h) small garnet crystal. All images except (h) are at crossed polars.

https://doi.org/10.3301/GFT.2024.09

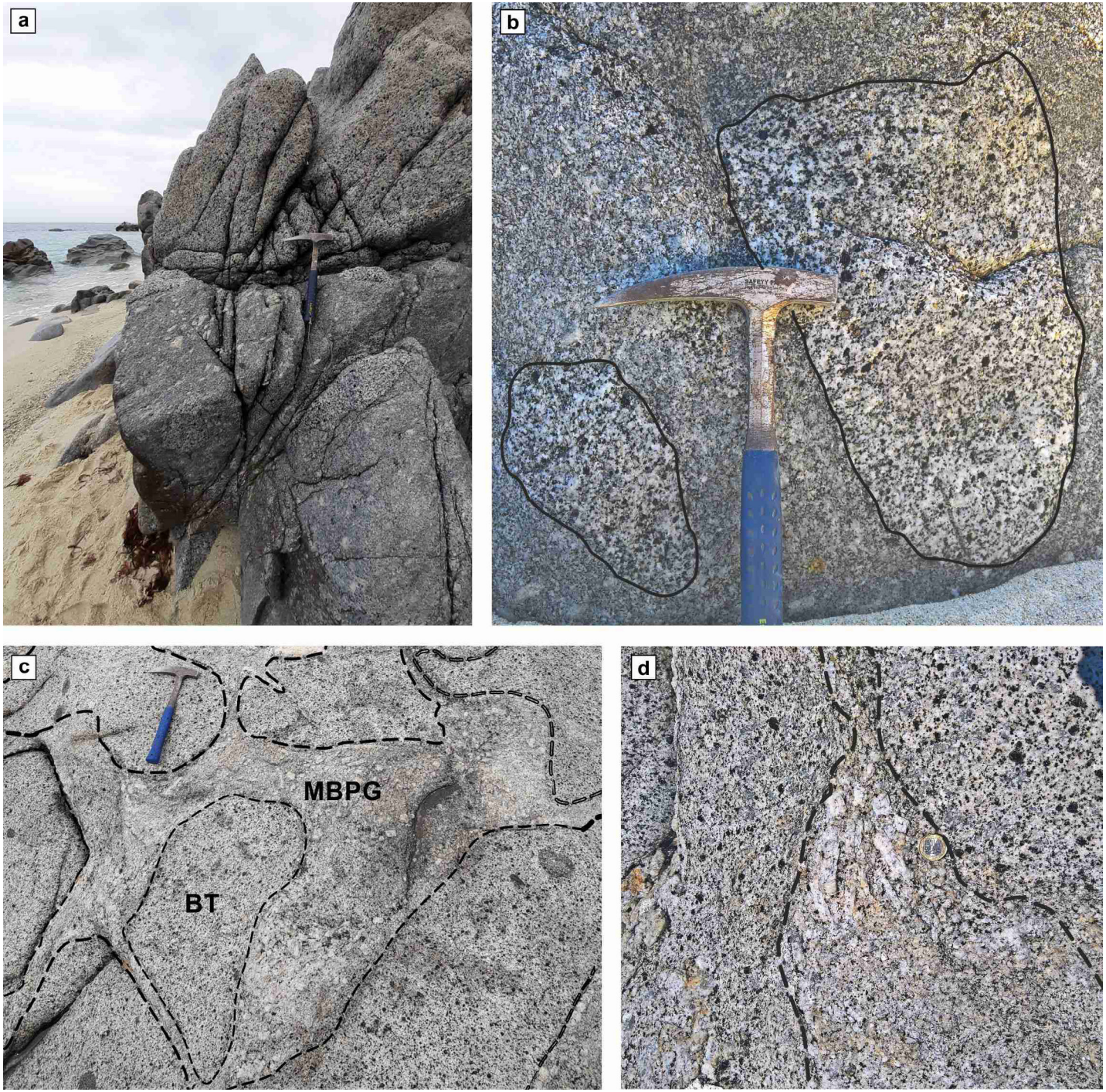

Fig. 36 - Magmatic contacts and magma-mush interactions between the intruding two-mica porphyritic magma and the tonalite mush. (a) Sharp contact between the two granitoid units; (b) rounded to angular tonalite blocks incorporated in the porphyritic granodioritic magma; (c) evidence of displacement to disaggregation into rounded to angular blocks of the mushy tonalite caused by the intrusion of the granodioritic magma; (d) K-feldspar mechanical accumulation with geometry indicating a filter-press mechanism.

https://doi.org/10.3301/GFT.2024.09

plagioclase up to 10 mm in size. The colour index is in the range of 15-35. The texture is usually hypidiomorphic with unzoned to weakly zoned euhedral to subhedral plagioclase (~ 55 vol. %), subhedral to anhedral biotite (~ 20 vol. %), both in clots and individual crystals and anhedral quartz (~ 25 vol. %). Rare interstitial microcline and small amounts of isolated platelets of muscovite occur in the most evolved terms. The typical accessory phases in the BT from CVP are epidote, allanite, ilmenite, titanite, apatite and zircon.

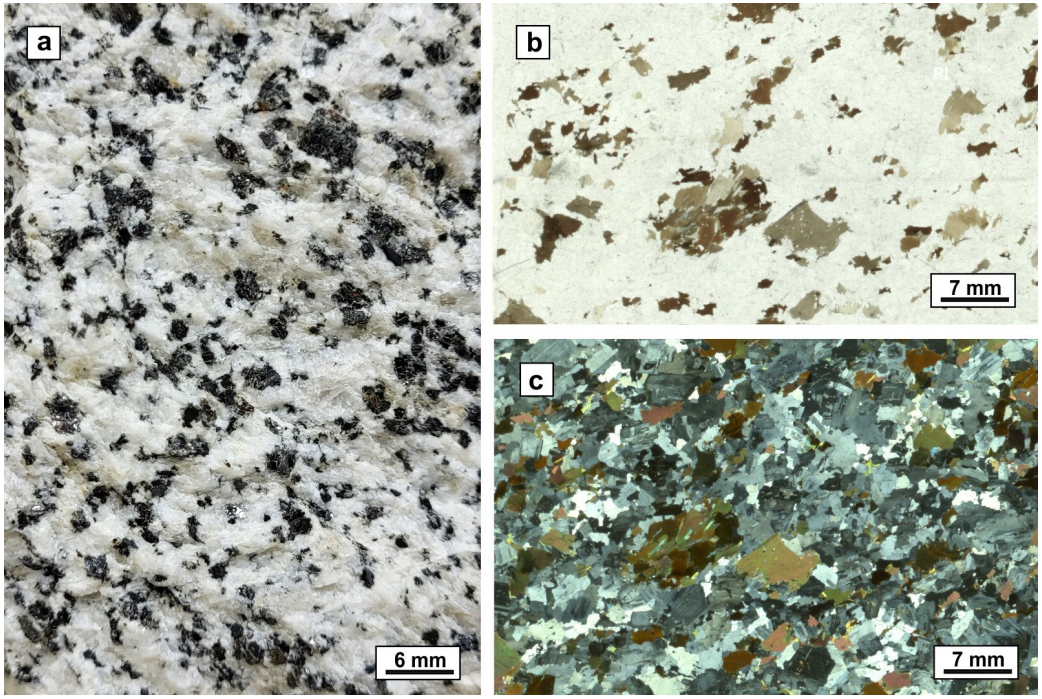

Fig. 37 - Mesoscopic (a) and microscopic (b-c) features of BT tonalites. (a) tonalite with a felsic composition and a weakly deformed structure, as typical for the tonalites from the top of the BT unit; (b-c) microdomains of a BT sample under parallel and crossed polars, showing the typical mineral assemblage and the hypidiomorphic texture with euhedral to subhedral plagioclase, subhedral to anhedral biotite in both clots and individual crystals, and anhedral quartz.

https://doi.org/10.3301/GFT.2024.09

DAY 3

MID- TO UPPER CRUSTAL GRANITOIDS, BUT ALSO «GEOLOGY AND HUMAN LIFE»

The third day will be partly devoted to the tight connections of the granitoids and other basement rocks with the architecture, productive activities and popular myths across central Calabria. The first stop will be at the Swabian-Norman castle of Vibo Valentia, still in the Capo Vaticano Promontory, largely built with the migmatitic paragneisses of the top of the lower crustal section. Then we will head to the Serre Massif, whose geology, in the areas far from the Ionian coast is largely hidden by forests. We will visit Serra San Bruno, a medieval «granite town» (~ 1100 B.C.), where most of the urban furniture, sidewalks and building elements are made of granite. The local granite consists of the same two-mica porphyritic granodiorites and granites of Capo Vaticano Promontory, in this area largely hidden by alluvial deposits and woodland. The next stop will be at a little quarry exposing the MBG. Then we will visit the «Megaliths of Nardodipace», masses of jointed and broken blocks of MBG, here transitional to the overlying granitoid unit, emerging from the bedrock up to ~ 8 metres. The next stop will be a few km southward, set in the shallowest and youngest (~ 292 Ma) main granitoid unit of the batholith, consisting in weakly peraluminous equigranular granodiorites (BG), with common MME occurrences. The last stop of the day will be at one of the locations where the BG are intruded by porphyritic dykes of dacite-rhyodacite composition.

Stop 3.1 - Swabian-Norman castle of Vibo Valentia

Coordinates: Lat. 38°40'16" N, Long. 16°6'30" E
Location: Vibo Valentia

The Swabian-Norman castle of Vibo Valentia (Fig. 38) is located in the area where once likely stood the Acropolis of Hipponion, one of the most important Greek colonies in Magna Graecia that became a Roman municipium with the name of Valentia in 182 B.C. and, finally, took the name of Vibo Valentia in 192 B.C.
Despite the first phase of construction of the castle structure being commonly attributed to the Norman era, it dates back to the Swabian period (1194-1266) and was then enlarged by Charles of Anjou in 1289, when it assumed a more or less similar appearance to today.
More interestingly, from a geological point of view, is that the Castle is located at the top of the hill made of the Stefanaconi paragneisses exposed at Stop 1.4 and that, as a natural consequence, migmatites are one of the building materials largely employed for the construction of the castle.

https://doi.org/10.3301/GFT.2024.09

Fig. 38 - Views of the Vibo Castle.

https://doi.org/10.3301/GFT.2024.09

Stop 3.2 - Serra San Bruno: the granite town

Coordinates: Lat. 38°34'42" N, Long. 16°19'55" E
Location: Serra San Bruno, old town and Certosa di Serra San Bruno

The cultural-geological visit to southern Calabria will continue with a walk in the historical centre of Serra San Bruno, whose origin is related to the arrival in Calabria of the monk Bruno di Colonia, founder of the Carthusian Order in 1053, who founded in 1092 the «Eremo of Santa Maria» in a forest area a few km south of the town; soon after, he started the construction of the Serra San Bruno Charterhouse, the most important Carthusian monastery in Italy and the second in Europe, after the Grande Chartreuse, mother house of the Carthusians, near Grenoble, in France.

The small town of Serra San Bruno was then built to host the men who worked at the construction of the Certosa. Unfortunately, the Certosa was nearly entirely destroyed, together with the Eremo di Santa Maria and the whole town, by the devastating 1783 earthquake. A few ruins remain of the original Carthusian complex, including those of the granite facade of the church. Both the Certosa, the Eremo of Santa Maria del Bosco and Serra San Bruno were then rebuilt, making large use of the local granite, here consisting of the two-mica porphyritic granodiorites and granites (PMBG).

Granite (of both local and external provenance) dominates the town, where most of the urban furniture, sidewalks and building elements in both civil and religious buildings are made of granite (Fig. 39).

In the Serre Massif, the PMBG pass southward to the overlying magmatic unit, consisting in two-mica equigranular granodiorites and granites. Field observations coupled with thin-section investigations revealed that the passage from the PMBG unit to the overlying MBG occurs through a transition zone, over an area ~ 500 m-wide (Russo et al., 2023). This width estimate mostly refers to the eastern boundary of the units, where the granitoids are characterised by better outcrop conditions and more continuous exposure. In more detail,

Fig. 39 - Examples of the employment of the Serre Batholith granitoids in Serra San Bruno monuments.

https://doi.org/10.3301/GFT.2024.09

the PMBG-MBG transition consists of a progressive decrease in the frequency of K-feldspar megacrysts. No systematic relationships between paleodepth and K-feldspar crystal shape or size was recorded, since the deepest regions of the unit are characterised by K-feldspar with a 0.5-12 cm length range; nevertheless, the largest megacrysts (>5-6 cm) do not occur in the uppermost levels. Quantitative density analysis of 1-6 cm long K-feldspar megacrysts, along several transects crossing the transition, revealed a gradual drop in megacryst occurrence at about 500 m approaching the MBG unit. In particular, megacryst density decreases from ~ 50 megacrysts/m^2 to ~ 20 megacrysts/m^2 in the first 400 m and then, from ~ 20 megacrysts/m^2 to no occurrence in about 100 m. According to Russo et al. (2023), such transition might reflect: (a) partial homogenisation of PMBG granitoids from the unit roof with the freshly emplaced overlying MBG magmas by crystal mush-magma mixing, or (b) remelting and recycling of PMBG granitoids into the younger MBG unit. Such processes have been envisaged by Žák and Paterson (2005) and Paterson et al. (2016), respectively, to explain transitional zones with similar size and features between granitoid units from the Tuolumne Intrusive Complex (Sierra Nevada Batholith).

Stop 3.3 - Quarry of two-mica equigranular granodiorites and granites

Coordinates: Lat. 38°30'06" N, Long. 16°21'06" E
Location: Quarry along the Serra San Bruno - Nardodipace statal road

This stop is at a small, abandoned quarry where typical two-mica equigranular granodiorites and granites from the intermediate-upper levels of the batholith are exposed (Fig. 40). The rocks from the MBG unit are often quite altered and those in this outcrop are not exception. The quarry however allows a relatively good observation of the field and mesoscopic features of these rocks.

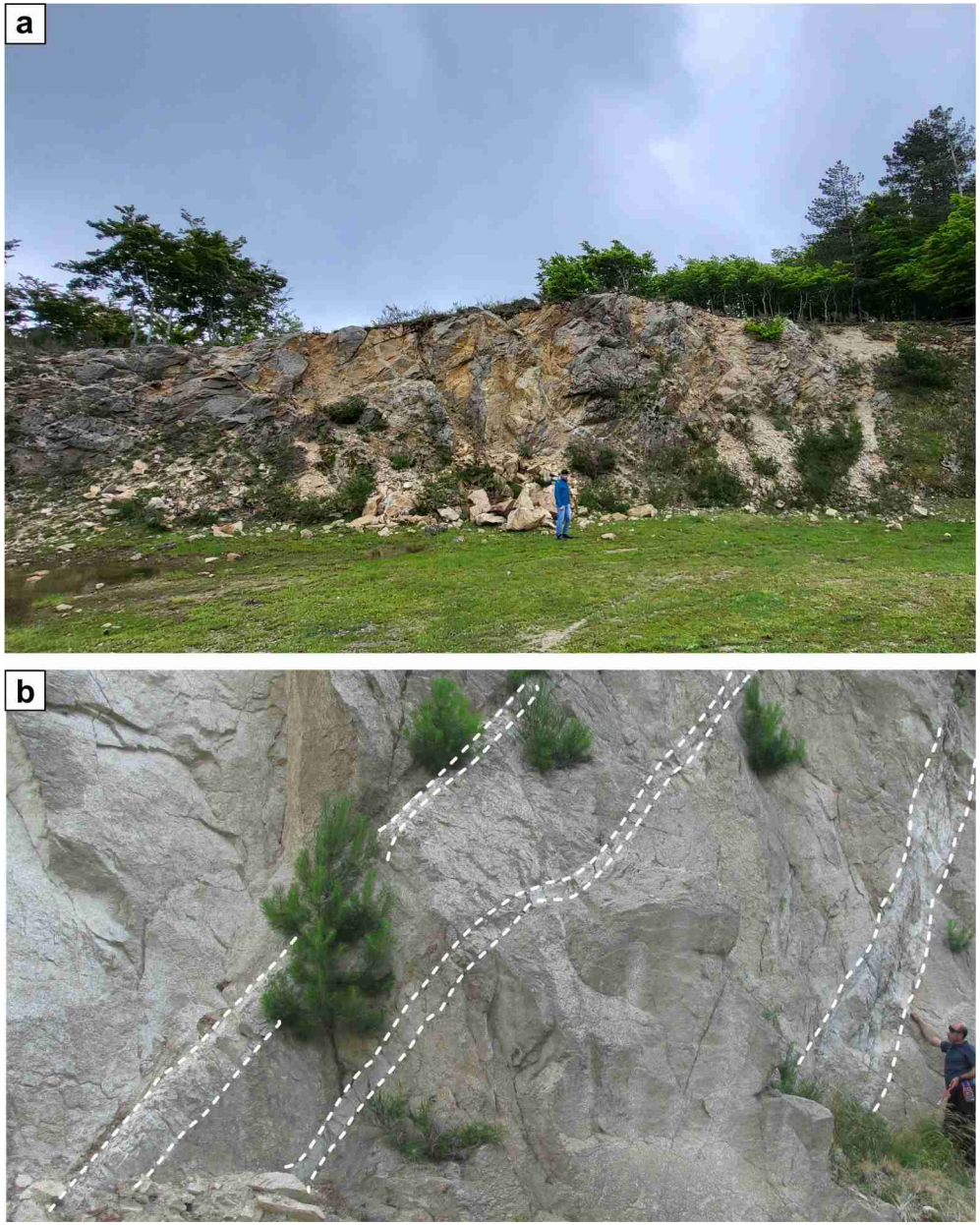

Fig. 40 - Field appearance of two-mica equigranular granodiorites and granites. (a) Abandoned quarry, with MBG cut by felsic dykes; b) MBG outcrop crossed by dm- to metre-thick steeply dipping felsic dykes with sharp intrusive contacts (after Fiannacca et al., 2021).

https://doi.org/10.3301/GFT.2024.09

MBG exhibit a slightly inequigranular medium grain size and a dominantly subhypidiomorphic and isotropic texture (Fig. 41). The main mineral assemblage consists of weakly zoned euhedral-subhedral plagioclase (~ 35 vol. %), anhedral quartz (~ 30 vol. %), subhedral K-feldspar (dominantly microcline, ~ 20 vol %), euhedral-subhedral biotite plates (~ 10 vol. %) and subhedral-anhedral muscovite plates (~ 5 vol. %). Zircon, apatite, monazite and ilmenite are the accessory phases.

Deformation microstructures (Fig. 42), described in detail by Fiannacca et al. (2021), include quartz chessboard, stretched mica aggregates wrapping feldspars, deformation twins in feldspars and kinked micas.

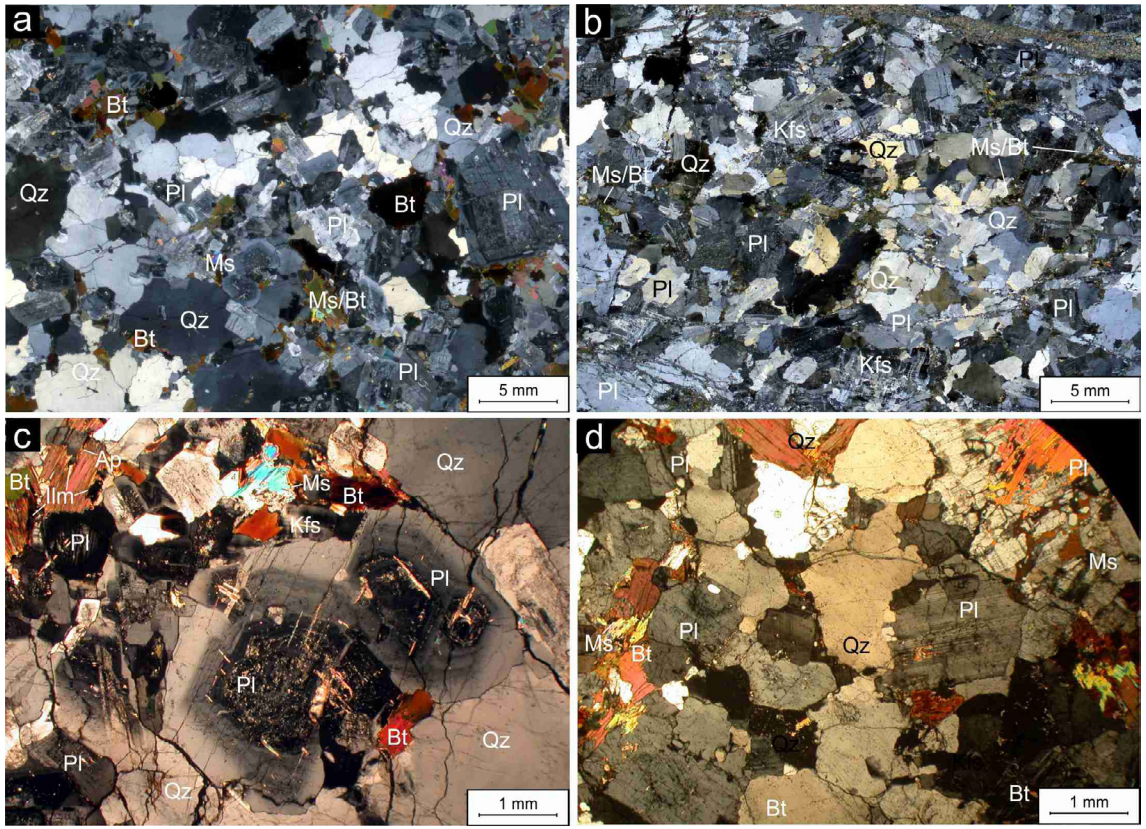

Fig. 41 - General petrographic features of the MBG (modified after Fiannacca et al., 2021). (a-b) Thin-section scans illustrating typical subhypidiomorphic to autoallotriomorphic microstructures; (c) MBG microdomain with zoned plagioclase, large quartz and finer-grained Ms-Bt-Pl aggregates; (d) MBG microdomain showing microcline-biotite and muscovite-biotite intergrowths together with roundish quartz largely exhibiting lobated boundaries.

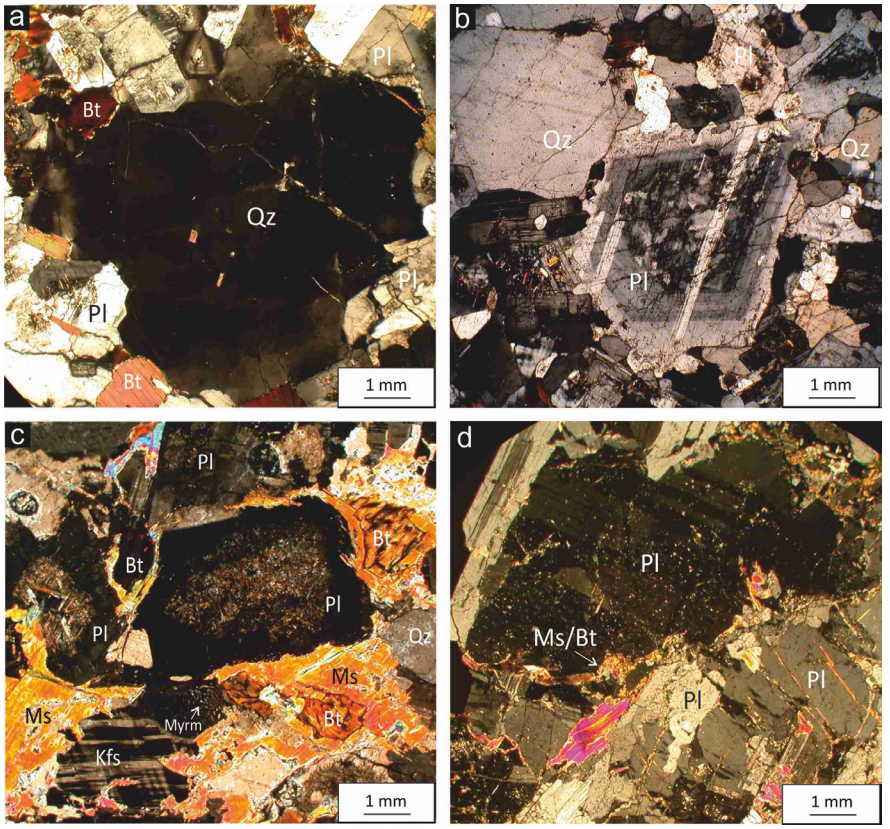

Fig. 42 - Deformation microstructures from submagmatic to solid-state low-temperature conditions in MBG (modified after Fiannacca et al., 2021). (a) Chessboard extinction in quartz; (b) strongly lobate boundaries indicative of GBM recrystallisation in zoned plagioclase; (c) slightly rounded feldspars bounded by deformed Bt/Ms aggregates; (d) deformation twins in plagioclase together with a mica fish indicating dextral sense of shearing.

https://doi.org/10.3301/GFT.2024.09

Stop 3.4 - The Nardodipace "megaliths"

Coordinates: Lat. 38°28'01" N, Long. 16°20'54" E
Location: Nardodipace Geosite B. Provincial Road, 2 km south of Nardodipace

Nardodipace "megaliths" are located in a forested area, 2 km south of the little town of Nardodipace. They were largely unknown until a large fire destroyed much of the dense vegetation in the area in the early 2000s.
With their imposing size and geometric regularity, these structures immediately aroused great attention and, in the last 20 years, they have been locally reported as human artefacts and many theories about their origin have been proposed, such as that they were erected by ancient populations as the Laestrygones from the Greek mythology. Many people in Calabria refer to these granite tors as the Calabrian Stonehenge.
Two main tors, about 6 and 8 m in height, are located at a distance of ~ 1 km from each other, and locally named Nardodipace Geosite A and Nardodipace Geosite B, respectively (Fig. 43). As typical for these landforms, the Nardodipace tors consist of castellated masses of jointed and rounded blocks emerging from the bedrock after denudation of the surrounding soil (e.g, Migoń, 2006; Raab et al., 2019).
The tors are made of two-mica granodiorites and granites like in the previous stop, but the MBG are here transitional to the Bt ± Am granodiorites forming the overlying BG granitoid unit.
Gradational contacts also typify the passage to the overlaying BG unit (Russo et al., 2023), as previously highlighted by Fornelli et al. (1994) and Servizio Geologico d'Italia (2016). In addition, Russo et al. (2023) described in detail the transition zone in the north-eastern Serre Massif and quantified its width as ~ 1.5 km in the western part of the studied area, and progressively decreasing to the east. The transition zone comprises granitoids with coexisting MBG- and BG-like features. The transition from MBG to BG has been defined by progressive: a) muscovite decreasing in both abundance and size; b) biotite increasing in abundance and size, and passing from tabular to stubby prismatic crystals; c) decreasing monazite abundance; d)

Fig. 43 - Nardodipace geosites. (a, b) Geosite A; (c) geosite B.

https://doi.org/10.3301/GFT.2024.09

increasing titanite, allanite and magmatic epidote; and e) K-feldspar passing from microcline to orthoclase. The transitional zone between MBG and BG is interpreted, as proposed for the PMBG-MBG transition, in terms of mixing between the MBG crystal mushes and the younger overlying BG magmas, or remelting and recycling of the MBG granitoids into the BG unit. Interaction of the uppermost MBG with the overlying BG magmas is supported by widespread disequilibrium features observed in plagioclase from transitional MBG, suggestive of reaction with a more mafic magma (Fiannacca et al., 2016a).

Stop 3.5 - The batholith roof: Bt ± Am granodiorites and MME at Fiumara Allaro

Coordinates: Lat. 38°26'44" N, Long. 16°20'32" E
Location: Fiumara Allaro, 500 m W of Nardodipace

In this outcrop on the banks of the Fiumara Allaro (Fig. 44a), the biotite granodiorites forming the shallowest and youngest main magmatic unit of the Serre Batholith (BG unit) are well exposed in both wall, pavement and boulder outcrops. The term "Fiumara" in southern Italy denotes a stream (more rarely a river) with a mostly short course, a very low flow rate in the warm seasons and, typically, a very wide, pebbly bed. Nevertheless, in the Nardodipace area, the course of Fiumara Allaro is characterised by narrow gorges up to about 6 km to the southeast.

The BG are here smooth and fresh and widely injected by dm- to m-sized mafic microgranular enclaves, usually globular, but locally flattened and stretched (Fig. 44 b-c). Dm- to m-thick pegmatitic and aplitic dykes, as well as dacite-rhyodacite porphyritic dykes, locally cut the BG.

Evidence of deformation and narrow shear zones locally occur within the BG (Fig.45), sometimes evolving into mylonitic bands up to 5 cm thick.

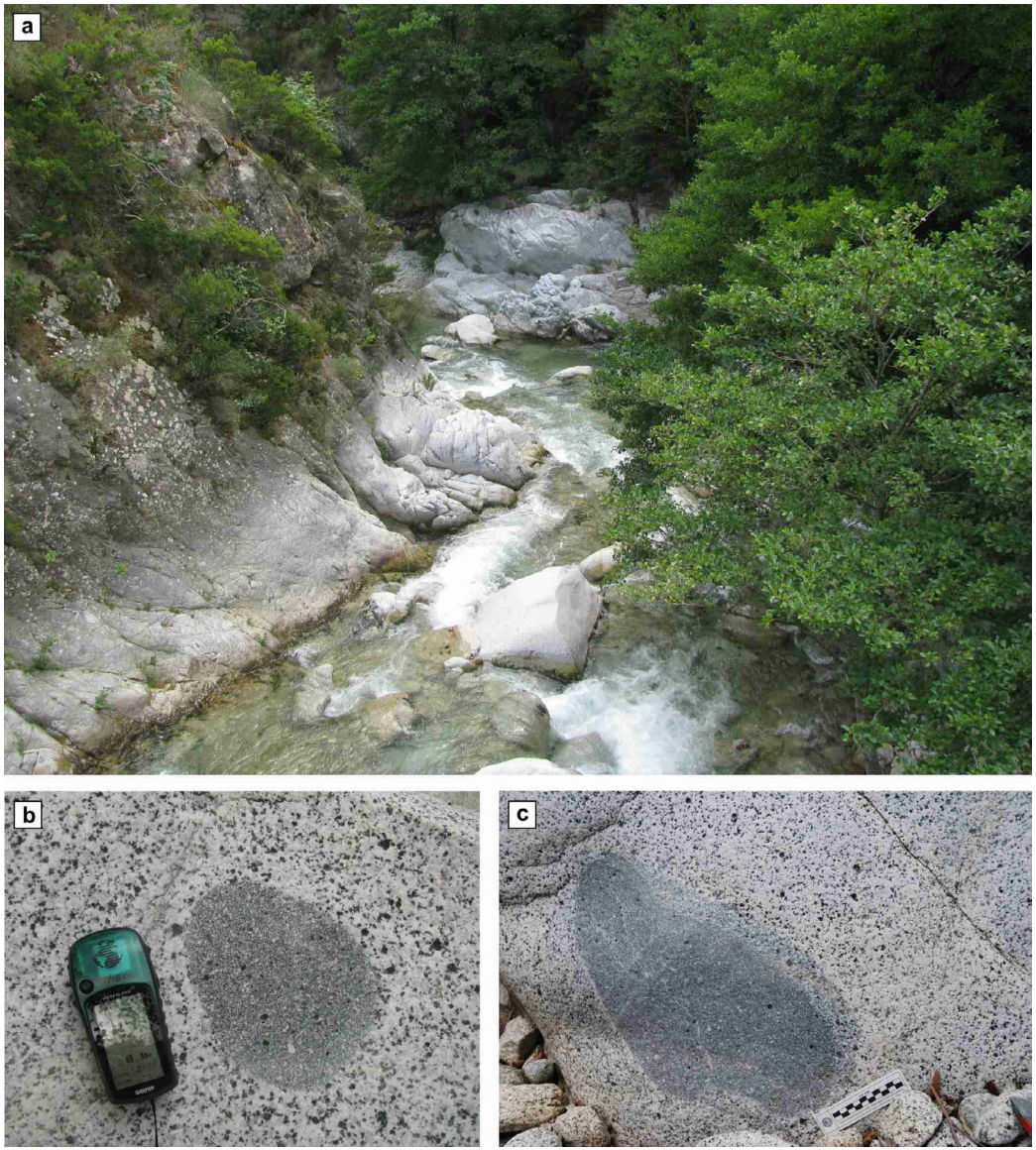

Fig. 44 - (a) View of the Fiumara Allaro from Ragonà bridge; rounded (b) to elongated (c) MME, the latter exhibiting a partly hybridised rim. Fig. 44c is from Cirrincione et al. (2015).

https://doi.org/10.3301/GFT.2024.09

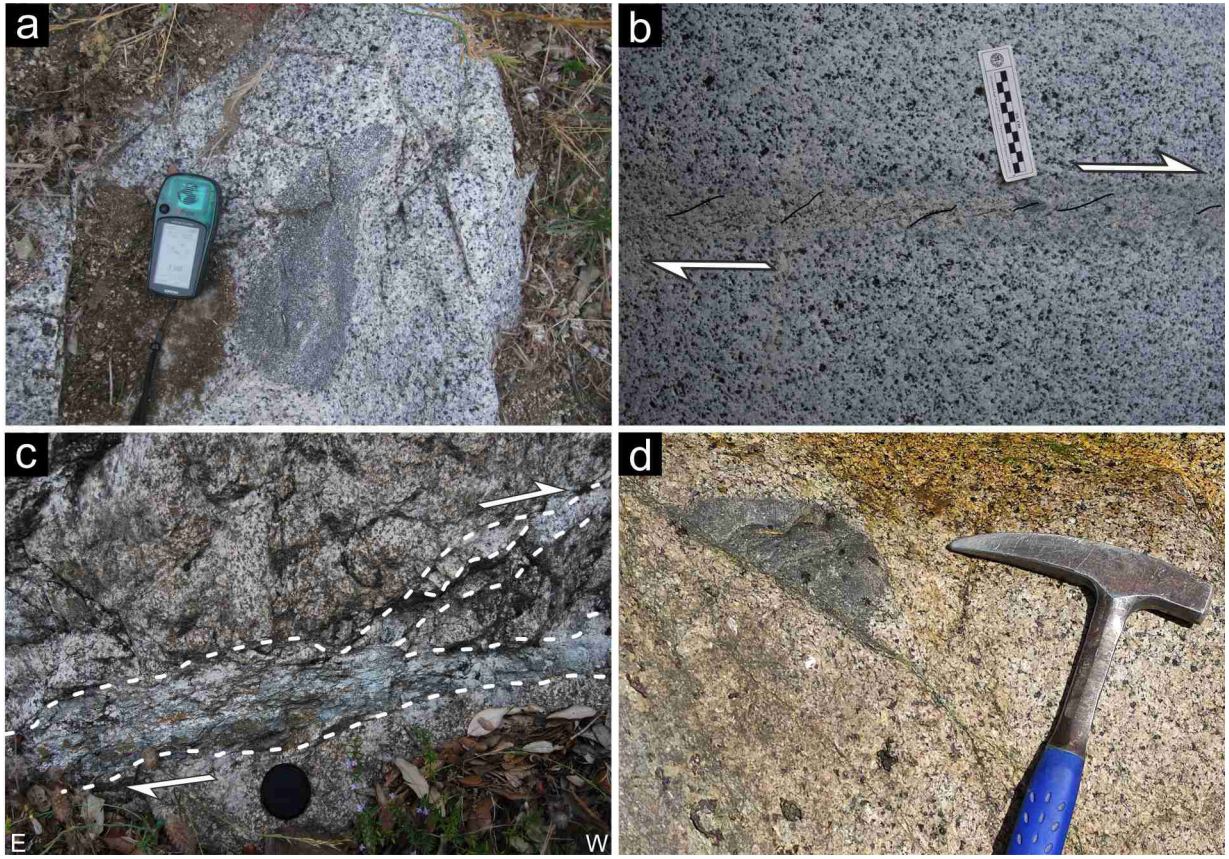

Fig. 45 - Evidence of deformation in the BG from the stop area (modified after Fiannacca et al., 2021). (a) Elongated mafic microgranular enclave; (b) narrow shear zone showing a dextral sense of shear; c) anastomosed shear zone with a dextral sense of shear; d) mafic enclave decapitated by a narrow shear zone; a weak fabric can be detected in close proximity of the tectonic structure.

Observed in thin section (Fig. 46), BG are mainly sub-hypidiomorphic and medium-fine-grained rocks, sometimes slightly porphyritic with larger plagioclase, quartz and biotite. Typical BG are made up of well-zoned euhedral-subhedral plagioclase (~ 35%), anhedral quartz (~ 30%), anhedral K-feldspar (~ 15%), and euhedral-subhedral biotite (~ 20%). K-feldspar mainly occurs as orthoclase, locally poikilitic with inclusions of quartz, biotite and plagioclase. Biotite typically occurs in euhedral barrel-shaped grains up to 1 cm thick. Hornblende rarely occurs, mostly as relicts partially replaced by biotite and fine-grained aggregates (Fig. 10f). Muscovite is mostly secondary, with platelets of primary origin only rarely occurring in some evolved compositions. Accessories consist of zircon, apatite, allanite, titanite, ilmenite and rare epidote. Allanite is always associated to biotite, often occurring in a metamict state. Epidote is mostly secondary, formed by alteration of biotite.

The microstructure is generally isotropic, a weak oriented fabric is locally observed in areas close to the contact with the upper crustal metamorphic host rocks. Most samples, from the whole unit, locally exhibit deformation microstructures such as quartz chessboard, submagmatic fractures, mica-fishes, deformation twins in feldspar and kinked biotite (Fig. 47; see Fiannacca et al., 2021 for details).

It is here interesting to remark that deformation microstructures are present in the granitoids from all the magmatic units of the batholith, from the deepest and oldest ABT-BT to the shallower and youngest BG; they range from typical submagmatic conditions (>650 °C) to low-temperature subsolidus conditions (<450 °C), with the latter largely obliterating the previous ones. This implies that a tectonic stress was active during all the cooling phases of the plutons, starting when melt was still present.

https://doi.org/10.3301/GFT.2024.09

A strong difference in fabric in the different granitoid units, already pointed out by Caggianelli et al. (1997, 2000), is very evident by comparing the shallow granodiorites and granites with no, or weak fabric, with the deep-seated strongly foliated quartz diorites and tonalites. Nevertheless, microstructural investigations of the shallowest and youngest main units (MBG and BG) by Fiannacca et al. (2021) highlighted a non-linear relationship between depth of emplacement and developed fabric, since not only a massive structure is typically observed in both MBG and BG, but also no relevant differences in deformation microstructures emerge from the comparison between the shallowest BG and the underlying MBG (Fig. 48). This would imply no significant change in the tectonic regime during the progressive emplacement of the strongly peraluminous MBG and the weakly peraluminous BG.

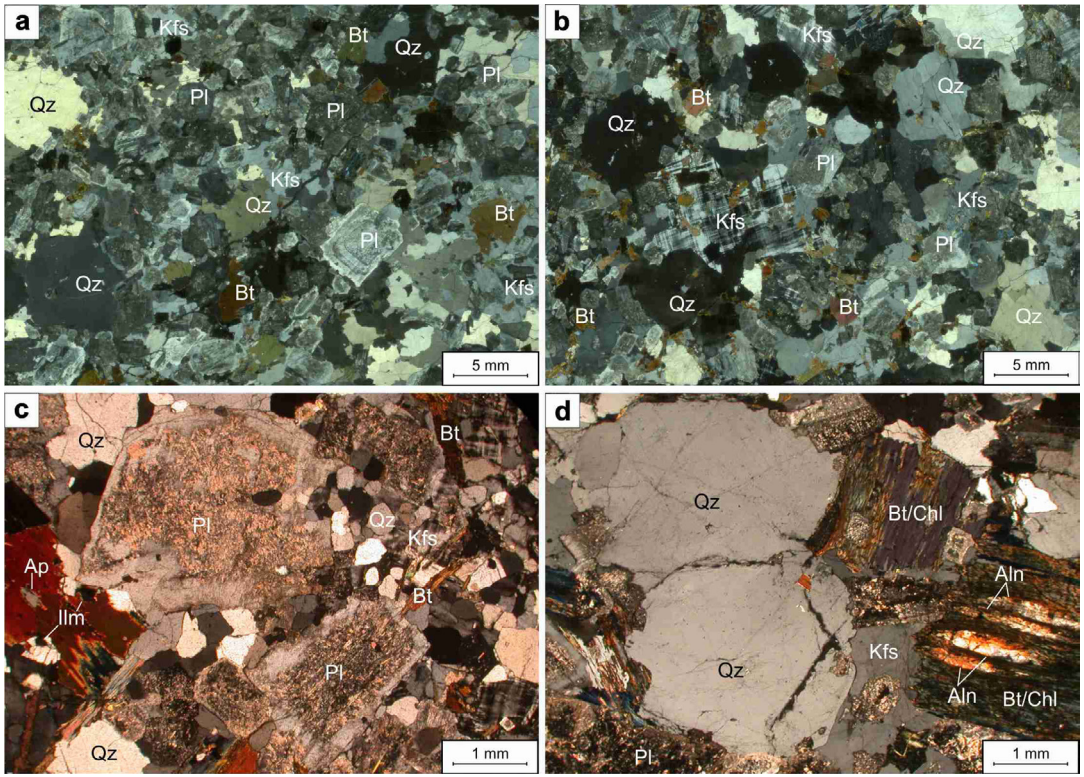

Fig. 46 - Thin section features of BG (modified after Fiannacca et al., 2021). (a-b) Thin-section scans showing a slightly inequigranular hypidiomorphic textures; (c) subhedral plagioclase crystals with sericitic core and unaltered rims surrounded by fine-grained recrystallised quartz aggregates; (d) subhedral quartz crystals, altered plagioclase grains and partially chloritised biotite with local inclusions of metamict allanite.

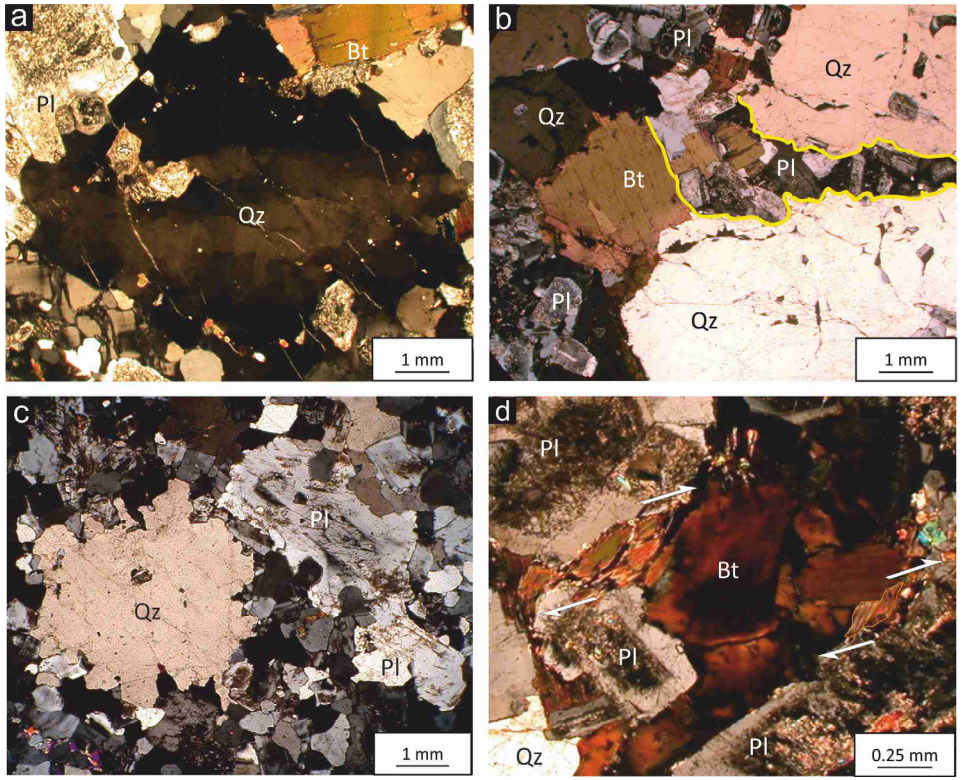

Fig. 47 - Deformation microstructures from submagmatic to solid-state domain in BG rocks (modified after Fiannacca et al., 2021. (a) Quartz crystal characterised by chessboard extinction overprinted by undulose extinction; (b) submagmatic microfracture (marked by yellow lines) filled by subhedral plagioclase and biotite after breaking apart a large quartz crystal; (c) quartz and plagioclase crystals with extremely lobed rims indicating high-temperature recrystallisation; (d) sub-millimetric biotite mica-fishes suggesting dextral sense of shearing.

https://doi.org/10.3301/GFT.2024.09

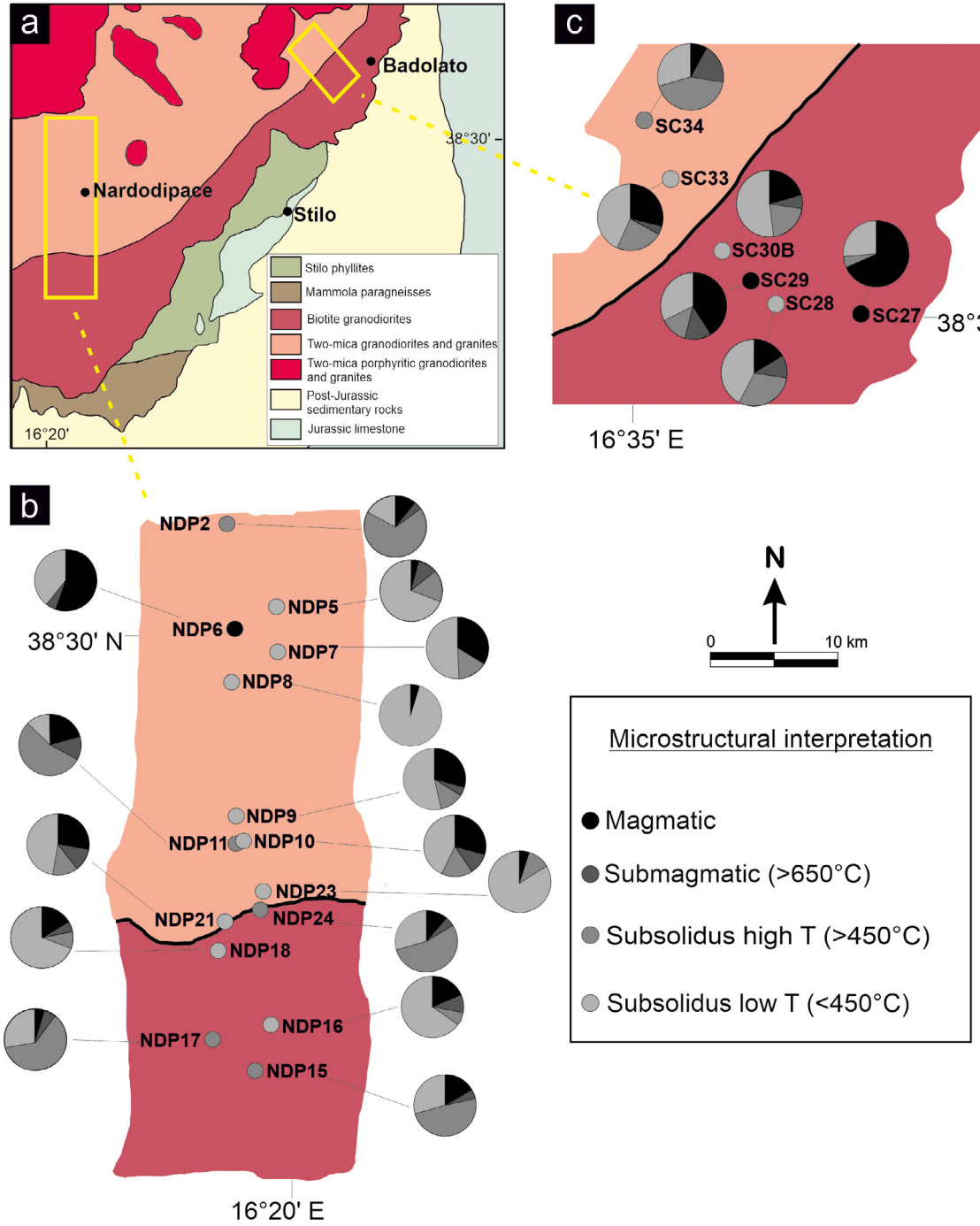

In addition, despite the upper crustal granitoids developed only very locally an oriented fabric at the micro- or mesoscale, preliminary AMS investigations by Fiannacca et al. (2021) detected an internal magnetic foliation in these apparently isotropic granitoids, represented by a mainly oblate AMS ellipsoid. In more detail, magnetic foliations and lineations are consistent with a stress field characterised by a shortening axis roughly oriented NW-SE (Fig. 49).
This, in association with local occurrence of field and microstructural evidence for shear-related deformation, might support the idea that the emplacement of the shallow-seated Serre granitoids was influenced by shear zone activity, in a likely waning stage, whose geometry and tectonic regime are still being investigated.

Stop 3.6 - The end of late Variscan magmatism

Coordinates: Lat. 38°27'41" N, Long. 16°22'16" E
Location: Country road, Santo Todaro Village

Late- to post-orogenic subvolcanic dykes, ranging in composition from rhyolite to dacite with minor andesites and basaltic andesites, extensively intruded the Bt±Am granodiorites from the Serre Batholith roof and the overlying

Fig. 48 -Semi-quantitative depiction of the different microstructures developed from supra- to LT subsolidus conditions in MBG and BG from the south-eastern Serre Massif (a), along two transects in the Nardodipace (b) and Badolato (c) area. Relative proportions of the different microstructural categories estimated in each studied sample are represented through pie charts. The different shades of grey of the location spot indicates the dominant microstructure in the related sample. Modified after Fiannacca et al. (2021).

https://doi.org/10.3301/GFT.2024.09

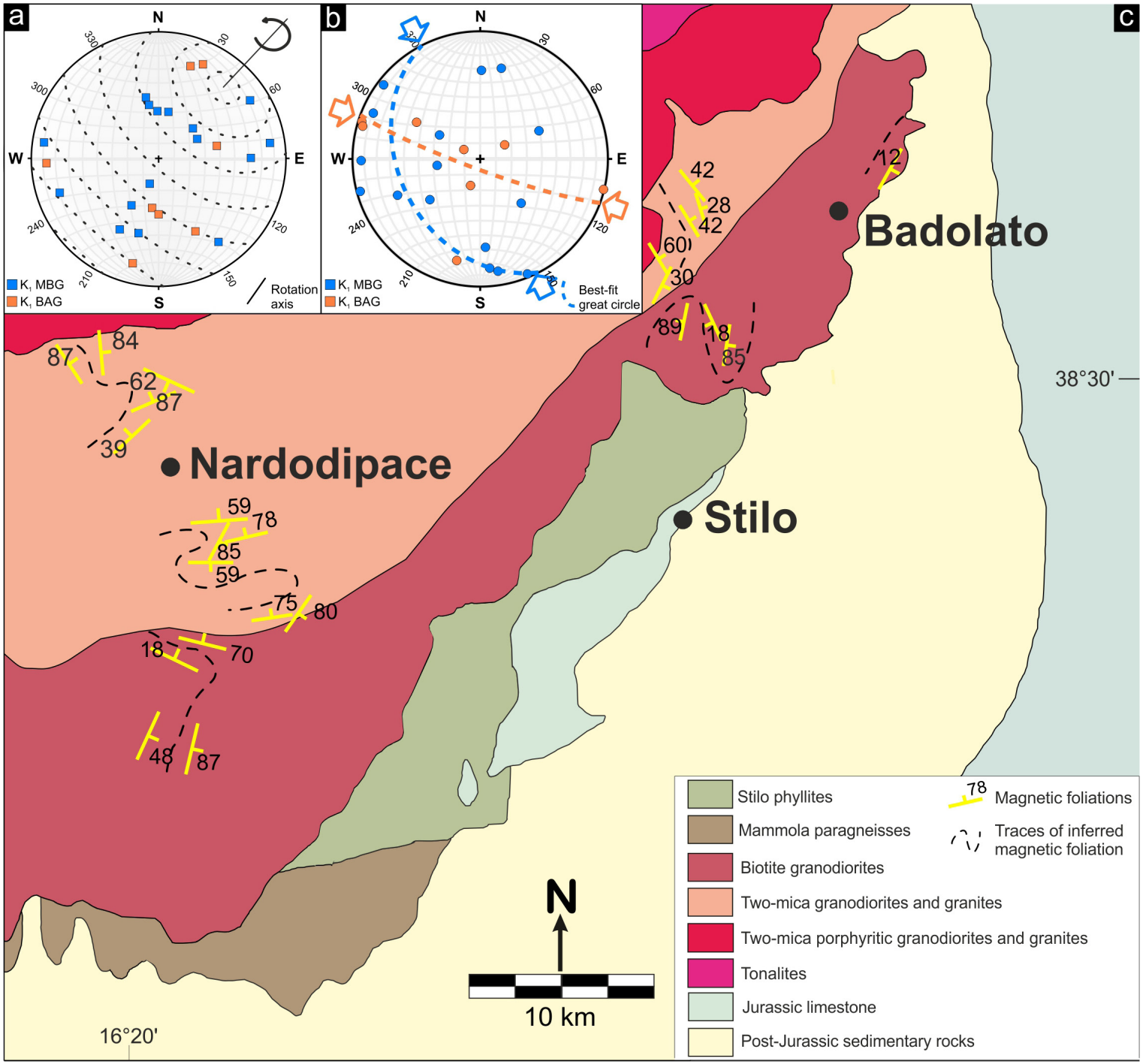

upper crustal metamorphic host rocks, marking the end of late Paleozoic magmatism in southern Calabria (Romano et al., 2011, and references therein). Swarms of dykes with similar composition and emplacement levels widely intruded also the Sila Massif, in northern Calabria, at ~ 280 Ma (Festa et al., 2010). These Calabrian subvolcanic products are framed in the felsic-intermediate and minor mafic subvolcanic magmatism which affected large areas of the west-European Variscan Belt in the early Permian (e.g., Pyrenees, Massif Central, Bohemian Massif, Spanish Central System, Sardinian-Corsica Domain; Romano et al., 2011, and references therein).

Fig. 49 - Magnetic data of the upper-seated granitoids of the Serre Batholith (modified after Fiannacca et al., 2021). (a) Stereographic projections of magnetic lineations (K1), dispersed around a NE-dipping gently inclined rotation axis; (b) Stereographic projections of poles to magnetic foliations (K3) with a dominant NW-SE distribution marked by inferred shortening axes (arrows); (c) sketch map of the study area with interpreted magnetic foliation trajectories.

https://doi.org/10.3301/GFT.2024.09

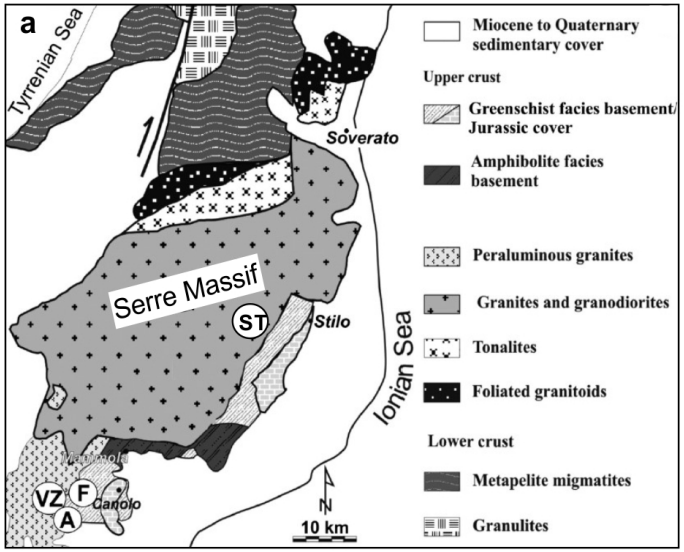

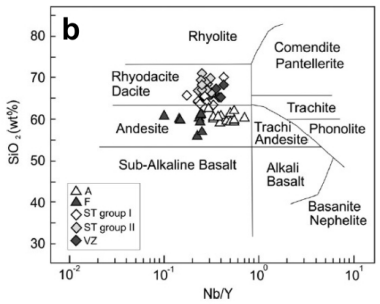

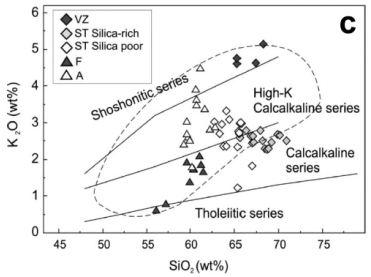

Fig. 50 - Geographical distribution, classification and affinity of subvolcanic rocks from the southern Serre Massif (modified after Romano et al., 2011). (a) Sketch map of the Serre Massif, with dyke locations. A: Antonimina, VZ: Villaggio Zomaro, F: Foletti Valley, ST: Santo Todaro; (b) SiO_2 vs. Nb/Y diagram (Winchester and Floyd, 1977) and (c) K_2O vs. SiO_2 diagram (Peccerillo and Taylor, 1976). The dashed area in (c) represents the field of the calc-alkaline post-Variscan dykes from the Sardinia-Corsica Domain (after Romano et al., 2011, and references therein).

In southern Calabria, four groups of intermediate to felsic dykes cropping out in the central-southern Serre Massif, have been investigated by Romano et al. (2011).

The dykes crop out in the Antonimina, Villaggio Zomaro, Foletti Valley and Santo Todaro areas (labelled as A, VZ, F and ST, respectively, in Fig. 50a). A and F dykes classify as andesites, whereas ST and VZ dykes are mostly dacites-rhyodacites, with some andesites among the more mafic ST dykes (Fig. 50b). The andesites have calcalkaline (F) to high-K calcalkaline (A) affinity, with a few Antonimina samples classifying as shoshonitic. The VZ dacite-rhyodacites are shoshonitic. The ST dacite-rhyodacites can be separated into silica-rich and silica-poor varieties, having calc-alkaline and high-K calc-alkaline affinity, respectively (Fig. 50c)

Stop 3.6 is located in an area where the BG are diffusively intruded by porphyritic dykes of dacite-rhyodacite composition (ST).

The ST dykes are dark brown in the field, porphyritic and 1-10 m thick, with tabular or lenticular shape. The dyke exposed at this stop is tabular and ~ 4 m-thick, with sharp contacts with the granitoid host rocks (Fig. 51).

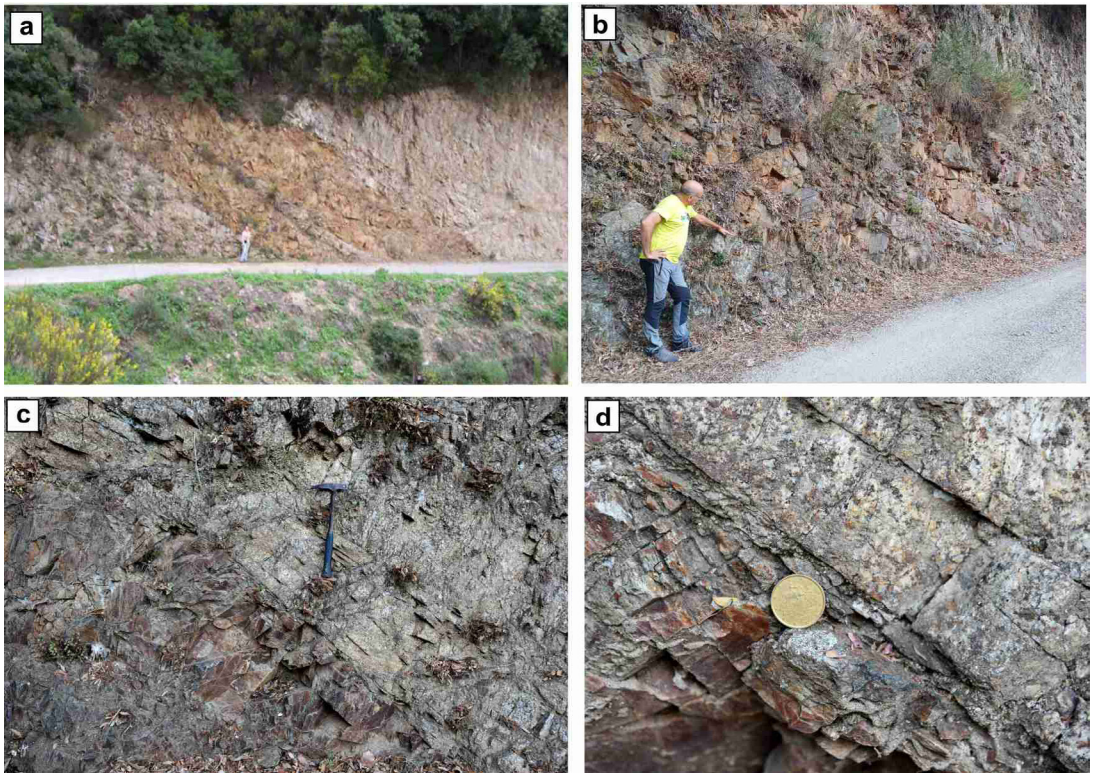

Fig. 51 – (a-d) Field appearance of the ST dacitic dyke exposed at Stop 3.6, with contacts with the host BG highlighted at different scales.

https://doi.org/10.3301/GFT.2024.09

In thin section (Fig. 52), ST dykes can be subdivided into two sub-groups:

- group I, with porphyritic texture, fine-grained matrix and white mica-poor secondary assemblage;
- group II, with porphyritic to equigranular texture, fine to medium-grained matrix, as well as abundant white mica in interstitial plats and radial intergrowths. Micrographic and radiating quartz-K-feldspar intergrowths also occur.

The porphyritic index is <7%, with extensively altered plagioclase and K-feldspar phenocrysts. Former mafic phenocrysts, mostly biotite and possibly amphibole, are now completely replaced by chlorite + rutile ± titanite. Matrix minerals consist of plagioclase, quartz, chloritised biotite, K-feldspar and muscovite. The accessory phases are zircon, rutile and acicular apatite. Finally, mm-sized quartz xenocrysts, larger than average phenocrysts size, rarely occur.

A lack of genetic relationships between the two groups of ST dykes is indicated by separate trends in variation diagrams for specific major and trace elements (e.g., MgO, Al_2O_3, TiO_2 and P_2O_5 in Fig. 53). Romano et al. (2011) suggest a derivation by hybridisation of basaltic mantle magma with metapelites for the ST (and VZ) dacite-rhyodacites, and by pure partial melting of metapelitic crust for the more SiO_2-rich and peraluminous rhyodacites.

The andesitic dykes (A and F) have been considered by the same authors to have resulted from partial melting of an enriched mantle source metasomatised by crustal fluids/melts during former subduction, and to have then suffered minor, if any, contamination after assimilation of lower crustal metapelites.

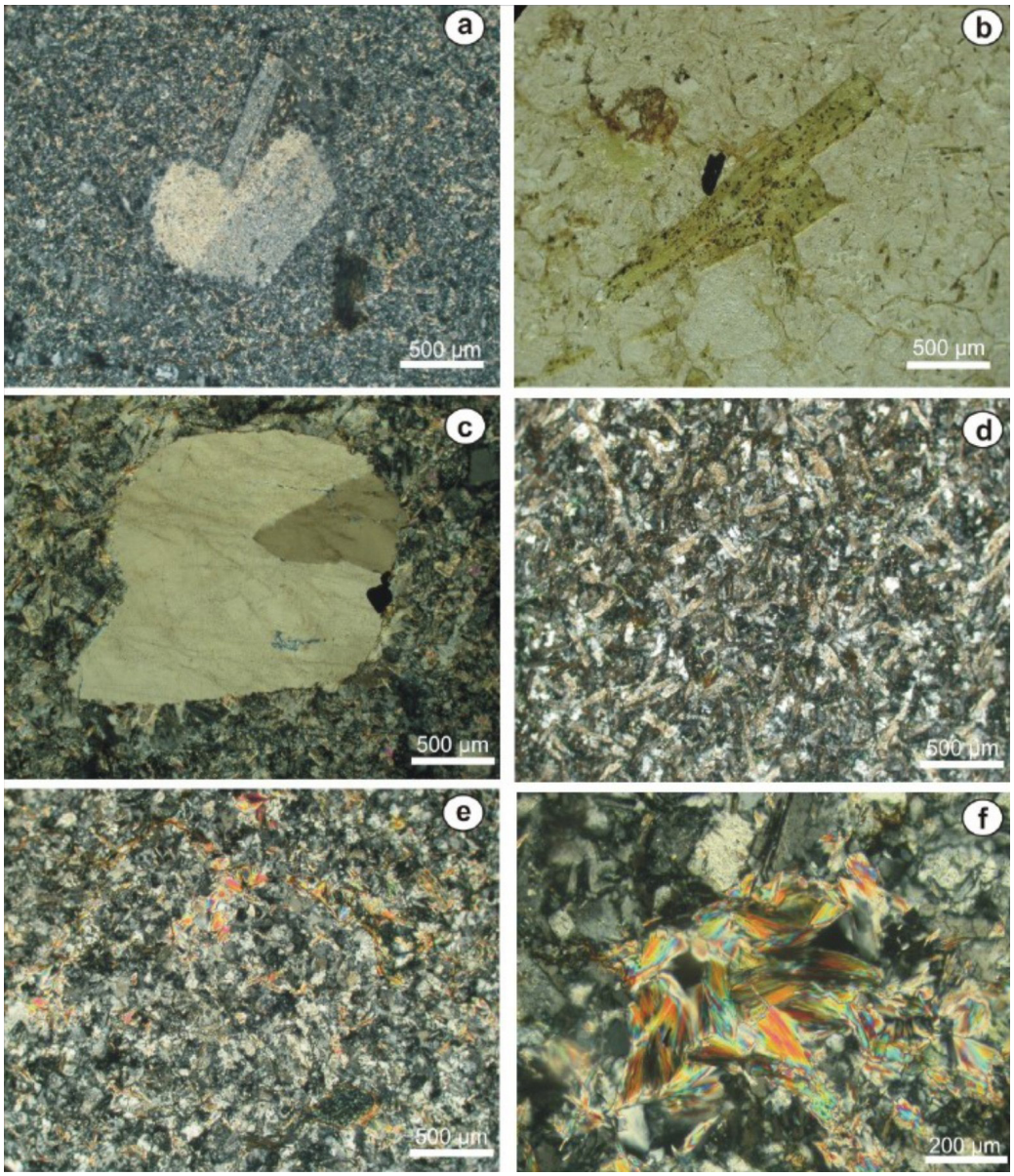

Fig. 52 - Petrographic features of ST subvolcanic rocks (after Romano, 2011). (a) Plagioclase and K-feldspar phenocrysts in a fine-grained groundmass mainly made of plagioclase, K-feldspar, quartz and chloritised biotite; (b) chlorite pseudomorphs; (c) quartz xenocrysts; (d) example of white mica-poor ST rock (group I); (e) example of white mica-rich ST rock (group II); (f) radiating white mica aggregated in Group II.

https://doi.org/10.3301/GFT.2024.09

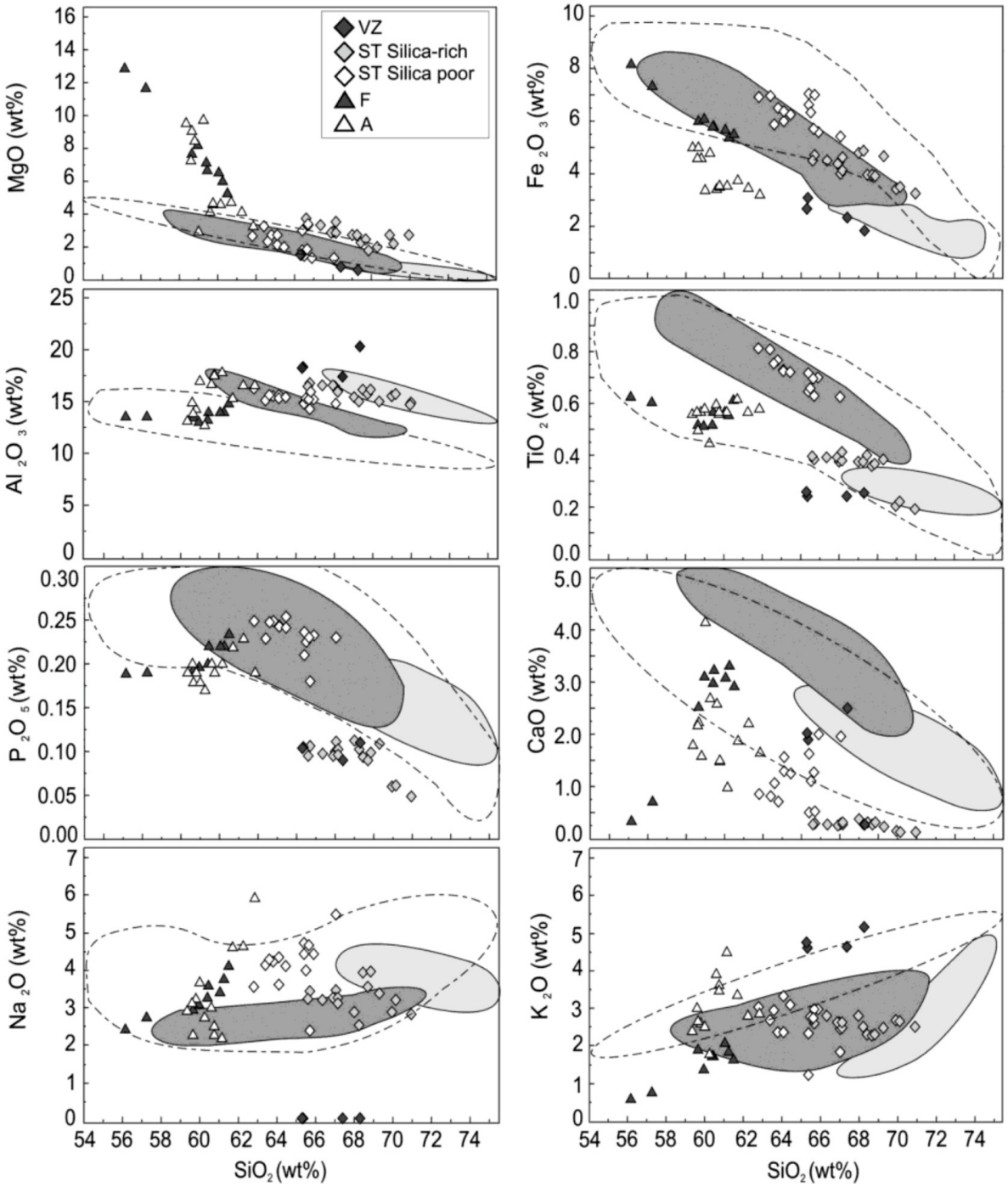

All the intermediate-felsic Serre dykes show indeed typical subduction-related geochemical signatures, as typical for post-collisional igneous rocks from the western European Variscan Belt. Overall, the calc-alkaline dykes, intruding Variscan phyllite and late-Variscan granitoid rocks, were likely generated in a post-collisional extensional context, characterised by lithosphere thinning promoting upwelling of hot asthenosphere. In such a context, the generation of both mantle, crustal and hybrid magmas can all take place. This is indeed the general framework envisaged for dykes of roughly similar composition widespread in Western Europe, for which a transition from a compressive to extensional geodynamic setting has been invoked to explain their geochemical features (Romano et al., 2011, and references therein). Calc-alkaline affinity and geochemical signatures of the hybrid post-collisional rocks have been interpreted as the result of interaction at varying extents with metasedimentary crust of mantle-derived magmas derived from subduction-modified lithospheric and/or asthenospheric mantle sources.

Fig. 53 - Major-element Harker diagrams for the subvolcanic rocks from the southern Serre Massif (after Romano et al., 2011). Symbols and dashed area as in Fig. 50. Grey and light grey areas: calc-alkaline and strongly peraluminous granitoids of Serre Massif, respectively (after Rottura et al., 1990).

https://doi.org/10.3301/GFT.2024.09

DAY 4

THE UPPER CRUST

The first stop of the day will be in the Stilo area, where we will observe a portion of the batholith's contact aureole, here consisting in spotted schists with porphyroblasts of biotite and cordierite. We will then visit a small stone quarrying and processing company, where the granites are not from typical quarries, but are instead the «Granitic stones of the Stilaro Valley», i.e., cobbles and boulders of alluvial origin. Then, we will visit outcrops documenting the final Permo-Carboniferous stages of granitic magmatism in Calabria, which produced swarms of pegmatite-aplite dykes, intruding both the upper crustal magmatic units and metamorphic host rocks. In particular, the leucogranitic dykes locally cut a well-developed mylonitic foliation, in the Mammola paragneisses, providing constraints on the Variscan age of the shear zone producing the mylonites. The final stop of the field trip will take us back again deep in the crust at the transition between the lower crustal migmatites and the syntectonic tonalites from the floor of the batholith, at Palmi. Here the Variscan metamorphic and magmatic rocks have been spectacularly deformed within a regional-scale Alpine shear zone (Palmi Shear Zone), associated with the tectonic juxtaposition of the Serre crustal section with the poly-orogenic (Cadomian-Variscan-Alpine) basement of the Aspromonte Massif, to the south.

Stop 4.1 - Spotted schists

Coordinates: Lat. 38°29'44" N, Long. 16°26'40" E
Location: Torrente Pardalà, Bivongi

Intrusion at shallow depth of the BG magmas produced a contact aureole, ~2 km wide, resulting in a post-tectonic metamorphic overprint in the host rocks, mainly consisting in paragneisses (Mammola Paragneiss Unit) and phyllites (Stilo Phyllite Unit). Thermal metamorphism partially, or completely obliterated the regional metamorphic texture. A cornubianitic texture is defined by static biotite, cordierite and andalusite appearing sequentially in spotted schists and hornfelses approaching the intrusive contact. The peak assemblage equilibrated at temperatures ranging from 535 to 590 °C and pressures from 1.75 to 2.00 MPa, verified by Al-in-hornblende barometry on granodiorite (Festa et al., 2013).
At this stop, the Stilo Phyllite Unit exhibits spotted schists (Fig. 54). These schists are typically grey in color, with a spotted appearance due to abundant static crystallisation of various minerals, predominantly cordierite porphyroblasts. Caggianelli et al. (2013) also reported andalusite up to a few centimetres in size. The field foliation S_1 (Fig. 54a) is affected by folding with metric to decimetric wavelength, locally highlighted by folded quartz layers (Fig. 54b).

https://doi.org/10.3301/GFT.2024.09

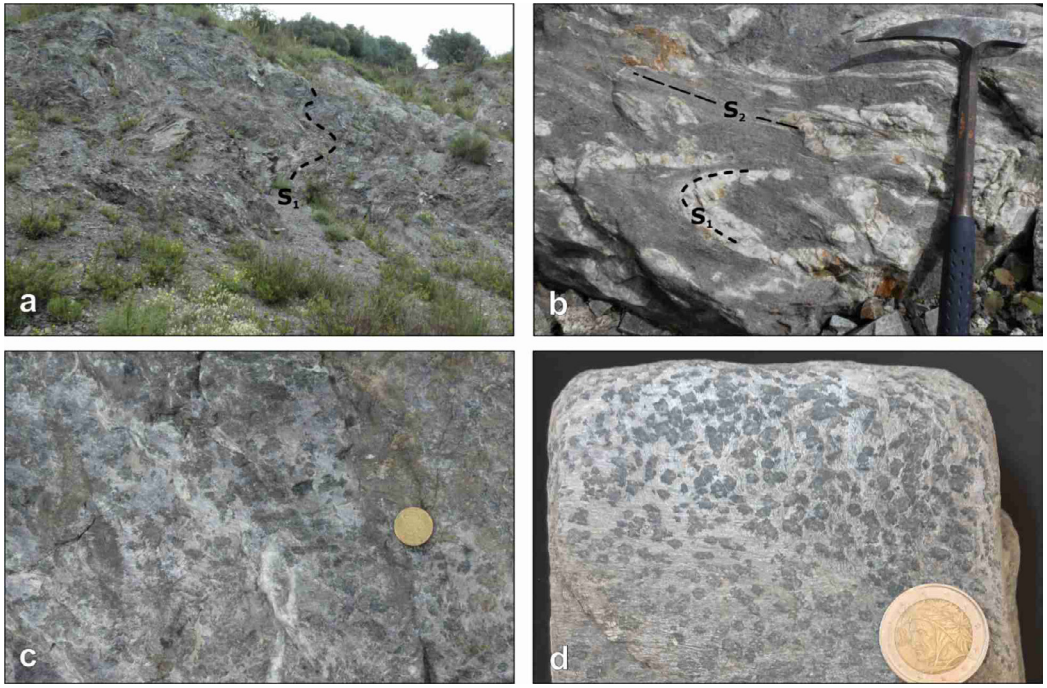

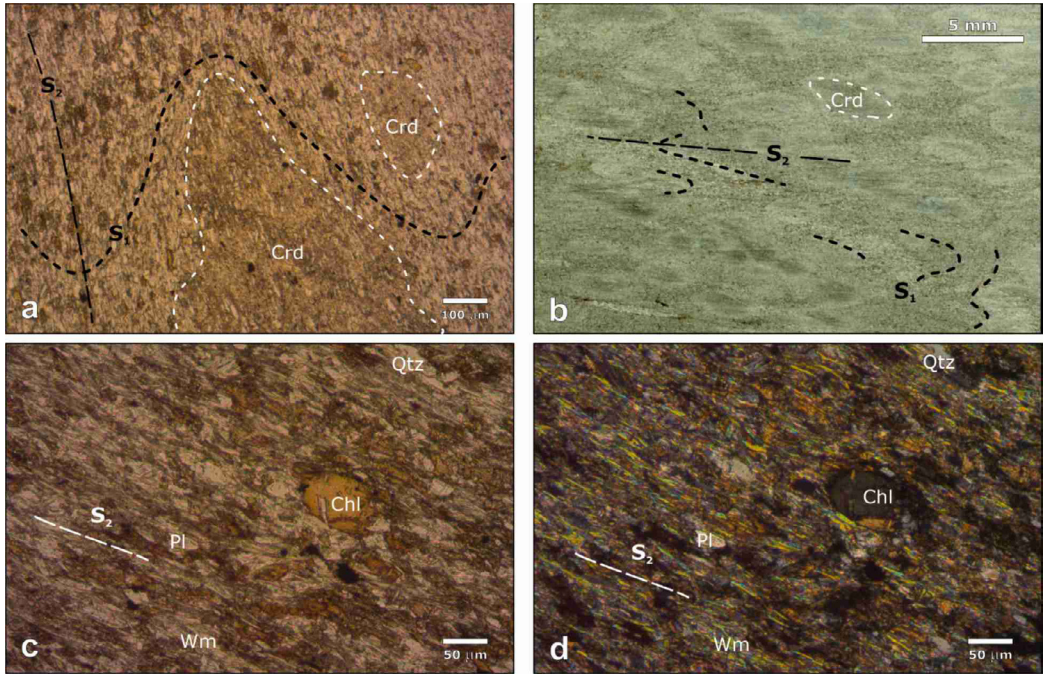

Fig. 54 - (a) Overview of the spotted schists exposure at Pardalà River; (b) S_1 foliation nearly isoclinally folded, forming a new planar axial surface foliation S_2; (c) static blastesis of cordierite is observable as dark spots on the outcrop surface; in the lower right part some porphyroblasts show a dark rim; (d) highly foliated hand-specimen with diffuse static growth of cordierite porphyroblasts.

Under the microscope (Fig. 55), the schists display a S_1 foliation that is crenulated and transposed into a new S_2 foliation. This new foliation has been overprinted by static crystallisation of relatively large porphyroblasts (up to a few mm) that have been nearly completely pinitised (ghost crystals of cordierite).

Stop 4.2 - Boulder granite quarry

Coordinates: Lat. 38°27'56" N, Long. 16°29'22" E
Location: Provincial Road 9 at Fiumara Stilaro, Stilo

This stop is at a small stone quarrying and processing company that has now ceased its activity. The particularity of this activity is that the granites were not extracted in quarries set in a late Variscan magmatic unit of the Serre Batholith (e.g., the BG, which are the closest to the stop), but are instead the «Granitic stones of the Stilaro Valley», i.e., cobbles and boulders of alluvial origin (Fig. 56).

Fig. 55 - Thin-section features of the spotted schists. (a) Crenulation of the S1 foliation (main field foliation) is developing a new axial plane surface, S2 foliation. A large cordierite porphyroblast (ghost crystal) is visible at the bottom centre of the picture (parallel polars); (b) a thin section scan of the spotted schist (parallel polars). Fine-grained white mica, biotite, plagioclase, quartz, ilmenite, and epidote are aligned along the S_1 foliation. The foliation appears locally microfolded, while ghost porphyroblasts (cordierite) with light-coloured halos are mainly oriented with their longer axes parallel to the S_2 foliation; (c-d) S_2 foliation is marked by the alignment of mica flakes (primarily white mica and minor biotite), quartz, plagioclase, and chlorite replacing biotite (parallel polars on the left, and crossed polars on the right).

https://doi.org/10.3301/GFT.2024.09

The quarry is indeed located on the right bank of the Fiumara Stilaro, a main fiumara in Calabria that in this area has deeply carved the basal conglomerate member of the Stilo-Capo d'Orlando Formation, which is a Miocene transgressive turbiditic unit covering non-conformably the basement of the southern CPO (Cavazza, 1989; Bonardi et al., 2002). The cobbles and boulders of the sedimentary succession largely consist of metamorphic and magmatic rocks, also including large amounts of granitoids. A Sardinian provenance of the sedimentary formation was proposed by Cirrincione (1996), based on the affinity of porphyrite pebbles included in the conglomerate member exposed in the Peloritani Mountains with late-Variscan high-K calc-alkaline dykes from central-eastern Sardinia. Nevertheless, the matching of petrological parameters in the sandstones and conglomerates with the upper crustal metamorphic and granitoid rocks of the Serre Massif (e.g., Cavazza, 1989; Critelli, 2018; Critelli and Martin-Martin, 2022), is mostly considered to indicate a local provenance of the Stilo-Capo d'Orlando Formation and, therefore, also of the "Granitic stones of the Stilaro Valley".

Stop 4.3 - Mylonitic paragneisses intruded by felsic dykes

Coordinates: Lat. 38°22'03" N, Long. 16°13'13" E
Location: Provincial road 5, Mammola

The upper crustal rocks exposed at this stop are the mylonitic paragneisses of the Mammola Paragneiss Unit, which are here intruded by different generations of late Variscan felsic dykes with thicknesses ranging from a few cm to ~ 1 m (Fig. 57), a clear indication that the shearing event was Variscan itself.
In more detail, most dykes are post-tectonic, either concordant or discordant with the steep mylonitic foliation. Nevertheless, a minor dyke generation consists of late-tectonic weakly sheared dykes, which attest to shear zone activity still taking place during the final stages of Variscan magmatism in the area.
As for the tectono-metamorphic evolution of the Mammola paragneisses, two different metamorphic cycles have been identified by Angì et al. (2010), and confirmed by

Fig. 57 - (a) Outcrop of Mammola paragneisses intruded by decimetric to metric felsic dykes both concordant and discordant with the steep mylonitic foliation; (b) detail of the mylonitic foliation; (c) detail of post-tectonic concordant dykes (modified after Ortolano et al., 2022, and references therein); (d) same outcrop with thin late-tectonic discordant dyke (modified after Ortolano et al., 2022); (e) detail of (d) showing the interfingered boundary with evidence of mylonitic deformation between the late-tectonic dyke and the host paragneiss.

https://doi.org/10.3301/GFT.2024.09

Tursi et al. (2020) and Ortolano et al. (2022), based on field and thin section investigations (Fig. 58):

- polyphase orogenic metamorphism with $D_1 \rightarrow M_1$ and $D_2 \rightarrow M_2$ phases and a final retrograde mylonitic evolution ($D_3 \rightarrow M_3$), during which, according to Angì et al. (2010) and Fiannacca et al. (2017), the granitoids forming the main magmatic units of the Serre Batholith were emplaced at progressively decreasing depth;
- late to post-tectonic thermal metamorphism caused by the intrusion of the upper crustal late Variscan granitoids.

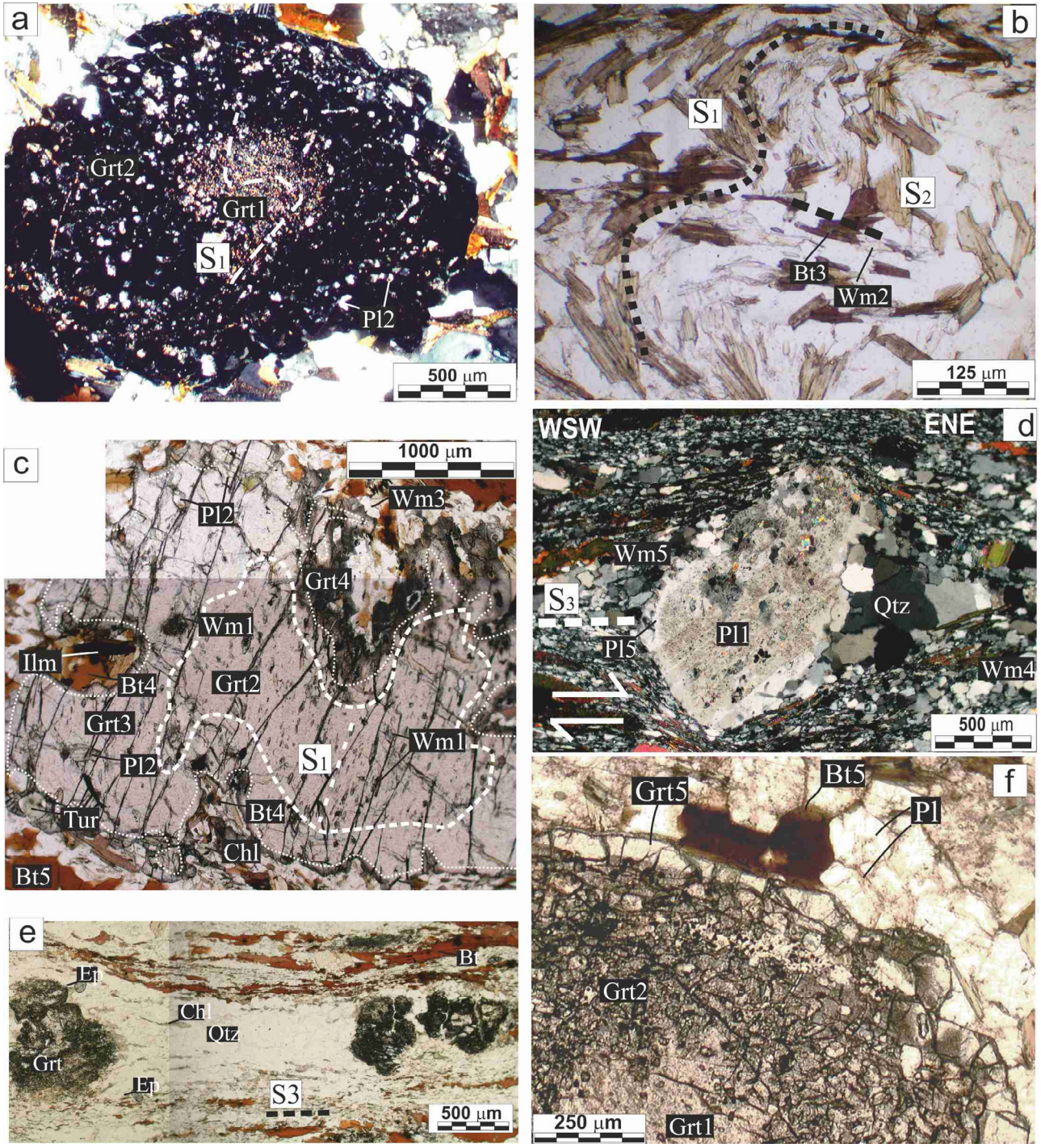

Fig. 58 - Microphotographs documenting sequential blasto-deformational stages in Mammola paragneisses (modified after Angì et al., 2010). (a) Early-M1 assemblage consisting in zoisite inclusion trails in garnet core (Grt_1) in equilibrium with Pl_1, Bt_1, and Qtz and prograde garnet overgrowth (Grt_2) in equilibrium with Pl_2 and $Wmca_1$ (crossed polars); (b) crenulation event D_2 producing folding of S_1 schistosity and development of S_2 schistosity defined by Qtz+$Wmca_2$±Bt_3 (parallel polars); (c) prograde to peak assemblages given by zoisite-free garnet outer core (Grt_2) in association with $Wmca_1$ and Bt_2 and by Grt_3 overgrowths in equilibrium with Pl_2. Garnet embayments filled by $Wmca_3$+Pl_3+Bt_4+Chl+Ilm intergrowths in equilibrium with garnet rim overgrowth (Grt_4) represent early-M_3 retrograde stage (parallel polars); (d-e) late-M_3 stage, producing a $Wmca_4$+Chl+Ep+Pl_5 retrograde assemblage and non-coaxial syn-mylonitic structures; (d) σ-type porphyroclast providing a top-to-ENE–NE sense of shear (crossed polars); (e) boudinaged garnet porphyroclasts attesting to mylonitic deformation in an extensional regime (parallel polars); (f) thermal metamorphic stage documented by static blastesis of Grt_5 in equilibrium with Pl_5 and Bt_5 porphyroblasts, forming limpid rims on syn-tectonic garnet (parallel polars).

https://doi.org/10.3301/GFT.2024.09

The main foliation in the Mammola paragneisses is the mylonitic foliation related to the retrograde mylonitic evolution, even if the subsequent thermal cycle induced a significant mineralogical-textural re-equilibration that partly obliterated the previous fabrics by annealing recrystallisation. In addition to the crystallisation of static garnet rims and randomly oriented Bt and Pl porphyroblasts, the annealing process is documented by strongly recovered ribbon-like quartz levels and quartz-feldspar microdomains with polygonal granoblastic texture.

A summary of the structural and petrographic features associated to the different stages of the tectono-metamorphic evolution of the Mammola paragneisses, compared to the same features in Stilo-Pazzano phyllites (Ortolano et al., 2022), is reported in Fig. 59.

Fig. 60 reports the P-T path obtained by Angì et al. (2010), with the different tectono-metamorphic stages illustrated by schemes of the associated blasto-deformational features; comparable P-T constraints have been subsequently obtained by Tursi et al. (2020).

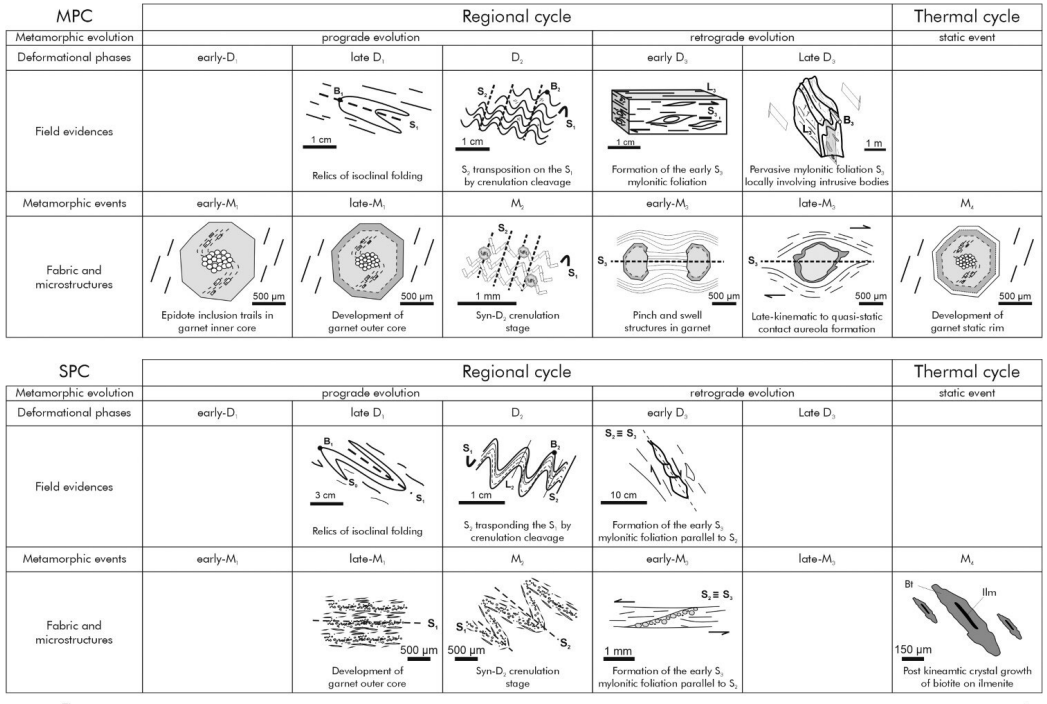

Fig. 59 - Summary of the field and petrographic evidence documenting the different stages of the tectono-metamorphic evolution of the Mammola Paragneiss Unit (MPU) and Stilo Phyllite Unit (SPU) (after Ortolano et al., 2022).

In more detail, the first deformational stage (D_1) led to development of a penetrative and pervasive foliation surface (S_1), more visible in the Stilo-Pazzano phyllites than in the Mammola paragneisses where it is locally preserved as relict isoclinal fold hinges within the mylonitic foliation. D_1 was followed by a D_2 crenulation stage, also this is rarely visible in the paragneisses.

These early stages, consistent with eo-Variscan crustal thickening or, according to Tursi et al. (2020), a first mylonitic event in a subduction context, were followed by the retrograde mylonitic stage D_3, recently divided by Ortolano et al. (2022) in an early extensional stage, mostly visible in thin section, and a subsequent transpressional stage.

According to both Tursi et al. (2020) and Ortolano et al. (2022), the early-D_3 stage was related to orogenic collapse and associated crustal thinning stage and was responsible for the detachment or the shallower phyllite levels of the late Variscan crustal section (i.e., SPC) from the higher-degree and deeper paragneisses of the MPC.

This extensional mylonitic stage was followed by a transpressional stage (Ortolano et al., 2022), leading to the development of the pervasive mylonitic field foliation, and likely assisting intrusion of the granitoid magmas up to the latest magmatic stages, as testified by late-tectonic felsic dykes

https://doi.org/10.3301/GFT.2024.09

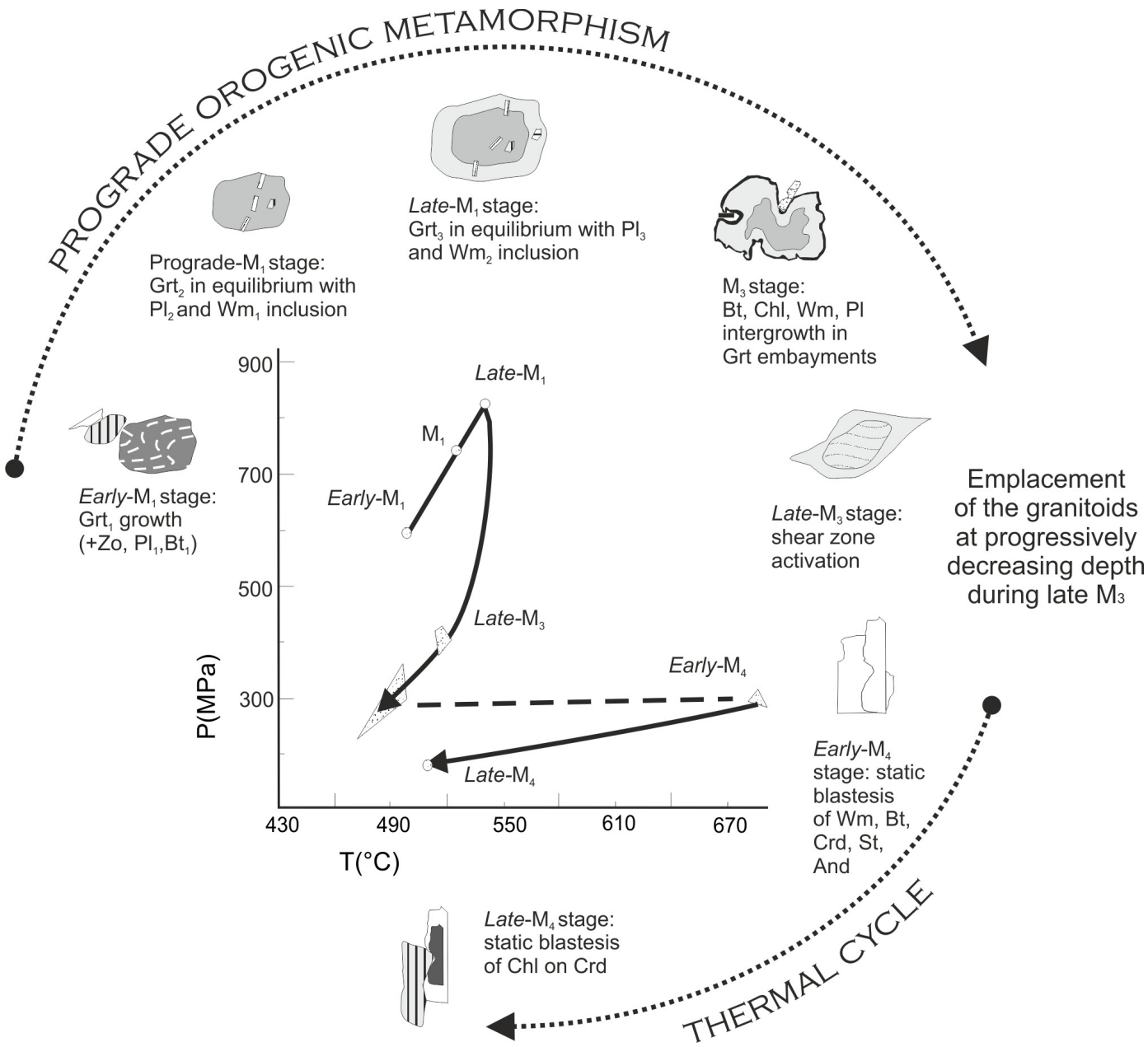

Fig. 60 - P–T path of the Mammola Paragneiss Unit, accompanied by schemes of multi-stage mineral growth marking discrete stages of the tectono-metamorphic evolution (modified after Angì et al., 2010).

exhibiting clear evidence of supra-solidus deformation. Finally, late Variscan magmatism ended with the intrusion of totally undeformed post-tectonic felsic dykes, paraconcordant to discordant and characterised by sharp contacts with the host paragneisses.

Shear zone activity in a transpressional regime has been considered by the above authors consistent with the mechanisms of batholith construction proposed by Fiannacca et al. (2017), and supported by deformation microstructures developed in the granitoids from submagmatic to low-temperature sub-solidus conditions, as well as by the internal magnetic fabric recorded by Fiannacca et al. (2021) in the apparently isotropic granitoids from the uppermost levels of the Serre Batholith (MBG and BG), suggesting a shortening axis roughly oriented NW–SE (Fig. 49). According to Ortolano et al. (2022), this shortening axis can be correlated with the attitudes orientation pattern of the mylonitic field foliation of the Mammola paragneisses (S_3), which is consistent with a folding system characterised by a sub-horizontal axis, oriented from NE-SW to ENE-WSW and by a stretching-lineation L_3 with a main ENE-WSW trend; such structures are consistent with dextral strike-slip tectonics, which can be

https://doi.org/10.3301/GFT.2024.09

ascribed to the late-D_3 transpressional stage. In addition, this interpretation would support the involvement of southern Calabria in the activity of the East Variscan Shear Zone, in line with results by Fazio et al. (2020) that suggest location of the NE Peloritani Mountains (southernmost CPO) within a peripheral branch of the EVSZ, based on evidence of long-lasting shear zone activity and associated granitoid magmatism during post-collisional exhumation of the Variscan middle crust.

Stop 4.4 - Alpine mylonites at the batholith-lower crust interface

Coordinates: Lat. 38°22'53" N, Long. 15°51'34" E
Location: Ulivarella Beach, Palmi

Palmi area (Fig. 3), at the boundary zone between the Aspromonte and Serre crustal domains, hosts late Variscan metamorphic and magmatic rocks from the deep-intermediate portion of the Serre crustal section. In particular, the area mostly hosts migmatitic paragneisses, intruded by the oldest and deepest plutonic rocks of the Serre Batholith, consisting in the foliated tonalites and quartz diorites (ABT-BT) emplaced at a depth of ~ 20-23 km (Caggianelli et al., 2000) and diffusively intruded by deformed to undeformed pegmatite-aplite dykes.
This area is of large interest since it hosts the Palmi Shear Zone (PSZ), a strike-slip crustal-scale shear zone of Alpine age (57 Ma; Prosser et al., 2003), exposed along the Calabrian Tyrrhenian coast near the village of Palmi (Fig. 61). The PSZ, which is characterised by a roughly E-W trending sub-vertical mylonitic foliation, separates late Variscan foliated tonalites and felsic dykes to the south, from migmatitic paragneisses, marbles and Ca-silicate rocks to the north. As common in high-strain zones dominated by strike-slip tectonics, the PSZ is characterised by a complex evolution and kinematics, well expressed by a range of intricate structures at both outcrop- (Fig. 62) and thin-section (Fig. 63) scale.

Fig. 61 - (a) Panoramic view of the Palmi Shear Zone; (b) near isoclinal fold (FA_1) of the field mylonitic foliation (S_m); (c) foliated tonalite with folded felsic dyke.

https://doi.org/10.3301/GFT.2024.09

The PSZ exhibits high structural complexity for many reasons: previous rock fabrics (magmatic or tectonic) at the time of deformation, different lithotypes involved (marbles, skarns, migmatitic paragneisses, tonalites, pegmatites) with highly contrasting rheology (e.g., the viscosity contrast between pegmatites and tonalites is between 50 and 250; Alsop et al., 2021), occurrence of folding interference patterns and, possibly, reactivation of the shear zone with opposite shear sense.

his complexity accounts for the conflicting interpretations of the kinematics of the PSZ and its possible links to other shear zones. Some authors (Prosser et al., 2003) recognised a sinistral shear sense, which was confirmed by Festa et al. (2016), who also proposed a possible connection of this shear zone with those exposed in Alpine Corsica, and which could hypothetically mark the front of the Alpine chain; other authors (Ortolano et al., 2020b) reported a bulk dextral shear direction and a possible correlation with other strike-slip zone branches exposed between southern Sardinia and the Balearic terrane. More recently, Fazio et al. (2024) found evidence for Alpine dextral reactivation of an ancient sinistral shear zone. Microstructural investigations (RGN - rigid grain net analysis) carried out in the PSZ by Ortolano et al. (2020b) revealed a sub-simple shear with a dominant pure shear component (67% for the mylonitic tonalites; 64% for the mylonitic paragneisses; and 60% for the mylonitic skarns). Quartz paleopiezometry combined with various flow laws gives

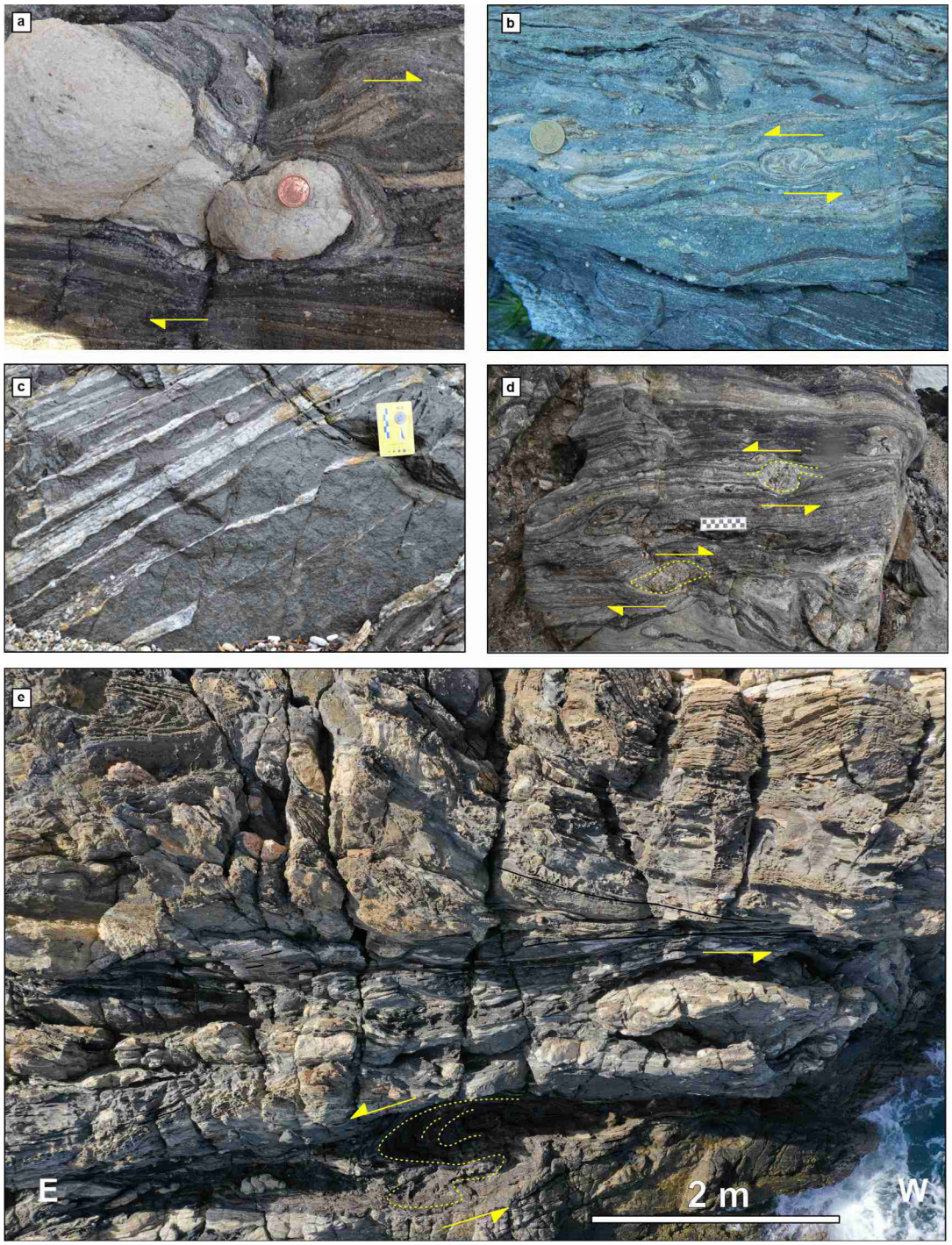

Fig. 62 - Mesoscopic structural features of the Palmi Shear Zone. (a) High viscosity contrast between felsic dyke and hosting skarns (dextral shear sense); (b) anticlockwise rotation of a spiral fold in the mylonitic skarns; (c) migmatitic paragneisses; (d) contrasting kinematic indicators on the same outcrop surface; (e) aerial view of the outcrop showing asymmetric drag folds and sub-vertical shear planes with a sinistral sense of shear.

https://doi.org/10.3301/GFT.2024.09

shear strain-rate values ranging from $1.14*10^{-12}$ (1/s) for mylonitic paragneisses to $5.91*10^{-12}$ (1/s) for mylonitic tonalites (Ortolano et al., 2020b), in agreement with typical values found for high strain zones in natural settings.

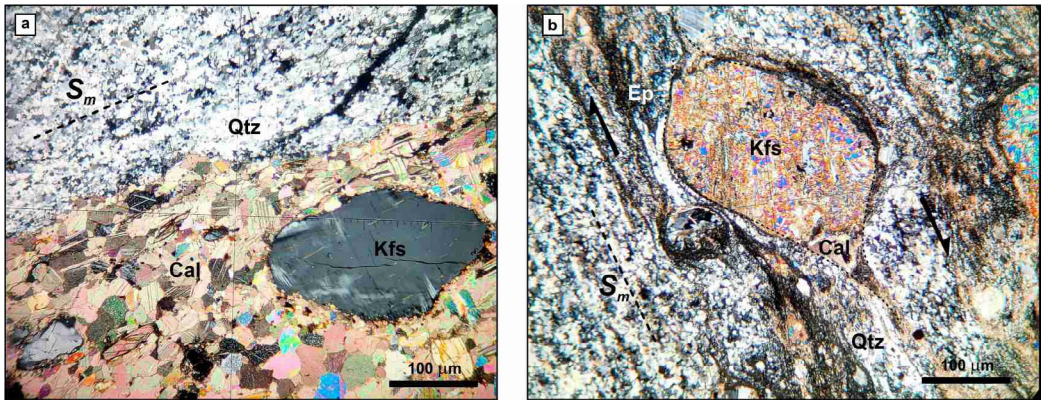

Fig. 63 - Microstructural features of Palmi mylonitic rocks: a) Mylonitic foliation (S_m) subparallel to the contact between the quartz-rich layer (top) and calcite-rich layer (bottom) in a calc-silicate rock. b) sigmoid clast of strongly sericitised K-feldspar indicating dextral kinematics with calcite tails parallel to the mylonitic foliation (S_m).

Stop 4.5 - Metapelitic migmatites just outside the Palmi shear zone

Coordinates: Lat. 38°23'42" N, Long. 15°51'42" E
Location: Scoglio dell'Isola, Palmi

We end this field trip in Palmi, ~ 2 km north of Stop 4.4, at the top of the Variscan lower crust. In this location, two well-exposed outcrops of dominant migmatitic paragneisses make up the cliff below the Taureana tower, and the Scoglio dell'Isola (Fig. 64) at the beach in front of the cliff. In this area, migmatitic paragneisses are not affected by the same Alpine shearing observed at the previous stop, even if they show evidence of high-temperature mylonitic deformation.
Migmatites from Scoglio dell'Isola consist of medium-coarse-grained melanosomes mostly consisting of garnet, biotite, and plagioclase, alternated to concordant leucosomes comprising quartz, feldspar, garnet and biotite (Fig. 65).

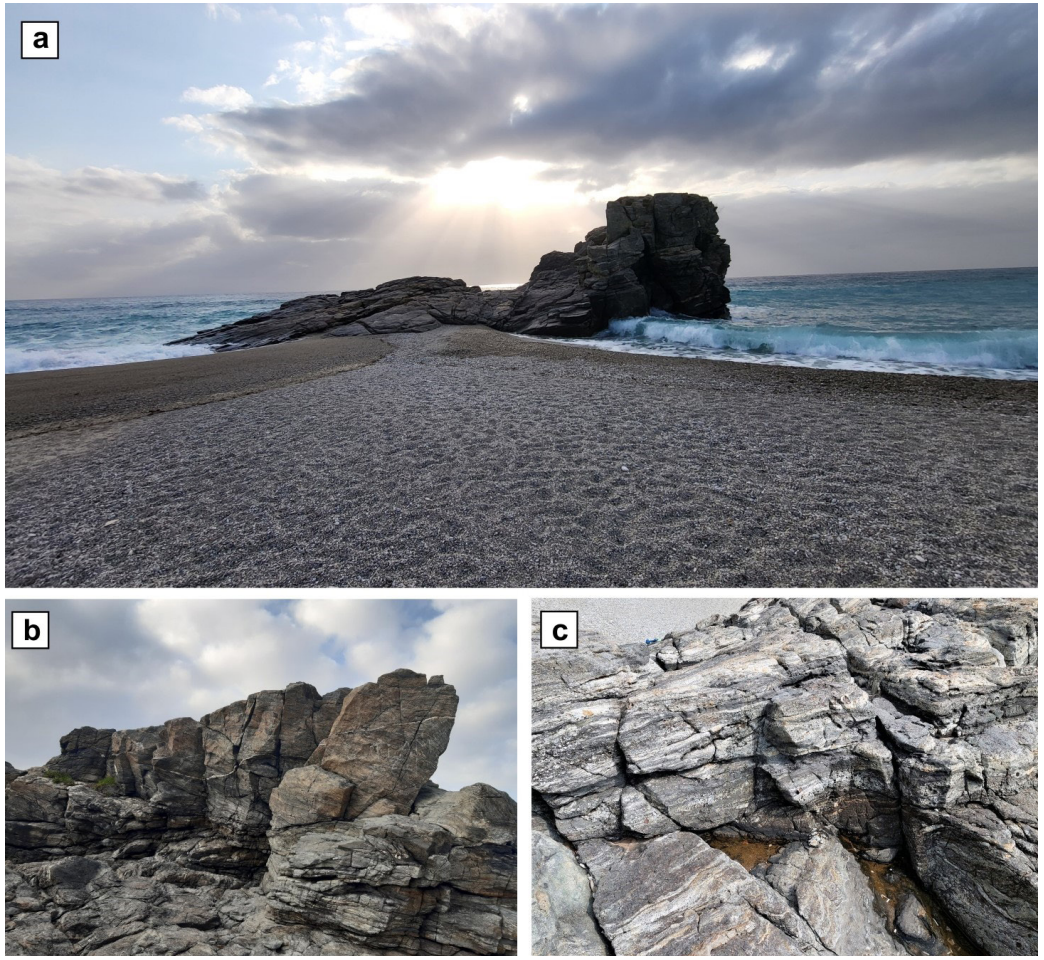

Fig. 64 - Field appearance of the Scoglio dell'Isola migmatites. (a) Panoramic view of the outcrop; (b-c) close-up views of the outcrop showing a well-developed migmatitic layering mostly having a 1-2 cm spacing.

https://doi.org/10.3301/GFT.2024.09

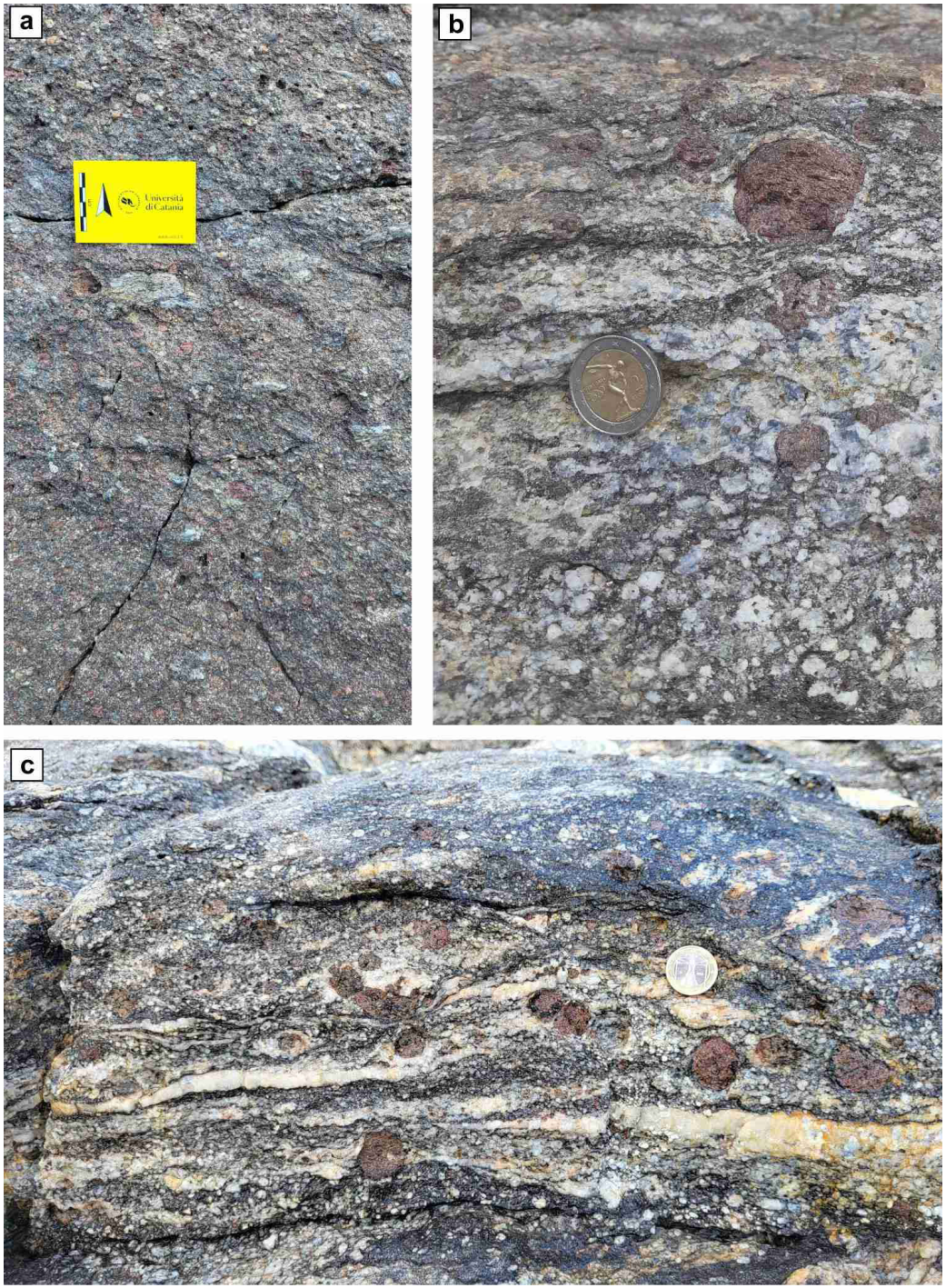

Sillimanite is also frequently present in the melanosomes, and it can form large aggregates up to 7 cm-long (Fig. 65a). Garnet is also outstanding in this outcrop, forming large porphyroblasts that are locally flattened, or wrapped by the quartz-feldspar-biotite matrix forming together sigmoidal objects (e.g., large porphyroblast in Fig. 65b) suggesting possible simple shear deformation; in addition, both Grt-bearing and Grt-free leucosomes appear clearly stretched along the main foliation (Fig. 65b-c).

Thin section observations reveal that two different types of leucosomes are present at the Scoglio dell'Isola, granitic (Fig. 66a-c), as already reported by Caggianelli et al. (2013), but also trondhjemitic (Fig. 66d). The two leucosome types have a similar appearance in the field, as they are quartz-rich, garnet-bearing, and can contain large feldspar crystals, up to 1 cm-long.

As visible in the thin section, the granitic leucosomes can contain large and euhedral-subhedral microcline crystals, up to 8 mm-long in Fig. 66a, and are associated with large peritectic garnet with inclusions of iso-oriented prismatic sillimanite (Fig. 66b), depicting an internal schistosity parallel to the main foliation. The amount of K-feldspar originally crystallising from the anatectic melt was larger, as testified by microdomains with evidence of replacement of microcline by secondary plagioclase (Fig. 66c). Anyhow, the granitic composition together with sillimanite and biotite inclusions in peritectic garnet is a clear evidence for the formation of granitic melt by biotite dehydration melting.

Fig. 65 - (a) Pavement outcrop with large oriented sillimanite clusters lying on the foliation surface; (b) variously deformed garnet porphyroblasts, with the largest one defining a s-shape geometry together with the surrounding leucosome; (c) stretched leucosomes marking the migmatitic foliation.

https://doi.org/10.3301/GFT.2024.09

On the other hand, trondhjemitic leucosomes (Fig. 66d) contain plagioclase as the only feldspar phase and lack sillimanite. They also contain garnet, visibly larger than the garnet in the mesosome, which would also point to biotite incongruent melting; however, this is at odds with the trondhjemitic composition of the leucosome. A few leucosome domains are characterised by a cumulate texture defined by aggregates of euhedral-subhedral plagioclase, which might suggest that some granitic melt may have escaped. Nevertheless, most of the plagioclase, euhedral to anhedral, and submillimetric to 7 mm-long in Fig. 66d, is surrounded by quartz in medium-grained aggregates and large crystals up to 6 mm in size, attesting to such leucosomes representing crystallisation from a trondhjemitic melt.

ACKNOWLEDGEMENTS

We are extremely grateful to the participants of the post-congress excursion of the 10th Hutton Symposium for their enthusiastic participation and stimulating discussions. We would like to thank the Editor-in-Chief Marco Malusà for editorial handling and the reviewers for constructive suggestions and comments. Careful editorial handling and helpful suggestions and comments by Associate Editor Matteo Massironi have been highly appreciated. We express special thanks to the Editorial Manager Fabio Petti for his precious work and infinite patience.
This work was supported by funds from University of Catania, (PIAno di inCEntivi per la RIcerca di Ateneo 2020/2022—Pia.Ce.Ri), Grant Number: 22722132153, within the project “GeoPetroMat”.

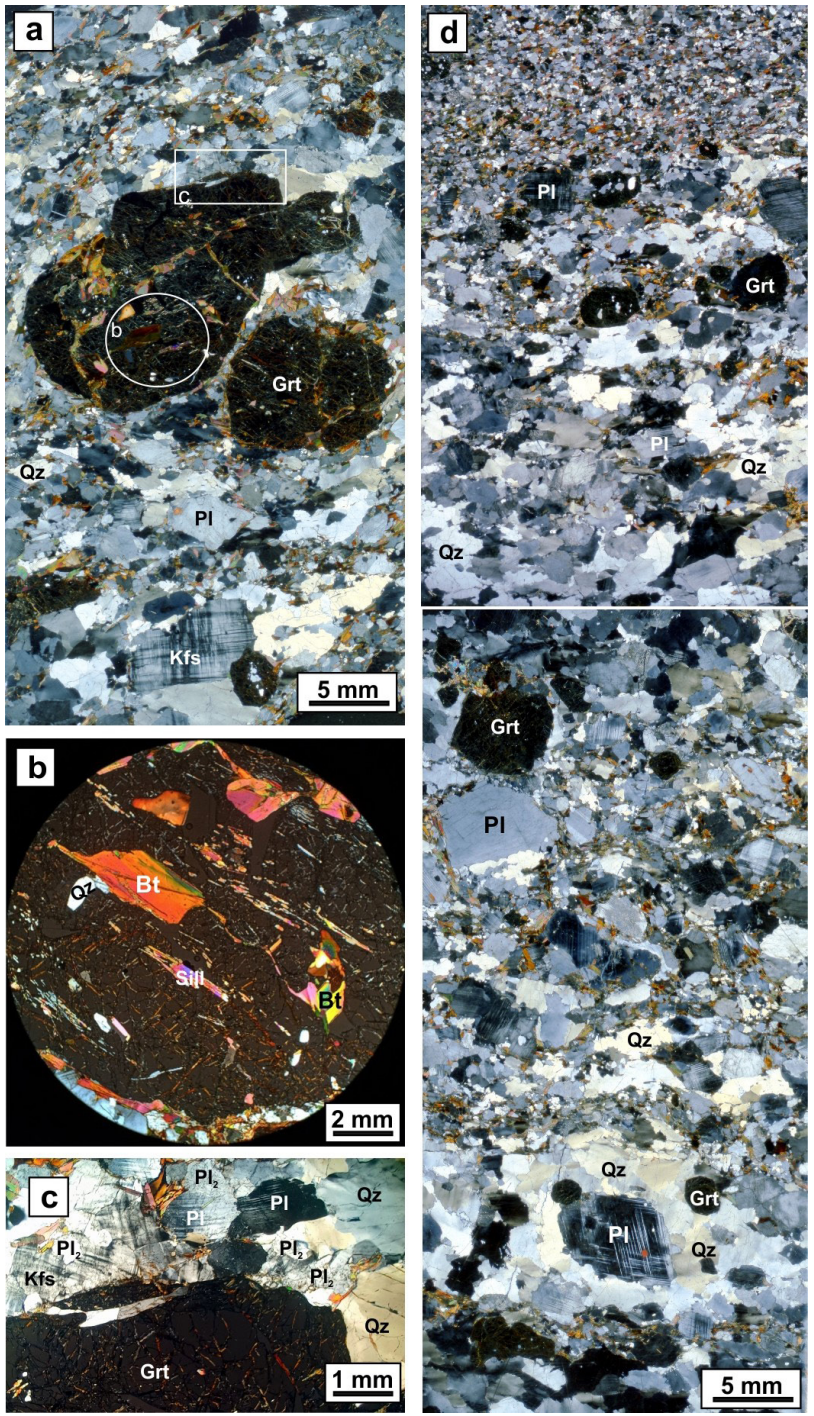

Fig. 66 - Thin section features of Scoglio dell’Isola migmatites. (a) Leucosome with large microcline crystal; smaller K-feldspar grains also occur scattered in the thin section; (b) zoom of (a) showing biotite and sillimanite inclusions in garnet; (c) zoom of (a) illustrating microcline grains partially replaced by secondary plagioclase (Pl_2); (d) scans of two adjacent thin sections, perpendicular to the migmatitic foliation, showing garnet-bearing fine- to medium-grained melanosomes and medium-coarse grained leucosomes with plagioclase as the only feldspar phase.

https://doi.org/10.3301/GFT.2024.09

REFERENCES

Acquafredda P., Lorenzoni S., Lorenzoni E. Z. (1994) - Palaeozoic sequences and evolution of the Calabrian-Peloritan Arc (Southern Italy). Terra Nova, 6(6), 582-594.

Acquafredda P. Caggianelli A., Di Battista P. (1995) - Contrasting features of foliated and massive Hercynian granitoids from Calabria (Italy). Mineral. Petrogr. Acta, 38, 9-24.

Acquafredda P., Fornelli A., Paglionico A., Piccarreta G. (2006) - Petrological evidence for crustal thickening and extension in the Serre granulite terrane (Calabria, southern Italy). Geol. Mag., 143(2), 145-163.

Acquafredda P., Fornelli A., Piccarreta G., Pascazio A. (2008) - Multi-stage dehydration–decompression in the metagabbros from the lower crustal rocks of the Serre (southern Calabria, Italy). Geol. Mag., 145(3), 397-411.

Alsop G.I., Strachan R.A., Holdsworth R.E., Burns I.M. (2021) - Geometry of folded and boudinaged pegmatite veins emplaced within a strike-slip shear zone: A case study from the Caledonian orogen, northern Scotland. J. Struct. Geol., 142, 104233.

Angì G., Cirrincione R., Fazio E., Fiannacca P., Ortolano G., Pezzino A. (2010) - Metamorphic evolution of preserved Hercynian crustal section in the Serre Massif (Calabria-Peloritani Orogen, southern Italy). Lithos, 115, 237-262.

Appel P., Cirrincione R., Fiannacca P., Pezzino A. (2011) - Age constraints on Late Paleozoic evolution of continental crust from electron microprobe dating of monazite in the Peloritani Mountains (southern Italy): another example of resetting of monazite ages in high-grade rocks. Int. J. Earth Sci., 100, 107-123.

Ayuso R.A., Messina A., De Vivo B., Russo S., Woodruff L.G., Sutter J.F., Belkin H.E. (1994) - Geochemistry and argon thermochronology of the Variscan Sila Batholith, southern Italy: source rocks and magma evolution. Contrib. Mineral. Petr., 117, 87-109.

Barca D., Cirrincione R., De Vuono E., Fiannacca P., Ietto F., Lo Giudice A. (2010) - The Triassic system in the northern Calabria-Peloritani Orogen: evidence from basaltic dyke magmatism in the San Donato Unit. Per. Mineral., 79, 61-72.

Bonardi G., de Capoa P., Di Staso A., Martín-Martín M., Martín-Rojas I., Perrone V., Tent-Manclús J. E. (2002) - New constraints to the geodynamic evolution of the southern sector of the Calabria–Peloritani Arc (Italy). C.R. Geosci., 334(6), 423-430.

Borsi S., Hieke-Merlin O., Lorenzoni S., Paglionico A., Zanettin-Lorenzoni E. (1976) - Stilo unit and 'dioritic-kinzigitic' unit in le Serre (Calabria, Italy). Geological, petrological, geochronological characters. Boll. Soc. Geol. It., 95, 219-45.

Brandt S. and Schenk V. (2020) - Metamorphic response to Alpine thrusting of a crustal-scale basement nappe in southern Calabria (Italy). J. Petrol., 61(11-12), egaa063.

Burton A.N. (1971) - Carta geologica della Calabria alla scala 1:25.000: relazione generale. Ufficio bonifiche. Ufficio piani di massima e studi.

Caggianelli A., Del Moro A., Paglionico A., Piccarreta G., Pinarelli L., Rottura A. (1991) - Lower crustal granite genesis connected with chemical fractionation in the continental crust of Calabria (Southern Italy). Eur. J. Mineral, 3, 159-180.

Caggianelli A., Del Moro A., Piccarreta G. (1994) - Petrology of basic and intermediate orogenic granitoids from the Sila Massif (Calabria, southern Italy). Geol. J., 29, 11-28.

Caggianelli A., Prosser G., Di Battista P. (1997) - Textural features and strain of granitoids emplaced at different depths: the example of the Hercynian tonalites and granodiorites from Calabria. Mineral. Petrogr. Acta, 40, 11-26.

Caggianelli A., Prosser G., Rottura A. (2000) - Thermal history vs. fabric anisotropy in granitoids emplaced at different crustal levels: An example from Calabria, southern Italy. Terra Nova,12(3), 109-116.

Caggianelli A., Moro A.D., Di Battista P., Prosser G., Rottura A. (2003) - Leucogranite genesis connected with low-pressure high-temperature metamorphism in the Sila basement (Calabria, Italy). Swiss Bull. Mineral. Petrol., 83(3), 301-316.

https://doi.org/10.3301/GFT.2024.09

Caggianelli A., Liotta D., Prosser G., Ranalli G. (2007) - Pressure–temperature evolution of the late Hercynian Calabria continental crust: compatibility with post-collisional extensional tectonics. Terra Nova, 19(6), 502-514.2013.
Caggianelli A., Prosser G., Festa V., Langone A., Spiess R. (2013) - From the upper to the lower continental crust exposed in Calabria. Geol. F. Trips, 4, 1-49.
Carosi R., Montomoli C., Tiepolo M., Frassi C. (2012) - Geochronological constraints on post-collisional shear zones in the Variscides of Sardinia (Italy). Terra Nova, 24(1), 42-51.
Cavazza W. (1989) - Detrital modes and provenance of the Stilo-Capo d'Orlando Formation (Miocene), southern Italy. Sedimentology, 36(6), 1077-1090.
Chappell B.W. and White A.J.R. (1974) - Two Contrasting Granite Types. Pacif. Geol., 8, 173-174.
Chappell B.W. and White A.J. (2001) - Two contrasting granite types: 25 years later. Aust. J. Earth Sci., 48(4), 489-499.
Cirrincione R. (1996) - Geochronologic and petrologic features of porphyrite rocks in the Tortonian conglomerate of north-eastern Sicily: hypothesis on their provenance. Per. Mineral., 65(1-2), 21-33.
Cirrincione R., Fiannacca P., Lo Giudice A., Pezzino A. (2005) - Evidence of early Palaeozoic continental rifting from mafic metavolcanics of southern Peloritani Mountains (North-Eastern Sicily, Italy). Ofioliti, 30, 15-25.
Cirrincione R., Fiannacca P., Ortolano G., Pezzino A., Punturo R. (2013) - Granitoid stones from Calabria (southern Italy): Petrographic, geochemical and petrophysical characterization of ancient quarries of Roman age. Per. Mineral., 82(1), 41-59.
Cirrincione R., Fiannacca P., Lustrino M., Romano V., Tranchina A. (2014) - Late Triassic tholeiitic magmatism in Western Sicily: A possible extension of the Central Atlantic Magmatic Province (CAMP) in the Central Mediterranean area? Lithos, 188, 60-71.
Cirrincione R., Fazio E., Fiannacca P., Ortolano G., Pezzino A., Punturo R. (2015) - The Calabria-Peloritani Orogen, a composite terrane in Central Mediterranean; its overall architecture and geodynamic significance for a pre-Alpine scenario around the Tethyan basin. Per. Mineral., 84(3B), 701-749.
Cirrincione R., Fiannacca P., Lustrino M., Romano V., Tranchina A., Villa I. M. (2016) - Enriched asthenosphere melting beneath the nascent North African margin: trace element and Nd isotope evidence in middle–late Triassic alkali basalts from central Sicily (Italy). Int. J. Earth Sci., 105, 595-609.
Clarke D.B. and Rottura A. (1994) - Garnet-forming and garnet-eliminating reactions in a quartz diorite intrusion at Capo Vaticano, Calabria, Italy. Can. Mineral., 32(3), 623-635.
Clemens J.D., Darbyshire D.P.F., Flinders J. (2009). Sources of post-orogenic calcalkaline magmas: the Arrochar and Garabal Hill-Glen Fyne complexes, Scotland. Lithos, 112, 524-542.
Colonna V., Lorenzoni S., Zanettin Lorenzoni E. (1973) - Sull'esistenza di due complessi metamorfici lungo il bordo sud-orientale del massiccio granitico delle Serre (Calabria). Boll. Soc. Geol. It., 92, 801-830.
Corsini M. and Rolland Y. (2009) - Late evolution of the southern European Variscan belt: Exhumation of the lower crust in a context of oblique convergence. C.R. Geosci., 341(2-3), 214-223.
Critelli S. (2018) - Provenance of Mesozoic to Cenozoic circum-Mediterranean sandstones in relation to tectonic setting. Earth Sci. Rev., 185, 624-648.
Critelli S. and Martín-Martín M. (2022) - Provenance, paleogeographic and paleotectonic interpretations of Oligocene-Lower Miocene sandstones of the western-central Mediterranean region: A review. J. Asian Earth Sci., 10, 100124.
Cruden A.R. and Weinberg R.F. (2018) - Mechanisms of magma transport and storage in the lower and middle crust — magma segregation, ascent and emplacement. In: Burchardt S. (Ed.), Volcanic and igneous plumbing systems, Elsevier, 13–53, https://doi.org/10.1016/B978-0-12-809749-6.00002-9.
D'Amico C., Rottura A., Maccarrone E., Puglisi G. (1982) - Peraluminous granitic suite of Calabria Peloritani arc (Southern Italy). Rend. Soc. Ital. Min. Petrol., 38, 35-52.
Del Moro A., Fornelli A., Paglionico A. (1994) - K-feldspar megacryst granitic suite in the Serre (Southern Calabria – Italy). Per. Mineral., 63, 19-33.
Domeier M. and Torsvik T.H. (2014) - Plate tectonics in the late Paleozoic. Geosci. Front., 5(3), 303-350.
Duchene S., Fornelli A., Micheletti F., Piccarreta G. (2013) - Sm-Nd chronology of porphyroblastic garnets from granulite facies metabasic rocks in Calabria (Southern Italy): inferences for preserved isotopic memory and resetting. Miner. Petrol., 107, 539-551.

https://doi.org/10.3301/GFT.2024.09

Fazio E., Cirrincione R., Pezzino A. (2015) - Tectono-metamorphic map of the south-western flank of the Aspromonte Massif (southern Calabria-Italy). J. Maps, 11(1), 85-100.

Fazio E., Fiannacca P., Russo D., Cirrincione R. (2020) - Submagmatic to solid-state deformation microstructures recorded in cooling granitoids during exhumation of late-Variscan crust in North-Eastern Sicily. Geosciences, 10(8), 311.

Fazio E., Ortolano G., Alsop G.I., D'Agostino A., Visalli R., Luzin V., Salvemini F., Cirrincione R. (2024) - Enhanced structural analysis through a hybrid analogue-digital mapping approach: Integrating field and UAV survey with microtomography to characterize metamorphic rocks. J. Struct. Geol., 187, 105213.

Festa V., Di Battista P., Caggianelli A., Liotta, D. (2003) - Exhumation and tilting of the late Hercynian continental crust in the Serre Massif (Southern Calabria, Italy). Boll. Soc. Geol. It., 2(1), 79-88.

Festa V., Langone A., Caggianelli A., Rottura A. (2010) - Dike magmatism in the Sila Grande (Calabria, southern Italy): evidence of Pennsylvanian–Early Permian exhumation. Geosphere, 6(5), 549-566.

Festa V., Caggianelli A., Langone A., Prosser G. (2013) - Time–space relationships among structural and metamorphic aureoles related to granite emplacement: A case study from the Serre Massif (southern Italy). Geol. Mag., 150(3), 441-454.

Festa V., Prosser G., Caggianelli A., Grande A., Langone A., Mele D. (2016) - Vorticity analysis of the Palmi shear zone mylonites: new insights for the Alpine tectonic evolution of the Calabria–Peloritani terrane (southern Italy). Geol. J., 51, 670-681.

Festa V., Tursi F., Caggianelli A., Spiess R. (2018) - The tectono-magmatic setting of the Hercynian upper continental crust exposed in Calabria (Italy) as revealed by the 1:10,000 structural-geological map of the Levadio stream area. Ital. J. Geosci., 137(2), 165-174.

Festa V., Cicala M., Tursi F. (2020) - The Curinga–Girifalco Line in the framework of the tectonic evolution of the remnant Alpine chain in Calabria (southern Italy). Int. J. Earth Sci., 109, 2583-2598.

Festa V., Fornelli A., Micheletti F., Spiess R., Tursi F. (2022) - Ductile shearing and focussed rejuvenation: Records of High-P (eo-) Alpine metamorphism in the Variscan lower crust (Serre Massif, Calabria—Southern Italy). Geosciences, 12(5), 212.

Festa V., Spiess R., Tursi F. (2024) - Garnet coalescence clogs melt extraction channels in migmatite. Lithos, 472-473, 107581.

Fiannacca P., Williams I.S., Cirrincione R., Pezzino A. (2008) - Crustal contributions to late Hercynian peraluminous magmatism in the southern Calabria–Peloritani Orogen, southern Italy: petrogenetic inferences and the Gondwana connection. J. Petrol., 49(8), 1497-1514.

Fiannacca P., Cirrincione R., Bonanno F., Carciotto M. (2015) - Source-inherited compositional diversity in granite batholiths: The geochemical message of Late Paleozoic intrusive magmatism in central Calabria (southern Italy). Lithos, 236, 123-140.

Fiannacca P., Lombardo R., Militello G.M., Cirrincione R. (2016a) - Plagioclase microstructures and compositions as tracers of mixing processes in weakly to strongly peraluminous granodiorites and granites from the Serre Batholith (southern Italy). Rend. Soc. Ital. Min. Petrol., 38, 43-46.

Fiannacca P., Williams I.S., Cirrincione R., Hegner, E. (2016b) - Suffering zircon from a Variscan lower crustal environment: U-Pb ages and oxygen isotopic compositions in mafic and felsic granulites from the Serre Massif (Calabria, Italy). VIII International SHRIMP Workshop, 26-28.

Fiannacca P., Williams I.S., Cirrincione R. (2017) - Timescales and mechanisms of batholith construction: Constraints from zircon oxygen isotopes and geochronology of the late Variscan Serre Batholith (Calabria, southern Italy). Lithos, 277, 302-314.

Fiannacca P., Williams I.S., Cirrincione R., Pezzino A. (2019) - Poly-orogenic melting of metasedimentary crust from a granite geochemistry and inherited zircon perspective (Southern Calabria-Peloritani Orogen, Italy). Front. Earth Sci., 7, 119.

Fiannacca P., Basei M. A., Cirrincione R., Pezzino A., Russo, D. (2020) - Water-assisted production of late-orogenic trondhjemites at magmatic and subsolidus conditions. Geol. Soc. London Spec. Pub., 491(1), 147-178.

Fiannacca P. and Cirrincione R. (2020) - Metasedimentary metatexites with trondhjemitic leucosomes from NE Sicily: Another example of prograde water-fluxed melting in collisional belts. Geosciences, 10(4), 123.

https://doi.org/10.3301/GFT.2024.09

Fiannacca P., Russo D., Fazio E., Cirrincione R., Mamtani M.A. (2021) - Fabric analysis in upper crustal post-collisional granitoids from the Serre Batholith (Southern Italy): Results from microstructural and AMS investigations. Geosciences, 11(10), 414.

Fornelli A. (1991) - Aspetti genetici e strutturali dei megacristalli di feldspato potassico dei granitoidi di Satriano (Serre orientali - Calabria). Mineral. Petrogr. Acta, 34, 95-102.

Fornelli A. (1994) - Metamorphic xenoliths and microgranular enclaves in the Serre granodiorites (Southern Calabria-Italy): their connection with granitoid genesis. Miner. Petrol., 51(1), 49-65.

Fornelli A., Caggianelli A., Del Moro A., Bargossi G.M., Paglionico A., Piccarreta G., Rottura A. (1994) - Petrology and evolution of the central Serre granitoids (Southern Calabria-Italy). Peri. Mineral., 63(1-3), 53-70.

Fornelli A., Piccarreta G., Del Moro A., Acquafredda P. (2002) - Multi-stage melting in the lower crust of the Serre (Southern Italy). J. Petrol., 43(12), 2191-2217.

Fornelli A., Piccarreta G., Acquafredda P., Micheletti F., Paglionico A. (2004) - Geochemical fractionation in migmatitic rocks from Serre granulitic terrane (Calabria, southern Italy). Per. Mineral., 73(2), 145-57.

Fornelli A., Langone A., Micheletti F., Piccarreta G. (2011) - Time and duration of Variscan high-temperature metamorphic processes in the south European Variscides: constraints from U-Pb chronology and trace element chemistry of zircon. Miner. Petrol., 103, 101-122.

Fornelli A., Pascazio A., Piccarreta G. (2012) - Diachronic and different metamorphic evolution in the fossil Variscan lower crust of Calabria. Int. J. Earth Sci., 101, 1191-1207.

Fornelli A., Langone A., Micheletti F., Pascazio A., Piccarreta G. (2014) - The role of trace element partitioning between garnet, zircon and orthopyroxene on the interpretation of zircon U–Pb ages: an example from high-grade basement in Calabria (Southern Italy). Int. J. Earth Sci., 103, 487-507.

Fornelli A., Langone A., Micheletti F., Piccarreta G. (2018) - REE partition among zircon, orthopyroxene, amphibole and garnet in a high-grade metabasic system. Geol. Mag., 155(8), 1705-1726.

Fornelli A., Festa V., Micheletti F., Spiess R., Tursi, F. (2020) - Building an orogen: Review of U-Pb zircon ages from the Calabria–Peloritani terrane to constrain the timing of the southern Variscan belt. Minerals, 10(11), 944.

Frost B.R., Arculus R.J., Barnes C.G., Collins W.J., Ellis D.J., Frost C.D. (2001) - A geochemical classification of granitic rocks. J. Petrol., 42, 2033-2048.

Frost B.R. and Frost C.D. (2008) - A geochemical classification for feldspathic igneous rocks. J. Petrol., 49, 11, 1955-1969.

Glazner A.F. and Johnson B.R. (2013) - Late crystallization of K-feldspar and the paradox of megacrystic granites. Contrib. Mineral. Petr., 166, 777-799.

Graessner T., Schenk V., Brocker M., Mezger K. (2000) - Geochronological constraints on timing of granitoid magmatism, metamorphism and postmetamorphic cooling in the Hercynian crustal cross-section of Calabria. J. Metam. Geol., 18, 409-421.

Graessner T. and Schenk V. (2001) - An exposed Hercynian deep crustal section in the Sila Massif of Northern Calabria: mineral chemistry, petrology and a P-T path of granulite-facies metapelitic migmatites and metabasites. J. Petrol., 42(5), 931-961.

Johnson B.R. and Glazner A.F. (2010) - Formation of K-feldspar megacrysts in granodioritic plutons by thermal cycling and late-stage textural coarsening. Contrib. Mineral. Petr., 159, 599-619.

Karakas O., Wotzlaw, J. F., Guillong M., Ulmer P., Brack P., Economos R., Bergantz G.W., Sinigoi S., Bachmann O. (2019) - The pace of crustal-scale magma accretion and differentiation beneath silicic caldera volcanoes. Geology, 47(8), 719-723.

Klötzli U.S., Sinigoi S., Quick J.E., Demarchi G., Tassinari C.C., Sato K., Günes Z. (2014) - Duration of igneous activity in the Sesia Magmatic System and implications for high-temperature metamorphism in the Ivrea–Verbano deep crust. Lithos, 206, 19-33.

Langone A., Gueguen E., Prosser G., Caggianelli A., Rottura A. (2006) - The Curinga-Girifalco fault zone (northern Serre, Calabria) and its significance within the Alpine tectonic evolution of the western Mediterranean. J. Geodyn., 42, 140-158.

Langone A., Caggianelli A., Festa V., Prosser G. (2014) - Time constraints on the building of the Serre Batholith: consequences for the thermal evolution of the Hercynian continental crust exposed in Calabria (southern Italy). J. Geol., 122(2), 183-199.

https://doi.org/10.3301/GFT.2024.09

Lombardo R., Fiannacca P., Cirrincione R. (2020) - Geochemical modelling of granitoid magma diversity at Capo Vaticano Promontory (Serre Batholith, southern Italy). Geochemistry, 80(2), 125599.

Lombardo R., Fiannacca P., Merlo R., Basei M. A., Cirrincione R. (2023) - Crustal vs. mantle origin of post collisional granitoids: insights from geochemistry and zircon Hf isotopes of late Variscan quartz diorites-tonalites from Capo Vaticano (Serre Batholith, Italy). 10th Hutton Symposium 2023, Baveno, Italy. Abstract volume p. 47.

Maccarrone E., Paglionico A., Piccarreta G., Rottura A. (1983) - Geochemical features of granulite-amphibolite facies metasediments from the Serre (Calabria, Southern Italy): their protholiths and the processes controlling their chemistry. Lithos, 16, 95-111.

Micheletti F., Barbey P., Fornelli A., Piccarreta G., Deloule E. (2007) - Latest Precambrian to Early Cambrian U–Pb zircon ages of augen gneisses from Calabria (Italy), with inference to the Alboran microplate in the evolution of the peri-Gondwana terranes. Int. J. Earth Sci., 96, 843-860.

Micheletti F., Fornelli A., Piccarreta G., Barbey P., Tiepolo M. (2008) - The basement of Calabria (southern Italy) within the context of the Southern European Variscides: LA-ICPMS and SIMS U-Pb zircon study. Lithos, 104, 1-11.

Migoń P. (2006) - Granite Landscapes of the World. Oxford University Press: New York.

Moresi M., Paglionico A., Piccarreta G., Rottura A. (1978) - The deep crust in Calabria (Polia-Copanello Unit): a comparison with the Ivrea-Verbano zone. Mem. Soc. Geol. Padova, 33, 233-242.

Moyen J.F., Laurent O., Chelle-Michou C., Couzinié S., Vanderhaeghe O., Zeh A., Villaros A., Gardien V. (2017) - Collision vs. subduction-related magmatism: two contrasting ways of granite formation and implications for crustal growth. Lithos, 277, 154-177.

Navas-Parejo P., Somma R., Martín-Algarra A., Perrone V., Rodríguez-Cañero R. (2009) - First record of Devonian orthoceratid-bearing limestones in southern Calabria (Italy). C.R. Palevol., 8(4), 365-373.

Novarese V. (1931) - La formazione diorito-kinzigitica in Italia. Boll. R. Com. Geol. It., 56(7), 1-62.

Ortolano G., Visalli R., Fazio E., Fiannacca P., Godard G., Pezzino A., Punturo R., Sacco V., Cirrincione R. (2020a) - Tectono-metamorphic evolution of the Calabria continental lower crust: The case of the Sila Piccola Massif. Int. J. Earth Sci., 109, 1295-1319.

Ortolano G., Fazio E., Visalli R., Alsop G.I., Pagano M., Cirrincione R. (2020b) - Quantitative microstructural analysis of mylonites formed during Alpine tectonics in the western Mediterranean realm. J. Struct. Geol., 131, 103956, https://doi.org/10.1016/j.jsg.2019.103956.

Ortolano G., Pagano M., Visalli R., Angì G., D'Agostino A., Muto F., Tripodi V., Critelli S., Cirrincione R. (2022) - Geology and structure of the Serre Massif upper crust: a look into the late-Variscan strike-slip kinematics of the Southern European Variscan chain. J. Maps, 18, 314-330.

Padovano M., Elter F. M., Pandeli E., Franceschelli M. (2012) - The East Variscan Shear Zone: New insights into its role in the late Carboniferous collision in Southern Europe. International Geology Review, 54(8), 957-970, https://doi.org/10.1080/00206814.2011.626120.

Padovano M., Dorr W., Elter F.M., Gerdes A. (2014) - The East Variscan Shear Zone: Geochronogical constraints from the capo Ferro area (NE Sardinia, Italy). Lithos, 196-197, 27-41.

Paglionico A., Piccarreta G., Rottura A. (1982) - Guida all'escursione nelle Serre attraverso le rocce di facies granulitica dell'unità Polia – Copanello. Rend. Soc. Ital. Min. Petrol. 38(3), 1153-1162.

Paterson S., Memeti V., Mundil R., Žák J. (2016) – Repeated, multiscale, magmatic erosion and recycling in an upper-crustal pluton: Implications for magma chamber dynamics and magma volume estimates. Am. Mineral., 101, 2176-2198.

Peccerillo A. and Taylor S.R. (1976) - Geochemistry of Eocene calcalkaline volcanic rocks from the Kastamonu area, northern Turkey. Contrib. Mineral. Petr., 58, 63-81.

Peressini G., Quick J.E., Sinigoi S., Hofmann A.W., Fanning M. (2007) - Duration of a large mafic intrusion and heat transfer in the lower crust: a SHRIMP U–Pb zircon study in the Ivrea–Verbano Zone (Western Alps, Italy). J. Petrol., 48(6), 1185-1218.

Prosser G., Caggianelli A., Rottura A., Moro A.D. (2003) - Strain localisation driven by marble layers: The Palmi shear zone (Calabria-Peloritani terrane, Southern Italy). GeoActa, 2, 155-166.

https://doi.org/10.3301/GFT.2024.09

Raab G., Egli M., Norton K., Dahms D., Brandová D., Christl M., Scarciglia F. (2019) - Climate and relief-induced controls on the temporal variability of denudation rates in a granitic upland. Earth Surf. Proc. Landf., 44(13), 2570-2586.

Redler C., Johnson T.E., White R.W., Kunz B.E. (2012) - Phase equilibrium constraints on a deep crustal metamorphic field gradient: metapelitic rocks from the Ivrea Zone (NW Italy). J. Metam. Geol., 30(3), 235-254.

Rizzo G., Piluso E., Morten L. (2005) - Tonalitic to trondhjemitic dykes within metabasic lower-crust rocks, Serre Massif, Calabrian-Peloritan arc. Boll. Soc. Geol. It., 45-52.

Romano V., Cirrincione R., Fiannacca P., Lustrino M., Tranchina, A. (2011) - Late-Hercynian post-collisional dyke magmatism in central Calabria (Serre Massif, southern Italy). Per. Mineral., 80(3).

Rottura A., Bargossi G.M., Caironi V., Del Moro A., Maccarrone E., Macera P., Paglionico A., Petrini R., Piccareta G., Poli G. (1990) - Petrogenesis of contrasting Hercynian granitoids from the Calabrian Arc, Southern Italy. Lithos, 24, 97-119.

Rottura A., Del Moro A., Pinarelli L., Petrini R., Peccerillo A., Caggianelli A., Piccarreta G. (1991) - Relationships between intermediate and acidic rocks in orogenic granitoid suites: Petrological, geochemical and isotopic (Sr, Nd, Pb) data from Capo Vaticano (southern Calabria, Italy). Chem. Geol., 92(1-3), 153-176.

Rottura A., Caggianelli A., Campana R., Del Moro A. (1993) - Petrogenesis of Hercynian peraluminous granites from the Calabrian Arc, Italy. Eur. J. Mineral., 5(4), 737-754.

Russo D., Fiannacca P., Fazio E., Cirrincione R., Mamtani, M.A. (2023) - From floor to roof of a batholith: geology and petrography of the north-eastern Serre Batholith (Calabria, southern Italy). J. Maps, 19(1), 2149358.

Schenk V. (1980) - U-Pb and Rb-Sr radiometric dates and their correlation with metamorphic events in the granulitic-facies basement of the Serre, Southern Calabria (Italy). Contrib. Mineral. Petr., 73, 23-38.

Schenk V. (1981). Synchronous uplift of the lower crust of the Ivrea Zone and of southern Calabria and its possible consequences for the Hercynian orogeny in southern Europe. Earth Planet. Sc. Lett., 56, 305-320.

Schenk V. (1984) - Petrology of felsic granulites, metapelites metabasics, ultramafics, and metacarbonates from southern Calabria (Italy): prograde metamorphism, uplift and cooling of a former lower crust. J. Petrol., 25, 255-298.

Schenk V. (1989) - PTt path of the lower crust in the Hercynian fold belt of southern Calabria. Geol. Soc. London Spec. Pub., 43(1), 337-342.

Schenk V. (1990) - The exposed crustal cross section of southern Calabria, Italy: structure and evolution of a segment of Hercynian crust. In: M.H. Salisbury, Fountain D.M. (Eds.). Exposed Cross Sections of the Continental Crust. Dordrecht: Kluwer, 21-42.

Schmid R. and Wood B.J. (1976). Phase relationships in granulitic metapelites from the Ivrea-Verbano zone (Northern Italy). Contrib. Mineral. Petr., 54(4), 255-279.

Servizio Geologico d'Italia (2016) - Carta Geologica d'Italia alla scala 1:50.0000, F. 580 Soverato. ISPRA, Roma. https://www.isprambiente.gov.it/Media/carg/580_SOVERATO/Foglio.html.

Streckeisen A.L. and Le Maitre R.W. (1979) - A chemical approximation to the modal QAPF classification of the igneous rock. Neues. Jb. Miner. Abh., 136, 169-206.

Thomson S.N. (1994) - Fission track analysis of the crystalline basement rocks of the Calabrian Arc, southern Italy: evidence of Oligo-Miocene late orogenic extension and erosion. Tectonophysics, 238, 331-35.

Tortorici G., Bianca M., De Guidi G., Monaco C., Tortorici L. (2003). Fault activity and marine terracing in the Capo Vaticano area (southern Calabria) during the Middle-Late Quaternary. Quatern. Int., 101, 269-278.

Tursi F., Spiess R., Festa V., Fregola R.A. (2020) - Hercynian subduction-related processes within the metamorphic continental crust in Calabria (Southern Italy). J. Metamorph. Geol., 38, 771-793.

Tursi F., Acquafredda P., Festa V., Fornelli A., Langone A., Micheletti F., Spiess R. (2021) - What can high-P sheared orthogneisses tell us? An example from the Curinga–Girifalco Line (Calabria, southern Italy). J. Metamorph. Geol., 39, 919-944.

Vernon R.H. and Paterson S.R. (2008) - How late are K-feldspar megacrysts in granites? Lithos, 104(1-4), 327-336.

https://doi.org/10.3301/GFT.2024.09

von Raumer J.F. and Stampfli G.M. (2008) - The birth of the Rheic Ocean—Early Palaeozoic subsidence patterns and subsequent tectonic plate scenarios. Tectonophysics, 461(1-4), 9-20.

von Raumer J.F., Bussy F., Schaltegger U., Schulz B., Stampfli G.M. (2013) - Pre-Mesozoic Alpine basements—their place in the European Paleozoic framework. Geol. Soc. Am. Bull., 125(1-2), 89-108.

von Raumer J.F., Finger F., Veselá P., Stampfli G.M. (2014) - Durbachites–Vaugnerites – a geodynamic marker in the central European Variscan orogen. Terra Nova, 26(2), 85-95.

Whalen J.B. and Frost C.D. (2013) - The Q-ANOR diagram: a tool for the petrogenetic and tectonomagmatic characterization of granitic suites. South-Central Section. Geol. Soc. Am. Abstracts with programs, 45(3), 24 (Paper No. 17-4.).

Whitney D.L. and Evans B.W. (2010) - Abbreviations for names of rock-forming minerals. Am. Mineral., 95(1), 185-187.

Winchester J.A. and Floyd P.A. (1977) - Geochemical discrimination of different magma series and their differentiation products using immobile elements. Chem. Geol., 20, 325-343.

Žák J. and Paterson S.R. (2005) - Characteristics of internal contacts in the Tuolumne Batholith, central Sierra Nevada, California (USA): Implications for episodic emplacement and physical processes in a continental arc magma chamber. Geol. Soc. Am. Bull., 117, 1242-1255.

Manuscript received 04 March 2024; accepted 07 November 2024; published online 18 December 2024;
editorial responsibility and handling by M. Massironi.

https://doi.org/10.3301/GFT.2024.09